UNCLASSIFIED

AD NUMBER

AD879878

NEW LIMITATION CHANGE

TO

Approved for public release, distribution unlimited

FROM

Distribution authorized to U.S. Gov't. agencies and their contractors; Critical Technology; JAN 1971. Other requests shall be referred to Air Force Rocket Prolpulsion Lab., Edwards AFB, CA.

AUTHORITY

AFRPL ltr, 29 Sep 1971

THIS PAGE IS UNCLASSIFIED

AFRPL-TR-70-153

AD879878

AD No. ____
DDC FILE COPY

ELECTROLYTIC IGNITION SYSTEM FOR A MILLIPOUND THRUSTER

(CONTRACT F04611-70-C-0070) NEW

PHASE I
SPECIAL REPORT
JANUARY, 1971

by

C.T. Brown

UNITED AIRCRAFT RESEARCH LABORATORIES
UNITED AIRCRAFT CORPORATION
EAST HARTFORD, CONNECTICUT

"This document is subject to special export controls and each transmittal to foreign governments or foreign nationals may be made only with prior approval of AFRPL (DOZT/STINFO). Edwards, California 93523"

Air Force Rocket Propulsion Laboratory
Directorate of Laboratories
Air Force Systems Command
United States Air Force
Edwards, California 93523

DDC
RECEIVED
FEB 10 1971
B

"When U. S. Government drawings, specifications, or other data are used for any purpose other than a definitely related Government procurement operation, the Government thereby incurs no responsibility nor any obligation whatsoever, and the fact that the Government may have formulated, furnished, or in any way supplied the said drawings, specifications, or other data, is not to be regarded by implication or otherwise, or in any manner licensing the holder or any other person or corporation, or conveying any rights or permission to manufacture use, or sell any patented invention that may in any way be related thereto."

ACCESSION for
CFSTI WHITE SECTION
DDC BUFF SECTION
UNANNOUNCED
JUSTIFICATION
BY
DISTRIBUTION/AVAILABILITY CODES
DIST. AVAIL. and/or SPECIAL

AFRPL-TR-70-153

ELECTROLYTIC IGNITION SYSTEM FOR A MILLIPOUND THRUSTER

Phase I Special Report
(Contract F04611-70-C-0070)

January 1971

by
C. T. Brown
United Aircraft Research Laboratories

This document is subject to special export controls and each transmittal to foreign governments or foreign nationals may be made only with prior approval of AFRPL (DOZT/STINFO) Edwards, California 93523

Air Force Rocket Propulsion Laboratory
Directorate of Laboratories
Air Force Systems Command
United States Air Force
Edwards, California 93523

FOREWORD

This work was done at the United Aircraft Research Laboratories, East Hartford, Connecticut, for the Air Force Rocket Propulsion Laboratory under Phase I of Contract F04611-70-C-0070. The work under this phase of the contract was carried out during the period July 15, 1970 through December 31, 1970.

Work under Phase I of the Contract F04611-70-C-0070 was performed under the direction of Dr. C. T. Brown, Principal Investigator.

This work was conducted under technical management of Capt. Douglas D. Huxtable, USAF/RPCL, and the contracting officer is G. M. Plock of Edwards Air Force Base, Edwards, California.

Publication of this report does not constitute Air Force approval of the report's findings or conclusions. It is published only for the exchange and stimulation of ideas.

Douglas D. Huxtable, Captain
Project Engineer

ABSTRACT

The United Aircraft Research Laboratories have conducted a research program under Phase I of Contract F04611-70-C-0070, which had as its objective the selection of an electrolyte and electrode materials for an electrolytic ignition system for millipound thrusters. This report describes the evaluation of electrode polarization effects, ohmic effects due to both electrolytes and electrodes, and possible catalytic effects on electrode surfaces. Electrical conductivity measurements indicate that hydrazine-based salts must be added to hydrazine in order to minimize ohmic effects and that the mixture of 77% hydrazine-23% hydrazine azide is the most promising electrolyte candidate. Polarization studies have shown that platinum or pyrolytic graphite should be the best anode material for the electrolytic cell and that AM350 or 304SS should be the best cathode material in terms of minimizing the power needs for the cell. These electrodes were also found to catalyze the propellant decomposition reaction in addition to providing simple electrolytic decomposition. This result indicates that the reaction will be self-propagating at power inputs considerably below theoretical.

Electrolytic Ignition System for a Millipound Thruster
Phase I Special Report

TABLE OF CONTENTS

	Page
INTRODUCTION	1
EXPERIMENTAL PROGRAM	3
Electrical Conductivity of Candidate Electrolytes	3
Experimental Approach	3
Materials	3
Apparatus	4
Procedure	4
Results	4
Polarization of Electrodes	5
Experimental Approach	6
Materials	6
Apparatus	6
Procedure	7
Potentiostatic Results	8
Flat Plate Electrodes	8
Stainless Steel Rod Electrodes	10
Pyrolytic versus Spectrographic Graphite	10
Effect of Azide Concentration	11
Potential Time Results at Constant Current	13
Electrolysis and Product Analysis	15
Experimental Approach	16

TABLE OF CONTENTS (Cont'd)

	Page
Materials	16
Apparatus	16
Procedure	17
Results	18
SUMMARY AND CONCLUSIONS	20
REFERENCES	23
TABLES I - XV	24
FIGURES 1 - 41	38

LIST OF FIGURES

FIGURE 1 Electrode Polarization Apparatus

FIGURE 2 Anodic Polarization of 17-7 PH in Hydrazine-Base Propellants

FIGURE 3 Anodic Polarization of 304SS in Hydrazine-Base Propellants

FIGURE 4 Anodic Polarization of AM350 in Hydrazine-Base Propellants

FIGURE 5 Anodic Polarization of HS1414 in Hydrazine-Base Propellants

FIGURE 6 Anodic Polarization of Platinum in Hydrazine-Base Propellants

FIGURE 7 Anodic Polarization of Graphite in Hydrazine-Base Propellants

FIGURE 8 Anodic Polarization of AA1100 in Hydrazine-Base Propellants

FIGURE 9 Anodic Polarization of AA6061-T6 in Hydrazine-Base Propellants

FIGURE 10 Cathodic Polarization of 17-7 PH in Hydrazine-Base Propellants

FIGURE 11 Cathodic Polarization of 304SS in Hydrazine-Base Propellants

FIGURE 12 Cathodic Polarization of AM350 in Hydrazine-Base Propellants

FIGURE 13 Cathodic Polarization of HS1414 in Hydrazine-Base Propellants

FIGURE 14 Cathodic Polarization of Platinum in Hydrazine-Base Propellants

FIGURE 15 Cathodic Polarization of Graphite in Hydrazine-Base Propellants

FIGURE 16 Cathodic Polarization of AA1100 in Hydrazine-Base Propellants

FIGURE 17 Cathodic Polarization of AA6061-T6 in Hydrazine-Base Propellants

FIGURE 18 Anodic Polarization of 17-7 PH in 77% Hydrazine-23% Hydrazine Azide

FIGURE 19 Cathodic Polarization of AM350 in 77% Hydrazine-23% Hydrazine Azide

FIGURE 20 Anodic Polarization of AM350 in 77% hydrazine-23% hydrazine azide and 88% hydrazine-12% hydrazine azide

FIGURE 21 Anodic Polarization of Graphite in 77% Hydrazine-23% Hydrazine Azide

LIST OF FIGURES (Cont'd)

FIGURE 22 Cathodic Polarization of Graphite in 77% Hydrazine-23% Hydrazine Azide

FIGURE 23 Anodic Polarization of 304SS as a Function of Azide Concentration

FIGURE 24 Anodic Polarization of AM350 as a Function of Azide Concentration

FIGURE 25 Anodic Polarization of Platinum as a Function of Azide Concentration

FIGURE 26 Anodic Polarization of Pyrolytic Graphite as a Function of Azide Concentration

FIGURE 27 Cathodic Polarization of 304SS as a Function of Azide Concentration

FIGURE 28 Cathodic Polarization of AM350 as a Function of Azide Concentration

FIGURE 29 Cathodic Polarization of Platinum as a Function of Azide Concentration

FIGURE 30 Cathodic Current Density vs. Azide Concentration at η = 1000 mv

FIGURE 31 Anodic Current Density vs. Azide Concentration at η = 1000 mv

FIGURE 32 Anodic Polarization of 304SS in 6% Hydrazine Nitrate and in 4.8% Hydrazine Azide

FIGURE 33 Anodic Polarization of AM350 in 6% Hydrazine Nitrate and in 4.8% Hydrazine Azide

FIGURE 34 Anodic Polarization of Platinum in 6% Hydrazine Nitrate and in 4.8% Hydrazine Azide

FIGURE 35 Anodic Polarization of Pyrolytic Graphite in 6% Hydrazine Nitrate and in 4.8% Hydrazine Azide

FIGURE 36 Cathodic Polarization of 304SS in 6% Hydrazine Nitrate and in 4.8% Hydrazine Azide

FIGURE 37 Cathodic Polarization of AM350 in 6% Hydrazine Nitrate and in 4.8% Hydrazine Azide

FIGURE 38 Cathodic Polarization of Platinum in 6% Hydrazine Nitrate and in 4.8% Hydrazine Azide

LIST OF FIGURES (Cont'd)

FIGURE 39 Potential-Time Relationships at 100 ma in 77% Hydrazine-23% Hydrazine Azide

FIGURE 40 Electrolysis Cell

FIGURE 41 Chromatographic Apparatus

LIST OF TABLES

TABLE I Specific Conductance of Selected Hydrazine-Base Propellants

TABLE II Anodic Polarization in Hydrazine-Base Propellants at 300°K

TABLE III Cathodic Polarization in Hydrazine-Base Propellants at 300°K

TABLE IV Comparison of Anodic and Cathodic Polarization of Stainless Steels in 77% Hydrazine-23% Hydrazine Azide at 300°K

TABLE V Anodic Polarization of AM350, 304SS, Pyrolytic Graphite and Platinum as a Function of Azide Concentration

TABLE VI Cathodic Polarization of AM350, 304SS, and Platinum as a Function of Azide Concentration

TABLE VII Comparison of Anodic and Cathodic Polarization in Azide and Nitrate Propellants

TABLE VIII Order of Cathodic Polarization at a Constant Current of 50 ma

TABLE IX Order of Anodic Polarization at a Constant Current of 50 ma

TABLE X Total Overpotential at 50 ma/cm^2 in 77% Hydrazine-23% Hydrazine Azide

TABLE XI Polarization as a Function of Azide Concentration at 50 ma

TABLE XII Comparison of Polarization in Hydrazine-Hydrazine Azide and Hydrazine-Hydrazine Nitrate at a Constant Current of 50 ma

TABLE XIII Electrolysis of Hydrazine Azide-Gas Analysis

TABLE XIV Polarization Data - Electrolysis Cell

TABLE XV Faradaic Efficiency for Electrolysis of 77% Hydrazine-23% Hydrazine Azide

SECTION I

INTRODUCTION

The advantages of monopropellants over bipropellants for specific rocket engine applications have long been recognized. These advantages include the simplicity and reliability of the system resulting from elimination of dual tankage and pumping requirements, as well as elimination of problems and inefficiencies associated with residual fuel or oxidizer at other than the design mixture ratio for bipropellant systems. Consequently, a considerable amount of research and development has been carried on during the past fifteen years to develop suitable monopropellants. This work has included studies of the quaternary ammonium salts (cavea-type compounds), hydrogen peroxide, n-propyl nitrate, tetranitromethane, hydrazine and a variety of other materials. In most instances, however, the simultaneous requirements of high performance and low shock sensitivity have screened out the candidate propellants.

Among the various candidate monopropellants, hydrazine was early recognized as presenting a good compromise between the requirements of performance and safety. Early work was hampered, however, by the need for relatively high bed temperatures to initiate the hydrazine decomposition in a reaction chamber and interest consequently lagged. However, the development of spontaneous low-temperature catalysts for monopropellant hydrazine has stimulated a considerable resurgence of interest during the past decade in the use of hydrazine and hydrazine-based mixtures as monopropellants for various applications in thrusters and gas generators and has led to the recent successful use of hydrazine monopropellant thrusters for satellite station-keeping operations.

One major problem remaining with the low-temperature catalyst for hydrazine-based monopropellants is the present requirement for substantial amounts of critical noble metals in systems which are to have multiple cold starts. Consequently, a number of alternatives to the use of noble metal catalysts for ignition have been suggested. In particular, the need for rapid ignition with high reliability over a wide range of temperature and engine sizes has resulted in interest in the development of an electrochemical means of ignition for hydrazine-based monopropellants in small thrusters. The development of an electrochemical ignition system circumvents problems associated with catalyst degradation caused by spallation, sintering, crystallite formation, and poisoning. In addition, such an ignition method would have a potential advantage in reduced chamber volume. An ignition system of this general type has been demonstrated on a small scale (Ref. 1) but substantial design information must still be obtained before an optimized system can be fabricated and tested.

An experimental program designed to provide the necessary design data is now being conducted by United Aircraft Research Laboratories (UARL) under AFRPL Contract F04611-70-C-0070. The work being performed under this contract comprises three phases which include: Phase I, Study of the mechanism of propellant decomposition; Phase II, Optimization of an electrolytic cell based on data obtained in Phase I; and Phase III, Fabrication and evaluation of an electrolytic ignition system designed for a propellant flow rate of approximately 5×10^{-4} lbs/sec.

The results obtained at UARL during Phase I of the contract are reported herein. Phase I had as its objective the selection of optimum electrode materials and electrolytes for the electrolytic cell in terms of minimizing power losses and maximizing heating effects. This work also included evaluation of the catalytic effects of various electrode materials on the propellant decomposition and the determination of the products of the electrolytic reaction. The latter can be used to predict heating effects.

SECTION II

EXPERIMENTAL PROGRAM

The Phase I experimental program comprised three basic studies: (1) the evaluation of the ohmic losses to be expected as a result of the resistivity (conductivity) of the electrolytes used; (2) the determination of polarization effects on various electrode materials as a function of the propellant/electrolyte used; and (3) electrolysis of propellant/electrolytes in order to determine the decomposition products formed and thus provide a basis for evaluating the theoretical heat output to be expected from the electrolysis.

1. ELECTRICAL CONDUCTIVITY OF CANDIDATE ELECTROLYTES

In order to provide the maximum current at minimum voltage in an electrolytic cell, it is necessary to have an electrolyte with as high an electrical conductivity as possible. Ohmic heating can represent a large power loss in the cell, and low conductivity severely limits the current available for direct-low temperature decomposition of the electrolyte.

Since the specific conductivity of pure hydrazine is of the order of 10^{-6} $ohms^{-1}$ cm^{-1} (or a resistivity of one million ohms per centimeter) (Ref. 2), it obviously cannot be used directly in an electrolytic cell. In order to raise the conductivity, it is necessary to use hydrazine-salt mixtures. Conductivity data for hydrazine-salt mixtures was found to be lacking, and it was thus necessary to determine this parameter for electrolytes of interest. Conductivity measurements were made at UARL for propellant grade hydrazine, hydrazine-2% hydrazine nitrate, hydrazine-2% hydrazine azide and hydrazine-23% hydrazine azide.

a. Experimental Approach

(1) Materials

For the determination of electrolytic conductance, platinum electrodes were used. The electrodes consisted of two parallel sheets of platinum foil (each approximately one cm^2); in order to aid in eliminating polarization effects due to the current, the electrodes were coated with a layer of finely divided platinum black.

The specific conductances of the following materials were determined: propellant grade hydrazine, hydrazine + 2% ammonium nitrate, and two solutions of hydrazine and hydrazine azide, one containing 23% hydrazine azide and the other containing 2% hydrazine azide. The nitrate solution was prepared by adding two weight percent of ammonium nitrate to propellant grade hydrazine. The 2% hydrazine azide solution was prepared by dilution of 23% hydrazine azide solution.

(2) Apparatus

The study of the conductance of hydrazine and hydrazine-based solutions was accomplished by the use of a conductance bridge in which the essential component is a precision impedance comparator (General Radio Co.). The other components were an adjustable resistance standard and a set of balancing capacitors. Capacitance decade boxes (Electronic Instrument Co.) connected in parallel with the resistance standard provided an auxiliary variable capacitor.

A constant temperature bath (Precision Scientific Co.) containing oil was used to maintain the solutions at the prescribed temperature.

Two H-shaped conductivity cells were used - one with an electrode spacing of one cm and one with a spacing of seven cm - in order to accommodate a wide range of resistances.

(3) Procedure

The conductivity cells were calibrated using a 0.01 Demal solution of KCl of known specific conductance. A cell constant was calculated from resistance measurements using the KCl solution according to the equation $\kappa = \underline{\kappa} R$ where $\underline{\kappa}$ is the specific conductance of the KCl and R is the measured resistance. This constant is then used to calculate the specific conductance of the hydrazine solutions. The resistance was measured at four frequences, 1KC, 2KC, 5KC, and 20KC and plotted against $1/\sqrt{f}$. The true resistance was found by extrapolating the plot to infinite frequency. The specific conductance of each solution was found at three temperatures, 25°C, 35°C, and 45°C.

b. Results

The conductivity data for the four propellants at three temperatures are summarized in Table I. It is apparent from these results that a small addition of a hydrazine salt has a large effect on the conductivity of the propellant (i.e., about two orders of magnitude for 2% nitrate and 2% azide). The use of the 23% azide provides another order of magnitude in the conductivity.

The fact that both the nitrate and azide mixtures have similar conductivities at similar concentrations indicates that the mechanism of conduction may be the same (i.e., both are completely ionized and the major conducting species is the $N_2H_5^+$ ion). The activation energies for the conduction process were determined from the equation:

$$\ln \kappa = \ln A - \frac{\Delta E}{RT}$$

where ΔE is the energy of activation for conduction in cal/mole, κ is the specific conductivity in ohm^{-1} cm^{-1}, and R is the gas constant expressed in cal/deg K/mole, A is an emprical constant, and T is the temperature in deg K. A plot of log κ versus 1/T yields a slope of $-\Delta E/2.303$ R and thus ΔE can be calculated. The values for the energies of activation obtained from plots of lnκ versus 1/T using data from Table I are 10.0, 1.6, 2.9, and 1.3 kcal/mole for N_2H_4, N_2H_4 - 2% NH_4NO_3, N_2H_4 - 2% N_5H_5 and N_2H_4 - 23% N_5H_5, respectively. Although the high value of 2.9 for the 2% N_5H_5 is unexplained, it is apparent that the values for the energies of activation for the propellants containing the two additives studied are all substantially smaller than the value of 10 kcal/mole measured for N_2H_4. These results add further credence to the premise that the conduction mechanisms are similar for these additives and it is not necessary to screen a further large group of additives for the sole purpose of finding one which will greatly increase the conductivity of the propellant.

The use of azide additive is to be preferred over use of the nitrate, since the azide decomposition products should be the same as those for neat hydrazine. Other additives such as nitrates would be expected to yield a wide variety of products.

2. POLARIZATION OF ELECTRODES

Electrode polarization or voltage loss (overvoltage) due to electrode-electrolyte effects becomes important as the internal resistance effects are minimized. The polarization effects are due to a slow step in the electron transfer reaction in the vicinity of the electrode surface (activation polarization) or to slow diffusion of a reacting species into the electrolyte-electrode zone (diffusion polarization). The latter case is usually important when the reacting species is present in low concentrations in an electrochemically inert solvent. This solvent can be an electrolyte whose ionic species are not discharged in the normal range of applied potentials. Since the source of reactants in this case is hydrazine azide, which is present in excess, there should be little or no diffusion polarization.

The preferred methods for electrode reaction studies are based on potentiostatic (controlled potential) or galvanostatic (controlled current) techniques. In either case, a noncurrent-carrying reference electrode is used to monitor potential changes at the anode and cathode separately. In the studies reported herein, a stable reversible reference electrode developed earlier at UARL was used.

Potentiostatic devices are used to maintain a set potential between the reference electrode and the electrode under study and provide the current necessary to maintain this potential. The system can be rapidly scanned and it is particularly applicable to anode polarization studies where, for example, the presence of an oxide film or of other protective films on the anode is easily detected as a plateau in the current-voltage curves. The applied voltage in excess of the natural voltage of the system can thus be measured in terms of the current flow through the cell.

This excess voltage may be termed the voltage loss due to reactions at the electrode surface. Another voltage loss which may also be present near the electrode surface is due to pseudo-resistances that occurs because of films that form on the surface of the electrode or the layers of non-reacting ions that may build up near the electrode surface.

Measurements of pseudo-resistance effects were accomplished in this program by applying a known constant current to the cell (galvamostatic techniques). The circuit is opened by means of a mercury-wetted reed switch and the potential decay noted as a function of time using an oscilloscope as a recorder. Since transition times for resistance effects are on the order of 10^{-5} sec, while decay of the potential due to capacitance effects in the electrolyte layer near the electrode surface and/or diffusion of reactant species requires times of the order of 10^{-4} to 10^{-3} sec, both effects are determined in the same experiment.

Descriptions of both the potentiostatic and constant current devices are contained in subsequent paragraphs.

a. Experimental Approach

(1) Materials

The electrolytes used were propellant grade hydrazine, 77% hydrazine - 23% hydrazine azide and two dilutions of the latter containing 12% hydrazine azide and 4.8% hydrazine azide. Hydrazine with additions of 5% and 6% ammonium nitrate were also used.

The first set of electrodes tested were flat plate electrodes of known surface area (approximately 2 cm^2). Each was spot welded to a wire of the same material. Electrode materials used were platinum; the stainless steels, AM350, 304SS and 17-7 PH; two aluminum alloys, AA1100 and AA6061-T6; and HS1414, a gold nickel brazing alloy.

The second set of electrodes were rods of varying diameters. These were adjusted in the cell so that a surface area of 2 cm^2 was obtained in all cases. Materials for these electrodes were the three stainless steels cited above and two types of graphite, pyrolytic, and spectrographic grade.

(2) Apparatus

The cell used in polarization experiments is shown in Fig. 1 (Item 1). This cell consists of three compartments, and was designed to eliminate electrolyte resistance effects through the use of a Luggen probe, which consists of a capillary tube extending from the center compartment to one of the side compartments. Thus, problems due to the wide range in conductivity of electrolytes should not effect the results of polarization experiments. A fritted disk below the center chamber allows nitrogen to be bubbled constantly through the solution in the cell. Three elec-

trodes are used: (1) the test or working electrode in the center chamber; (2) the counter-electrode which was always a spectrographic graphite rod located in one side chamber; and (3) a saturated calomel reference electrode in the other side chamber which fixes the potential of the electrode with respect to the hydrazine-containing electrolyte. The solution in the cell was maintained at a constant temperature, 28° C, by immersion in an oil bath [Precision Scientific Co. (Fig. 1, Item 10)].

Current-voltage relationships were measured by means of a Wenking potentiostat (Fig. 1, Item 8), a Wavetek Model 116 Function Generator (Fig. 1, Item 7) and a DC Offset Device (Fig. 1, Item 6). A triangular wave output from the function generator is fed to the potentiostat to provide the control signal between the referencing and working electrodes. The initial voltage of the triangular wave output is set by means of the DC offset device. The voltage range and sweep rate is set by means of the function generator amplitude and frequency controls, respectively. The potentiostat automatically provides the current flow between the working and counter electrode necessary to maintain the potential difference between the reference and working electrodes. The reference versus working potential is monitored using a Kiethly Model 200B Vacuum Tube Voltmeter (Fig. 1, Item 5) and the current-voltage relationships are recorded using a Tektronix Type 536, X-Y oscilloscope using Type G differential plug-in units (Fig. 1, Item 9). Permanent records of the traces were made using a C-12 Polaroid camera assembly.

Potential-time relationships were made using a regulated power supply [Dressen and Barnes model 62-112 (Fig. 1, Item 4)] in conjunction with a decade resistor [General Radio (Fig. 1, Item 2)] to maintain a constant cell current. A mercury-wetted reeed switch (Fig. 1, Item 3) was used as a triggering device for the current output. The oscilloscope was used to record the voltage-time relationship using the Type G differential plug-in unit for voltage, and a Type T, time base generator, plug-in unit for time.

(3) Procedure

(a) Current-voltage

The cell was filled with 40 ml of the electrolyte solution and placed in the oil bath at 28°C. The electrodes were immersed in the electrolyte to the proper depth and connected to the potentiostat and voltmeter. The function generator was always set to give a triangular wave pattern, a span of one volt, and a frequency of 0.03 cycles per second equivalent to a scanning rate of 400 mv/min. The initial voltage was set to the rest potential of the cell using the DC offset device. Once vertical and horizontal adjustments on the oscilloscope had been made, a five-minute picture was taken for both the anodic and cathodic process.

From the pictures, points were plotted of the overpotential versus the log of the current density (milliamps/cm^2) to directly compare the different electrodes and electrolyte solutions.

(b) Potential-Time

The cell was set up in the same manner as for current-voltage runs, and leads were connected from the electrodes to the voltmeter and regulated power supply. The leads from the power supply were connected to the working and counter electrodes with polarity appropriately adjusted to make either anodic or cathodic runs. Currents of 10 ma, 50 ma, 75 ma, and 100 ma were set by the power supply and a resistance of 100 ohms was set by the resistance box for each of the currents used. The horizontal time control on the oscilliscope was set at 0.05 millisec/cm or less in order to give a smooth curve. The mercury-wetted reed switch assembly is provided with a time delay which first triggers the oscilloscope and after 0.8 milliseconds connects the power supply to the cell. Pictures of the traces were taken using a 10-sec. exposure.

b. Potentiostatic Results

(1) Flat Plate Electrodes

Anodic and cathodic current-voltage curves have been measured for flat plate electrodes having areas of approximately 2 cm^2. The following electrode materials were investigated: 304SS, AM350, 17-7 PH, spectrographic graphite, platinum, HS1414 (gold-nickel brazing alloy), AA1100 and AA6061-T6. The latter aluminum alloys were used for comparison purposes only, since earlier work at UARL had indicated that these alloys are highly polarized in hydrazine-based propellants. The electrolytes used were propellant grade hydrazine ($\approx$ 1 percent H_2O), hydrazine - 5% hydrazine nitrate and hydrazine - 23% hydrazine azide.

The anodic polarization curves for the eight materials studied are illustrated in Figs. 2-9. The graphs include those for all three electrolytes studied for easy comparison. A Luggen probe was used in order to minimize resistance effects so that differences in the curves should not reflect differences in the conductivites of the electrolytes. The stainless steels, as well as platinum, graphite and HS1414 all indicate much lower anodic polarization effects in the nitrate and azide electrolytes than in propellant-grade hydrazine. These materials also show a lower polarization in azide than in the nitrate electrolyte with the exception of 17-7 PH which indicates the opposite effect (Fig. 2). The relative smoothness of the anodic polarization plots in hydrazine azide and hydrazine nitrate indicate a lack of surface inhibition of the anodic decomposition process. Slight dips are noted in the hydrazine curves for 17-7 PH (Fig. 2) and graphite (Fig. 7) at an overpotential of about 500 mv indicating the formation of an intermediate species on these surfaces. A pronounced double oxidation peak is noted on AA6061-T6 in hydrazine nitrate (Fig. 9) indicating very complex reaction on this surface.

In order to compare the relative merits of anode materials, the current density was used at an overpotential of 1000 mv. The data for the anodic current densities

at this overpotential are summarized in Table II. The aluminum alloys are obviously the poorest anode materials in all three electrolytes, probably due to the ease with which oxides are formed on the surface under oxidizing conditions. The alloys were used for comparison purposes only and were not studied in subsequent experiments. Platinum, HS1414, and spectrographic graphite are all good candidate anode materials, but graphite is less promising that expected. The stainless steels show polarizations about an order of magnitude less than the former group.

The cathodic polarization curves for the eight materials studied in the three electrolytes are illustrated in Figs. 10-17. A summary of the cathodic current densities at an overpotential of 1000 mv is shown in Table III. The cathodic process in the azide electrolyte is much less inhibited than the anodic. Similarly, the cathodic process on the two aluminum alloys appears to be much less inhibited than the anodic process, since it is observed that current densities for these two materials at an overpotential of 1000 mv are of the same order as on the stainless steels and graphite. Platinum and HS1414 show the most promise as cathode materials, but 17-7 PH also shows considerable promise. In hydrazine nitrate 17-7 PH is on a par with the more noble metals. Graphite is very poor as a cathode material in both azide and nitrate. The behavior of aluminum in the nitrate is considerably different than that of the azide which is surprising, since it was expected that both cathodic processes are due to the discharge of $N_2H_5^+$ ions. The cathodic process in propellant grade hydrazine is strongly inhibited for 304SS (Fig. 11), AM350 (Fig. 12), HS1414 (Fig. 13), and platinum (Fig. 14). In each case there is a permanent reduction current at high overpotentials indicating complete surface coverage by an intermediate species. There is also a partial inhibition at lower current densities in hydrazine azide for 17-7 PH (Fig. 10), 304SS (Fig. 11), AM350 (Fig. 12) and a pronounced plateau for HS1414 (Fig. 12) and graphite (Fig. 15). This effect at low overpotential is also apparent in hydrazine nitrate for AM350 (Fig. 12) and graphite (Fig. 15). These plateaus at lower overpotentials (300-500 mv) are not permanently inhibiting since much higher current densities are achieved at higher overpotentials. Evidently, the intermediate species responsible for the plateaus is reduced to a final product as the overpotential is increased. The stainless steels, as well as HS1414 and platinum, appear to be good candidate materials for the cathode of the electrolysis cell, while graphite is surprisingly poor.

As a result of this preliminary survey, it was decided to concentrate on the stainless steels, platinum and graphite in 23% azide. Although HS1414 and platinum both show the lowest polarization effects, they are expensive materials; however, the acquisition of platinum data was continued as a control for comparison of results. It was also decided to look at rod shaped electrodes, since a cylindrical configuration would probably be the most applicable to the design of an electrolytic cell. The graphite tests were also repeated at this time using pyrolytic graphite in order to determine if this material indicates improved behavior over that achieved for normal spectrographic grade graphite. The former material has a more regular surface than the spectrographic grade.

(2) Stainless Steel Rod Electrodes

Current-voltage polarization data was obtained using rod electrodes in a 23% hydrazine azide solution in the same manner as previously described. Comparison of the data between cleaned rod and flat plate electrodes show that anodic polarization of 304SS and AM350 is similar in the two cases, but that the 17-7 PH rod stock was much less polarized that flat plate stock. The polarization plots shown in Fig. 18 for 17-7 PH include data for the flat plate stock cleaned in the same manner as the rod stock. The initial polarization of the 17-7 PH rod stock is very high up to an overpotential of about 600 mv. Following this point, there is an abrupt rise in current which accounts for the improved behavior. This curve indicates existence of a passive film which is removed at high overpotentials. Repeated runs yielded erratic results, i.e., in some cases the passive state was retained up to overpotentials of 1200 mv, while in others a high current was obtained after 600 mv. Apparently, there is a condition of unstable passivity in this electrode-electrolyte combination which makes the usefulness of 17-7 PH as an anode doubtful.

Cathodic polarization of stainless steel rod electrodes in 77% hydrazine - 23% hydrazine azide indicates similar behavior for 304SS compared to the flat plate stock but erratic results for 17-7 PH. The polarization on AM350 showed slight improvement when the flat plate stock, previously used, was cleaned in the same manner as the rod. All materials were cleaned with fine emery paper followed by detergent cleaning, rinsing with deionized water, and air drying. The cathodic polarization curves for AM350 are shown in Fig. 19. The shapes of the three curves are similar, but the rod stock indicates a limiting current at 88 ma.

The data for AM350 and 17-7 PH rod stock was repeated many times and in most cases inconsistent data was obtained. The cathodic data for AM350 varied over a fairly limited range (i.e., from 50-90 ma/cm^2 at n = 1000 mv) with no regular pattern. However, the anodic AM350 data fell into two distinct groups, one set at about 17 ma/cm^2 and the other at about 50 ma/cm^2. Typical current-voltage curves for the two cases taken directly from the oscilloscope traces are shown in Fig. 20B. Traces similar to these were also obtained for 17-7 PH in both the anodic and cathodic case. It was found that cleaning of AM350 prior to use could, in most cases, yield a much lower polarization, but 17-7 PH yielded inconsistent results in spite of the use of cleaning procedures. Therefore, 17-7 PH was tentatively eliminated from future studies.

(3) Pyrolytic versus Spectrographic Graphite

The anodic and cathodic polarization curves for spectrographic grade and pyrolytic graphite in 23% azide solution are shown in Figs. 21 and 22, respectively. The anodic polarization of the two types of graphite are similar, but pyrolytic graphite indicates a 35 percent improvement in current density at an overpotential of 1000 mv.

The cathodic polarization is extremely high for both graphites and shows a definite "passivation" plateau in each case. (The more regular surface of pyrolytic graphite is more strongly affected than is that of spectrographic grade.) Because of this behavior, graphite has been eliminated as a candidate cathode material.

(4) Effect of Azide Concentration

The polarization curves of 304SS, AM350, platinum and pyrolytic graphite were measured as a function of azide concentration to ascertain if there is an optimum concentration where polarization and conductivity effects can be traded off. The optimization of these effects will be important in a practical ignition cell configuration where resistance effects will play an important part in determining the power necessary to achieve ignition.

The anodic polarization of 304SS, AM350, platinum and pyrolytic graphite as a function of azide concentration are shown in Figs. 23 through 26. The anodic current densities achieved at an overpotential of 1000 mv for each material at the three azide concentrations studied are summarized in Table V. The anodic data indicates that the polarization of pyrolytic graphite compares favorably with platinum and that pyrolytic graphite can probably be used as an anode material in an electrolytic cell. It is also apparent that the anodic polarization is a much stronger function of azide concentration for platinum and pyrolytic graphite than for either 304SS or AM350 and that the polarization for the latter two materials are linear functions of azide concentration. This behavior is shown in Fig. 31, which is a plot of current density at an overpotential of 1000 mv versus azide concentration.

It is also interesting to note that AM350 an an anode exhibits (Fig. 24) a cross-over point where the polarization is independent of azide concentration (about 8 ma/cm^2 at η = 700 mv) and that the reaction is strongly inhibited at higher azide concentrations at overpotentials less than 700 mv.

It was also found that the anodic behavior of AM350 was considerably different in 23% azide than previously measured (compare data in Table V with data in Table IV). The latter case was due to passivity, as previously shown in Fig. 20B. However, proper cleaning of AM350 surface followed by repeated runs yielded consistent current densities on the order of 50 ma/cm^2 at η = 1000 mv. The same anodic polarization behavior for AM350 was also observed in 12% and 4.8% azide, as shown in Fig. 20A.

The cathodic polarization of 304SS, AM350, and platinum as a function of azide concentration is shown in Figs. 27 through 29. The cathodic current densities achieved at an overpotential of 1000 mv for each material at the three azide concentrations studied are summarized in Table VI, and plots of the current density data versus azide concentration are shown in Fig. 30. The data for 304SS and AM350 are almost linear functions of azide concentration. The data for platinum indicate an irregular behavior as evidenced by the extremely low value at an azide concentration of 12%. The cathodic data for platinum at 12% azide was repeated many times and found to be between 35 and 40 ma/cm^2 at η = 1000 mv in each case. If the data at

12% azide is ignored, however, the slopes of linear plots for all three electrode materials are identical (i.e., ≈ 4 ma/cm^2/% azide) indicating a similar concentration controlled process in each case. It is apparent from the above data that the 304SS and AM350 are comparable to platinum as a cathode for the electrolytic cell and there is no optimum azide concentration below 23%. Even though there is some irregular behavior as a function of azide concentration, none of it is beneficial. It appears that the most promising electrolyte would be 23% azide, the concentration corresponding to the lowest melting point of any hydrazine-hydrazine azide solution.

As a corollary to this investigation, an evaluation of the relative merits of a nitrate and azide electrolyte was also made. Polarization data was obtained for platinum, pyrolytic graphite, 304SS and AM350 in hydrazine - 6% hydrazine nitrate. This nitrate concentration is equivalent on a mole basis to a 4.8% hydrazine azide concentration. Since the cathodic process is expected to be the same for both azide and nitrate electrolytes (i.e., the discharge of the $N_2H_5^+$ ion), the cathodic polarization should be similar in both cases. The polarization for the anodic process should be different, since the N_3^- ion is being discharged in the case of the azide and the NO_3^- ion in the case of the nitrate.

The anodic polarization curves are illustrated in Figs. 32 through 35 for 304SS, AM350, platinum, and pyrolytic graphite. A comparison of the current densities at an overpotential (η) of 1000 mv is summarized in Table VII. On the basis of this data, it is apparent that the anodic polarization of all of the materials except platinum is significantly different in the two electrolytes. Evidently, platinum can catalyze the reaction of both the azide and nitrate anions equally well. The AM350 is less polarized in the azide propellant, while 304SS and pyrolytic graphite are less polarized in nitrate.

Cathodic polarization curves for 304SS, AM350, and platinum are illustrated in Figs. 36 to 38. The cathodic polarization of AM350 and platinum were similar in both electrolytes as anticipated, since the $N_2H_5^+$ ion is involved in the cathodic reaction in both cases (the cathodic polarization of pyrolytic graphite was not included, since it has been shown to be highly polarized in all cases). The cathodic polarization in the two electrolytes was considerably different for 304SS. This alloy indicates a lower cathodic polarization in nitrate than in the azide which is consistent with the anodic results.

There does not seem to be any clear cut advantage for either propellant at these concentration levels, and an expected pattern for $N_2H_5^+$ and either N_3^- or NO_3^- discharge is not consistently confirmed by these experiments. However, it is known that propellants with high nitrate concentrations are quite unstable and would probably not have an advantage over the 23% azide. (For example, a 20% nitrate solution could not be used in the conductivity experiments because of its rapid decomposition in the presence of platinum.)

c. Potential-Time Results at Constant Current

The potentiostatic current-voltage data previously discussed were obtained by rapidly scanning over a voltage range and, therefore, primarily indicates transient effects. This technique is most applicable to the characterization of surface effects and provides a rapid means of surveying a large number of electrode materials.

An alternative approach, the steady-state constant current experiment, employing potential-time measurement at constant applied current more closely represents actual conditions of propellant electrolysis. By measuring the rapid potential rise upon application of the constant current and also determining the total steady-state overpotential, it is possible to obtain data in three important areas: (a) an initial rapid ($<10^{-5}$ sec) rise in potential corresponds to resistance effects uncompensated by the Luggen Probe (i.e., surface resistances as opposed to electrolyte resistivity); (b) the slope of the succeeding potential time curve yields information on the sequence of processes taking place as the electrode-electrolyte interface is charged; and (c) the true resistance-free total polarization at constant current can be obtained.

Potential-time measurements at constant applied current were taken for the original eight electrode materials in the three electrolytes. The measurements were obtained by rapidly (<0.1 msec) applying a fixed current to the experimental cell and recording the potential-time relationship on an oscilliscope. Potential-time data was obtained at 1, 5, 10, 25, and 50 ma in hydrazine-23% hydrazine azide and hydrazine-5% hydrazine nitrate; and at 1, 5, and 10 ma in propellant grade hydrazine. Subsequent runs with the rod electrodes were made at 10, 50, 75, and 100 ma. The resulting maximum current densities were approximately 25 ma/cm^2 in the azide and nitrate and 5 ma/cm^2 in propellant grade hydrazine.

The total resistance-free polarization data at constant current was adjusted for variation in electrode surface area. The order of preference of materials as both anodes and cathodes is based on mv/ma/cm^2 since all materials were run at a constant current in spite of differences in electrode surface area. The relative order of preference for cathode and anode materials based on this parameter is summarized in Table VIII and IX for azide and nitrate. Although there are slight variations, in general the order of merit for anode materials in azide and nitrate is unchanged when compared to the current-voltage data. Typical potential-time traces are shown in Fig. 39 for AM350, 304SS and pyrolytic graphite in 23% azide. During anodic polarization, no uncompensated resistance effects were noted for any material studied in the azide or nitrate electrolytes. Resistance effects in propellant grade hydrazine were so large that it was impossible to use this technique and obtain reliable data.

Cathodic resistance effects were noted in the case of 304SS only. In the example shown in Fig. 39, half of the total overpotential at 100 ma (50 ma/cm^2) is due to

uncompensated resistance. Cleaning techniques were applied to 304SS to no avail; the resistance effect was always present.

In most cases, the potential transients were found to have a simple logarithmic relationship with time. On occasion a curve similar to that shown for the anodic polarization of 304SS (Fig. 39) was obtained where the initial portion of the potential-time curve is linear. This portion of the curve may be due to the charging of the electrode-electrolyte interface or the removal of species adsorbed on the electrode surface and represents a voltage loss in addition to those due to electrolyte resistivity and the actual electrochemical discharge of a reacting ionic species. This effect was always present in the case of the anodic polarization of 304SS and could not be eliminated. It was found that this linear portion of the curve was present in some instances for AM350 and 17-7 PH.

A series of experiments were run in 23% azide to determine the IR drop and polarization characteristics of several materials using the oscillographic recording technique. A summary of this data for both the anodic and cathodic process is shown in Table X. Experiments in which cathodic and/or anodic deposits were electrolytically placed on the surface prior to anodic and cathodic polarization, respectively, show that these deposits result in abnormally high polarizations due to the extra current necessary to remove these deposits before normal polarization sets in. This effect is particularly apparent in the case of anodic polarization of AM350 and 17-7 PH. (The overpotential value of 1100 mv for 17-7 PH (Table X) is apparently due to a cathodic deposit, even though it was not deliberately placed on the surface.) It is these materials which seemed to yield inconsistent results. It is now apparent that these results were due to the prior polarization history of the electrodes. In each case the initial linear portion of the potential-time curve was present when this high overpotential was noted for AM350 and 17-7 PH. However, it has been found that platinum, 304SS, both anodic and cathodic, and pyrolytic graphite during anodic polarization only, are not subject to this prior history and are, therefore, more reliable electrodes (pyrolytic graphite as an anode only) for use in an electrolytic cell.

Constant current total overpotential data was also obtained as a function of azide and nitrate concentrations and is summarized in Tables XI and XII. In general, those results confirm the current-voltage data. Platinum and pyrolytic graphite are superior to the stainless steel as anodes at all concentrations, but the difference diminishes as the concentration is lowered. There is little difference between platinum, AM350 and 304SS as cathodes; however, based upon the equilibrium data platinum is best at both 12% and 4.8% azide. This latter data does not confirm the current-voltage results which show high platinum polarization at 12% azide, but the constant current data is considered more reliable for the purpose of designing an electrolytic cell.

The polarization data for the 6% nitrate and the 4.8% azide is summarized in Table XII for a constant current of 50 ma (25 ma/cm^2). The cathodic polarization is similar in both electrolytes for Pt, 304SS and AM350, but the data for pyrolytic graphite indicates a much higher polarization in hydrazine nitrate. The latter is not surprising, since the cathodic process on graphite has always been highly inhibited. It is possible that both azide and nitrate are preferentially adsorbed on the graphite surface or even react chemically with the graphite.

The anodic data indicates a large polarization difference in the two electrolytes for both platinum and pyrolytic graphite. The anodic process for 304SS is similar for both electrolytes, but the difference in the anodic process is much greater than the difference in the corresponding cathodic process. AM350 seems to be equally good in both electrolytes, indicating that the anodic process in this case is independent of the anodic species involved in the reaction.

The above data does not correspond to the current-voltage results summarized in Table VII. In the latter case, the anodic polarization of platinum was almost the same in azide and nitrate, while the rest of the electrodes indicated large anodic differences. The results are somewhat similar in the cathodic case with the exception of 304SS. The earlier results (current-voltage) indicate a large polarization difference in this case. Again, the constant-current data is considered to be the most reliable and seems to confirm the postulate that the cathodic species are the same in both cases (N_2H_5+).

3. ELECTROLYSIS AND PRODUCT ANALYSIS

Electrolysis experiments were performed using a dual-column chromatograph to analyze gaseous and liquid products from both anode and cathode compartments for specially constructed cells. On the basis of this product analysis, the relative proportions of nitrogen, hydrogen, and ammonia were determined.

The electrochemical reactions for the decomposition of hydrazine azide (N_5H_5) may be written as follows:

ionization of N_5H_5:

$$N_5H_5 \rightleftarrows N_2H_5^+ + N_3^-$$

anode:

$$2N_3^- \rightarrow 3N_2 + 2e^-$$

cathode (no NH_3 decomposition):

$$2N_2H_5^+ + 2e \rightarrow 2NH_3 + N_2 + 2H_2$$

cathode (complete NH_3 decomposition):

$$2\ N_2H_5^+ + 2e \rightarrow 2N_2 + 5H_2$$

overall (no NH_3 decomposition):

$$2\ N_5H_5 \rightarrow 2NH_3 + 4N_2 + 2H_2$$

overall (complete NH_3 decomposition):

$$2N_5H_5 \rightarrow 5N_2 + 5H_2$$

A generalized overall reaction for the decomposition of N_5H_5 may be written as:

$$2N_5H_5 \rightarrow 2(1 - x)NH_3 + (4 + x)N_2 + (2 + 3x)H_2$$

where x is the fraction of NH_3 decomposed. This equation is analogous to the generalized N_2H_4 decomposition reaction which is

$$3N_2H_4 \rightarrow 4(1 - x)NH_3 + 6x\ H_2 + (1 + 2x)N_2$$

The difference between the two decomposition reactions is the cathodic discharge of the $N_2H_5^+$ ion in N_5H_5 ion which requires the formation of H_2 in all cases, even if there is no catalytic decomposition of NH_3. For N_2H_4 the overall reaction can yield NH_3 and N_2 as the only products.

a. Experimental Approach

(1) Materials

Rod type electrodes of stainless steel and graphite and flat plate platinum electrodes previously described were used in these experiments.

In addition to the test electrolyte, 77% N_2H_4-23% N_5H_5, several standard solutions were used to calibrate the chromatograph. These were: hydrazine, hydrazine plus 1%, 5%, and 10% water; and hydrazine plus 1%, 5%, and 10% ammonia.

(2) Apparatus

The cell used for electrolysis is shown in Fig. 40. It consists of two cells joined by a glass frit (Fig. 40, Item 5), each cell having a gas inlet (Fig. 40, Item 8) located at the bottom. A rubber septum (Fig. 40, Item 4) for taking liquid samples, a reference electrode (Fig. 40, Item 3) and a working electrode (Fig. 40, Item 2) are fitted into the three openings of each cell. Lines from anode and cathode compartments of the cell are connected to a chromatograph by means of a special

valving system. This sytem provides for gas samples to be taken from one compartment while the other compartment is being vented.

The gas chromatograph used in these tests (Fig. 41) was developed at United Aircraft Research Laboratories and consists of two adsorption columns connected in series. One column separates gaseous ammonia, water and hydrazine. The other column separates the permanent gases - H_2, N_2, and O_2.

The carrier gas used in this chromatograph is 91.5% He - 8.5% H_2 at a pressure of 50 psig and a flow rate of 170 cc/min. The carrier gas flows through a heat exchanger coil which serves to equilibrate its temperature with that of the hot-wire detectors before flowing through the reference chambers. From there the carrier gas flows through a heated inlet which is used to vaporize liquid samples and then through a 10cc sample loop section of an automatic gas sampling valve (Beckman 102396). The sample is swept through the first column held at a temperature of 110-115° C. At this temperature, H_2, N_2, and O_2 are not held back, while the other components, i.e., ammonia, water, and hydrazine, are separated in that order. Each component gives rise to a separate peak on the recorder corresponding to the output of the first detector.

After the gases have emerged from the sample side of the detector, they enter a second column which separates the H_2, O_2, and N_2 into its components at 30-32°C.

The oven (Fig. 41, Item 1) is a Blue-M model OV8A modified with a circulating fan and a themistor-Triac-IC temperature controller.

The control unit of the chromatograph (Fig. 41, Item 2) consists of a power supply and attenuators for the detector output. The recorder is a Hewlett-Packard Model 7100 B dual-pen strip chart recorder with built-in integrator.

A Kiethly Model 600 B vacuum tube volt meter is used to measure rest potential of the cell and operating potential during electrolysis. The power supply (Harrison Labs Model 6201 A) supplies a constant current to the cell in conjunction with a General Radio decade resistor.

(3) Procedure

Calibration curves for liquid and gas samples were obtained using standard solutions for liquid samples and flowmeter calibrations for gas samples.

For any liquid a one microliter sample was taken with a Hamilton microliter syringe and injected into the rubber septum of the heated inlet, the plunger depressed and withdrawn after five seconds. The peaks were recorded on the strip chart recorder, and peak heights or areas calculated. Gas samples consist of mixtures of either nitrogen or hydrogen and the helium-hydrogen carrier gas.

In taking a gas sample, the gas mixtures were passed through the cell valving system (Fig. 40, Item 1) and then through the 10cc sample loop section of the automatic gas sampling valve. The sample switch on the chromatograph control unit opens the sample loop to the chromatograph, peaks corresponding to nitrogen, hydrogen and ammonia are recorded, and areas and peak heights calculated. Calibration curves were constructed by plotting the known percent of water, ammonia, or the gases N_2 and H_2, versus peak height and peak area.

During actual test operations, each compartment of the cell was filled with 20 ml of 77% hydrazine - 23% hydrazine azide. The electrodes were set in place and lines were connected from the valving system to the cell.

First, a liquid blank sample was taken with the microliter syringe. The helium-hydrogen carrier gas was then bubbled through the cell in order to remove all air. Gas samples from the cathode compartment were taken by means of the automatic gas sampling valve until the nitrogen and oxygen peaks had gone down sufficiently to insure replicate runs. The last run before electrolysis was the cathode gas blank. Leads were then connected from the power supply and voltmeter to the electrodes, and rest voltages for anode and cathode were recorded. A current of 30 ma with a resistance of 200 Ω was set by means of the power supply. After the onset of electrolysis, gas samples from the cathode compartment were taken at 10 minutes, 25 minutes, and 40 minutes and from the anode compartment at 55 minutes, 70 minutes, and 85 minutes. Then, liquid samples were taken from anode and cathode compartments just prior to termination of electrolysis. Cell voltages during electrolysis were also recorded.

The percent of ammonia, nitrogen, and hydrogen for blank and electrolysis runs were determined from the calibration curves. From these results, the percent increase for each component was found and the total percent of ammonia, nitrogen and hydrogen produced was determined. This procedure was followed for each of the following electrodes: platinum, pyrolytic graphite rod, 304SS rod, and AM350 rod.

b. Results

The gas analysis and the polarization of each electrode couple are summarized in Tables XIII and XIV, respectively. The gas analyses show that the value for x using the equations derived earlier in this section is zero for 304SS, AM350, and pyrolytic graphite, and is unity for platinum. The relative proportions for H_2, N_2, and NH_3 (where applicable) are in good agreement with the values predicted using the above equations. Apparently platinum catlyzes the thermal decomposition of NH_3 while the remainder of the materials do not. The total overpotentials using identical materials for both anode and cathode indicate that platinum would be the best electrode material. If platinum were excluded, the best electrode couple would be pyrolytic graphite as an anode and 304SS as a cathode for a total cell voltage of 1.01v at 30 ma/cm^2. If platinum were used as a cathode with a pyrolytic graphite as an anode, the total polarization would be 0.97v. Since platinum yields only H_2 and N_2

at the cathode, and thus less heat would be released, it is recommended that the pyrolytic graphite - 304SS couple be used. This couple should give the most heat output for the least power input based on electrolytic decomposition only.

The faradaic efficiency for the decomposition of the 77% hydrazine - 23% hydrazine azide was calculated on the basis of the amount of ammonia produced during electrolysis for 304SS, AM350, and pyrolytic graphite. The calculations were based on ammonia, since it was determined that ammonia analyses were the most accurate obtained using the chromatograph. The increase of dissolved ammonia in the electrolyte (40cc) was used as the basis of the calculations, and the amount of ammonia expected per faraday of electricity passed was based on the postulated decomposition equations (i.e., one mole NH_3 per faraday).

The results are summarized in Table XV. It is obvious from this data that much more ammonia was produced than predicted from electrolysis alone. About thirty times the expected amount was produced on electrolysis using AM350 and pyrolytic graphite and almost ten times the amount expected using 304SS.

Apparently, the cathodic reaction is highly catalyzed on the surface of these materials at essentially room temperature. This effect is extremely encouraging, since it suggests that the power levels that may have to be used in the electrolytic cell will be much less than those predicted on the basis of electrolysis as the sole source of decomposition energy.

SECTION III

SUMMARY AND CONCLUSIONS

In the course of the work done on Phase I of Contract F04611-70-C-0070, experimental investigations have been carried out on candidate electrolytes (propellants) and electrodes to determine their usefulness in an electrolytic ignition system for millipound thrusters. The primary objective of Phase I was to select electrodes and an electrolyte suitable for this purpose.

Electrical conductivity data was obtained as a function of temperature between 25°C and 45°C, for propellant grade hydrazine, hydrazine-20% hydrazine nitrate, hydrazine-2% hydrazine azide, and hydrazine-23% hydrazine azide. This data was of primary importance since ohmic losses due to poor electrolyte (propellant) conductivity in the electrolytic cell will be one of the primary factors in its design.

Voltage losses due to slow electrochemical processes at the electrode-electrolyte interface will also effect the design and performance of the electrolytic ignition cell. For this reason polarization studies (measurements of voltage losses under conditions of current flow) were carried out on platinum, pyrolytic, and spectrographic graphite, three types of stainless steel; AM350, 17-7PH, and 304SS, two aluminum alloys, AA1100, and AA6061-T6; and a gold-nickel brazing alloy, HS1414. The electrolytes used in these studies include propellant grade hydrazine, hydrazine-5% hydrazine nitrate, and hydrazine-23% hydrazine azide.

Preliminary electrolysis experiments (at low currents) were carried out and an analysis made of the products of the electrolysis reaction. These experiments were designed to determine the theoretical heat output, as well as the efficiency of the electrolysis process. Hydrazine-hydrazine azide was the only electrolyte used in these studies.

The results of the conductivity studies showed that the addition of small amounts of hydrazine-based salts enhances the conductivity of propellant grade hydrazine by at least two orders of magnitude. Both 2% hydrazine nitrate and 2% hydrazine azide additions showed conductivities of 3.0×10^{-2} and 3.5×10^{-2} $ohms^{-1}$ cm^{-1} at 25°C compared to 1.6×10^{-4} $ohms^{-1}$ cm^{-1} for propellant grade hydrazine at the same temperature. The addition of 23% hydrazine azide yielded a conductivity value of 1.8×10^{-1} ohm^{-1} cm^{-1}, another factor of ten better than obtained with the low percentage additions.

The polarization results were evaluated in terms of both transient and steady state effects. The former studies were designed to determine if any films were formed on the surface of the electrodes that would impede or stop the electrochemical process. The cell used in the experimental apparatus was designed to eliminate any effects due to differences in the conductivities of the electrolytes

used. It was found that all electrodes were highly polarized in propellant grade hydrazine and that the aluminum alloys performed very poorly as anodes in all the electrolytes studied. Almost without exception the best performance of all electrodes, anodic or cathodic, was obtained using the 23% hydrazine azide solution.

In hydrazine-23% hydrazine azide, platinum was found to be the least polarized material, as both an anode and a cathode. However, pyrolytic graphite was found to behave in a similar manner to platinum as an anode.

The three stainless steels were found to be relatively poor anodes but good cathodes with some notable reservations. It was found that the anodic and cathodic behavior of 17-7PH was unpredictable and often indicated very high polarization, and that the same effect applied to the cathodic behavior of AM350, although not to as great an extent. 304SS was the only low cost cathodic material that indicated consistant performance.

Steady state experiments were designed to evaluate resistance effects not connected with electrolytic resistivity and to compare total voltage losses at a steady current input to the cell. In general, the steady state results confirmed those obtained in the transient studies. The only true electrode resistance effects obtained were found under conditions of cathodic polarization of 304SS.

The effect of hydrazine azide concentration was also studied in the range of 2 to 23 weight percent azide to determine whether there was an optimum concentration where minimum polarization would be realized. However, the lowest polarization was always found at the 23% hydrazine azide level. The polarizations of the stainless steels were found to be linear functions of azide concentration while the relationship between polarization and azide concentration for platinum and graphite was irregular.

The products of electrolysis of hydrazine-23% hydrazine azide were determined using platinum, pyrolytic graphite, AM350, and 304SS. In all cases nitrogen was the only anodic product. The cathodic products for graphite, AM350, and 304SS were ammonia, nitrogen, and hydrogen in proportions consistent with the reactions:

$$2N_2H_5^+ + 2e \rightarrow 2NH_3 + N_2 + 2H_2$$

indicating no ammonia decomposition, and thus producing the highest heat output possible for the reaction. The cathodic process on platinum yielded nitrogen and hydrogen only, indicating catalytic decomposition of ammonia on the platinum surface, and thus a lower heat output.

The amount of ammonia produced during electrolysis was found to be almost ten times that predicted from current measurements for 304SS and thirty times that predicted for AM350 and pyrolytic graphite. These results indicate a substantial catalytic effect at the electrode surface not connected with the actual power input.

The power input data for the cell indicates that the best electrode combination would be a pyrolytic graphite anode and a 304SS cathode if platinum were excluded as an electrode material.

On the basis of the above results, the following conclusions have been reached.

(1) Hydrazine-23% hydrazine azide is the best electrolyte studied.

(2) Either platinum or pyrolytic graphite should be used as the anode of the electrolytic cell.

(3) One of the stainless steels (AM350 or 304SS) should be used as the cathode for the cell, since:

a. both electrodes yield ammonia as a cathodic product and thus provide maximum heat output, and

b. their polarization characteristics as cathodes are similar to platinum in 23% hydrazine azide.

A choice between the two cannot be made without further experimentation, since AM350 yields better catalytic effects, but may be unreliable for repeated runs, while the opposite is true of 304SS.

(4) There is a definite catalytic effect during electrolysis (even at room temperature) which indicates that the decomposition may be self-sustaining at relatively low power inputs.

REFERENCES

1. Breen, B. P., M. Gerstein and M. A. McLain: Electrolytic Ignition System for Monopropellants. AFRPL-TR-69-247 Final Report, January 1970.

2. Andrieth, L. F. and B. A. Ogg: The Chemistry of Hydrazine. John Wiley & Sons, Inc., New York, 1951.

TABLE I

SPECIFIC CONDUCTANCE OF SELECTED HYDRAZINE-BASE PROPELLANTS

Sample	Temperature (°C)	Specific Conductance (OHM^{-1} CM^{-1})
Propellant Grade Hydrazine	25°	0.000163
" " "	35°	0.000260
" " "	45°	0.000477
98% N_2H_4 + 2% NH_4NO_3	25°	0.02861
" " "	35°	0.03038
" " "	45°	0.03201
77% N_2H_4 + 23% N_5H_5	25°	0.19711
" " "	35°	0.20022
" " "	45°	0.22191
98% N_2H_4 + 2% N_5H_5	25°	0.03124
" " "	35°	0.03562
" " "	45°	0.04086

TABLE II

ANODIC POLARIZATION IN HYDRAZINE-BASE PROPELLANTS AT 300°K

Material	Current density (ma/cm^2) at η = 1000 mv		
	N_2H_4 - 23% N_5H_5	N_2H_4 - 5% $N_2H_5NO_3$	N_2H_4
17-7PH	5.5	24	0.40
304SS	19	8.0	0.13
AM350	16	7.4	0.35
HS1414	120	70	1.2
Pt	150	35	1.0
C	66	24	0.28
AA1100	0.012	0.016	0.052
AA6061-T6	0.11	0.019	0.043

TABLE III

CATHODIC POLARIZATION IN HYDRAZINE-BASE PROPELLANTS AT 300°K

Material	Current density (ma/cm^2) at η = -1000 mv		
	N_2H_4 - 23% N_5H_5	N_2H_4 - 5% $N_2H_5NO_3$	N_2H_4
17-7PH	86	102	0.34
304SS	70	6.2	0.08
AM350	48	70	0.17
HS1414	125	103	0.19
Pt	95	33	0.19
C	32	16	0.56
AA1100	48	1.5	0.13
AA6061-T6	50	0.88	0.08

TABLE IV

COMPARISON OF ANODIC AND CATHODIC POLARIZATION OF STAINLESS STEELS IN 77% HYDRAZINE - 23% HYDRAZINE AZIDE

	Current Density (ma/cm^2) at $\eta = \pm 1000$ mv					
	304SS		AM350		17-7PH	
Material Condition	Anode	Cathode	Anode	Cathode	Anode	Cathode
Rod-Cleaned	18	85	17	88	44	78
Plate-Uncleaned	19	70	16	48	5.5	86
Plate-Cleaned	19	70	17	68	5.5	20

TABLE V

ANODIC POLARIZATION OF AM350, 304SS PYROLYTIC GRAPHITE AND PLATINUM AS A FUNCTION OF AZIDE CONCENTRATION

Current density (ma/cm^2) at $\eta = 1000$mv

% Azide	304SS	AM350	Pt	PyC
23	18	54	100	92
12	4.9	32	78	70
4.8	1.3	21	27	26

TABLE VI

CATHODIC POLARIZATION OF AM350, 304SS AND PLATINUM AS A FUNCTION OF AZIDE CONCENTRATION

Current density (ma/cm^2) at η = -1000 mv

% Azide	304SS	AM350	Pt
23	85	90	95
12	45	47	39
4.8	13	18	27

TABLE VII

COMPARISON OF ANODIC AND CATHODIC
POLARIZATION IN AZIDE AND NITRATE PROPELLANTS

Material	Current Density (ma/cm^2) at $\eta = \pm 1000$ mv			
	92.5% N_2H_4 - 4.8% N_5H_5		94% N_2H_4 - 6% $N_2H_5NO_3$	
	Anodic	Cathodic	Anodic	Cathodic
AM350	21	18	7.4	15
304SS	1.3	13	7.5	24
Pyrolytic Graphite	26	--	55	--
Platinum	27	28	24	23

TABLE VIII

ORDER OF CATHODIC POLARIZATION AT A CONSTANT CURRENT OF 50ma

N_2H_4 - 23% N_5H_5			N_2H_4 - 5% $N_2H_5NO_3$		
Material	c.d. (ma/cm2)	Total Polarization (mv/ma/cm2)	Material	c.d. (ma/cm2)	Total Polarization (mv/ma/cm2)
Pt	31.8	11.3	Pt	31.8	18.9
C	25.0	18.8	HS1414	22.6	23.9
304SS	20.0	19.0	304SS	20.0	24.0
AM350	20.0	19.0	C	25.0	27.2
HS1414	22.5	19.5	17-7PH	24.7	32.4
17-7PH	23.6	26.6	AM350	19.4	36.0
AA6061-T6	21.0	88	AA1100	15.8	177
AA1100	17.0	127	AA6061-T6	21.8	179

TABLE IX

ORDER OF ANODIC POLARIZATION AT A CONSTANT CURRENT OF 50ma

N_2H_4 - 23% N_5H_5			N_2H_4- 5% $N_2H_5NO_3$		
Material	c.d. (ma/cm2)	Total Polarization (mv/ma/cm2)	Material	c.d. (ma/cm2)	Total Polarization (mv/ma/cm2)
Pt	31.8	14.8	Pt	31.8	18.2
C	25.0	23.2	C	25.0	26.4
HS1414	22.5	24.1	HS1414	22.6	28.8
304SS	20.0	40.0	304SS	20.0	38.0
17-7PH	23.6	46.6	17-7PH	24.7	52.6
AM350	20.0	47.5	AM350	19.4	53.6
AA6061-T6	21.0	95	AA6061-T6	21.8	229
AA1100	17.0	135	AA1100	15.8	247

TABLE X

TOTAL OVERPOTENTIAL AT 50 ma/cm^2
IN 77% HYDRAZINE - 23% HYDRAZINE AZIDE

Anodic				Cathodic			
Material	η (mv)	IR (mv)	IR Free η (mv)	Material	η (mv)	IR (mv)	IR Free η (mf)
AM350	900	-		AM350	510	-	
	900	-			600	-	
	980	-					
	1200	-	with cathodic deposit		780	-	with anodic deposit
	1250	-					
Pryolytic Graphite	590	-		Pyrolytic Graphite	1200	-	
	~ 500	-			1600	-	
304SS	1500	-		304SS	800	320	480
	1550	-			800	320	480
17-7PH	1100	-		17-7PH	720	-	
	840	-					
	1120	-	with cathodic deposit				
Platinum	540	-		Platinum	800	-	
	560				680	-	

TABLE XI

POLARIZATION AS A FUNCTION OF AZIDE CONCENTRATION AT 50ma

mv/ma/cm^2

Cathodic

Material	23% Azide	12% Azide	4.8% Azide
Pt	12.6	16.0	24.8
Py C	--	--	45.6
304SS	17.0	24.8	35.2
AM350	19.1	21.6	26.4

Anodic

Material	23% Azide	12% Azide	4.8% Azide
Pt	21.5	22.8	35.2
Py C	15.8	27.2	21.2
304SS	51.8	50.0	57.5
AM350	37.0	30.0	41.5

TABLE XII

COMPARISON OF POLARIZATION IN HYDRAZINE-HYDRAZINE AZIDE AND HYDRAZINE-HYDRAZINE NITRATE AT A CONSTANT CURRENT OF 50ma

Cathodic

	4.8% Azide		6.0% Nitrate	
Material	η (mv)	mv/ma/cm^2	η (mv)	mv/ma/cm^2
Pt	620	24.8	540	21.6
PyC	1140	45.6	1550	62.0
304SS	880	35.2	920	36.8
AM350	660	26.4	720	28.8

Anodic

	4.8% Azide		6.0% Nitrate	
Material	η (mv)	mv/ma/cm^2	η (mv)	mv/ma/cm^2
Pt	880	35.2	350	14.0
PyC	530	21.2	1020	40.9
304SS	1440	57.5	1550	62.0
AM350	1040	41.5	1050	42.0

TABLE XIII

ELECTROLYSIS OF HYDRAZINE AZIDE-GAS ANALYSIS

	Electrode	Electrolyte	% NH_3 Produced	% H_2 Produced	% N_2 Produced	% NH_3 Decomposed
Anodic	Pyrolytic graphite	77% N_2H_4 23% N_5H_5	0	0	100	
	304SS	77% N_2H_4 23% N_5H_5	0	0	100	
	AM350	77% N_2H_4 23% N_5H_5	0	0	100	
	Platinum	77% N_2H_4 23% N_5H_5	0	0	100	
Cathodic	Pyrolytic graphite	77% N_2H_4 23% N_5H_5	42	41	17	0
	304SS	77% N_2H_4 23% N_5H_5	44	31	25	0
	AM350	77% N_2H_4 23% N_5H_5	50	36	14	0
	Platinum	77% N_2H_4 23% N_5H_5	0	75	25	100
	Theoretical - No NH_3 decomposed		40	40	20	
	Theoretical - NH_3 decomposed		0	70	30	

TABLE XIV

POLARIZATION DATA
ELECTROLYSIS CELL

Electrode		Rest Voltage	Current	Power Supply Voltage	Resistance	Electrolysis Voltage	η	Total Cell η
AM350	Anodic	+ 0.94 v	30 ma	15 v	200 Ω	- 0.36 v	+1300 mv	2.00 v
AM350	Cathodic	+ 0.95 v	30 ma	15 v	200 Ω	+ 1.65 v	- 700 mv	
Pyrolytic graphite	Anodic	+ 0.69 v	30 ma	15.8 v	200 Ω	+ 0.20 v	+ 490 mv	1.51 v
Pyrolytic graphite	Cathodic	+ 0.70 v	30 ma	15.8 v	200 Ω	+ 1.72 v	-1020 mv	
304SS	Anodic	+ 1.02 v	30 ma	15 v	200 Ω	- 0.16 v	+1180 mv	1.70 v
304SS	Cathodic	+ 1.03 v	30 ma	15 v	200 Ω	+ 1.55 v	- 520 mv	
Platinum	Anodic	+ 0.98 v	30 ma	17 v	200 Ω	+ 0.30 v	+ 680 mv	1.46 v
Platinum	Cathodic	+ 0.98 v	30 ma	15 v	200 Ω	+ 1.46 v	- 480 mv	

TABLE XV

FARADAIC EFFICIENCY FOR ELECTROLYSIS
OF 77% HYDRAZINE-23% HYDRAZINE AZIDE

Material	Faradays	Moles NH_3 (Theoretical)	Moles NH_3 (Experimental)
304SS	2.52×10^{-3}	2.52×10^{-3}	2.12×10^{-2}
AM350	1.02×10^{-3}	1.02×10^{-3}	5.18×10^{-2}
PyC	1.68×10^{-3}	1.68×10^{-3}	3.06×10^{-2}

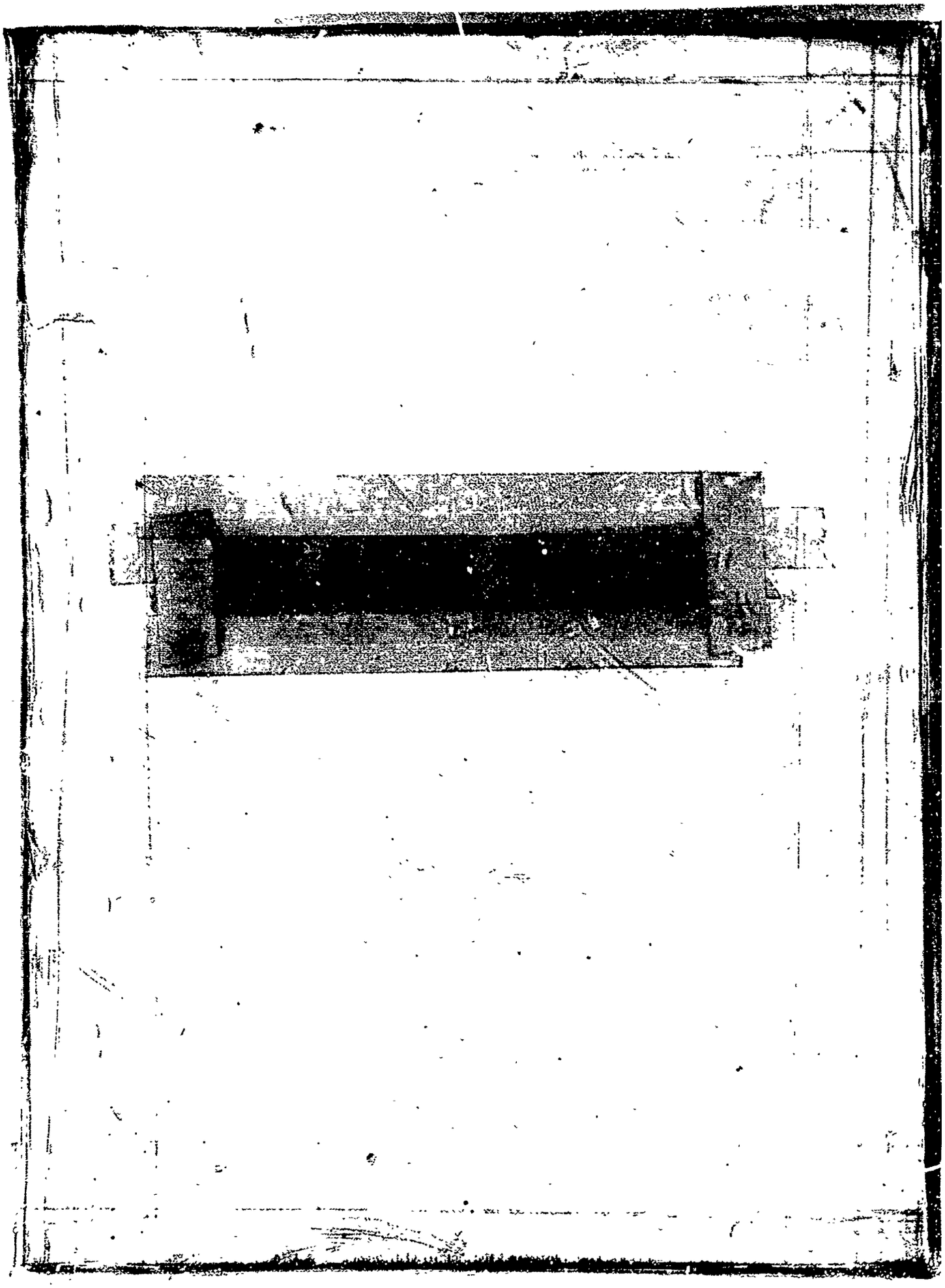

FIG. 1

ELECTRODE POLARIZATION APPARATUS

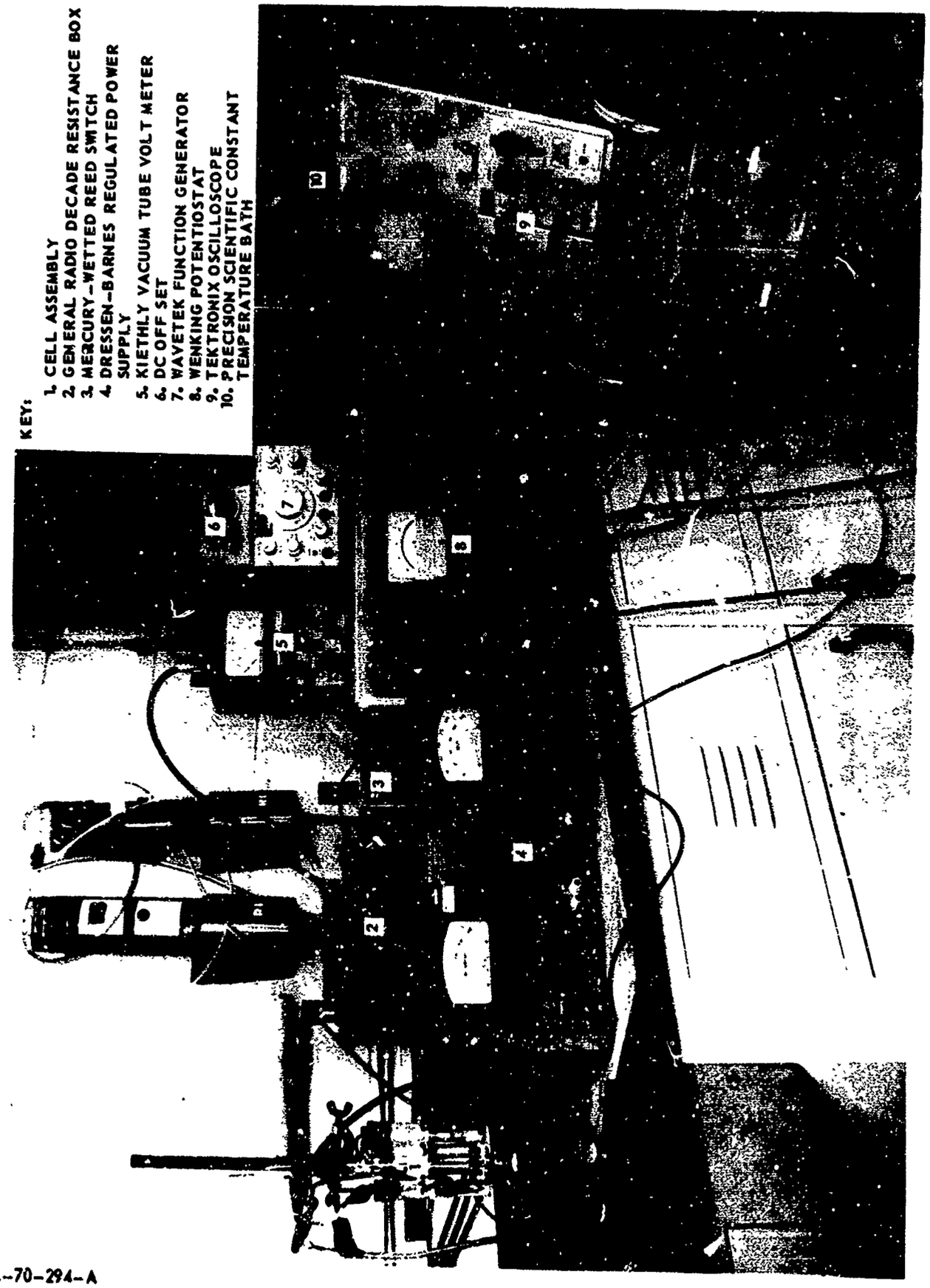

RI.-70-294-A

ANODIC POLARIZATION OF 17-7 PH IN HYDRAZINE-BASE PROPELLANTS

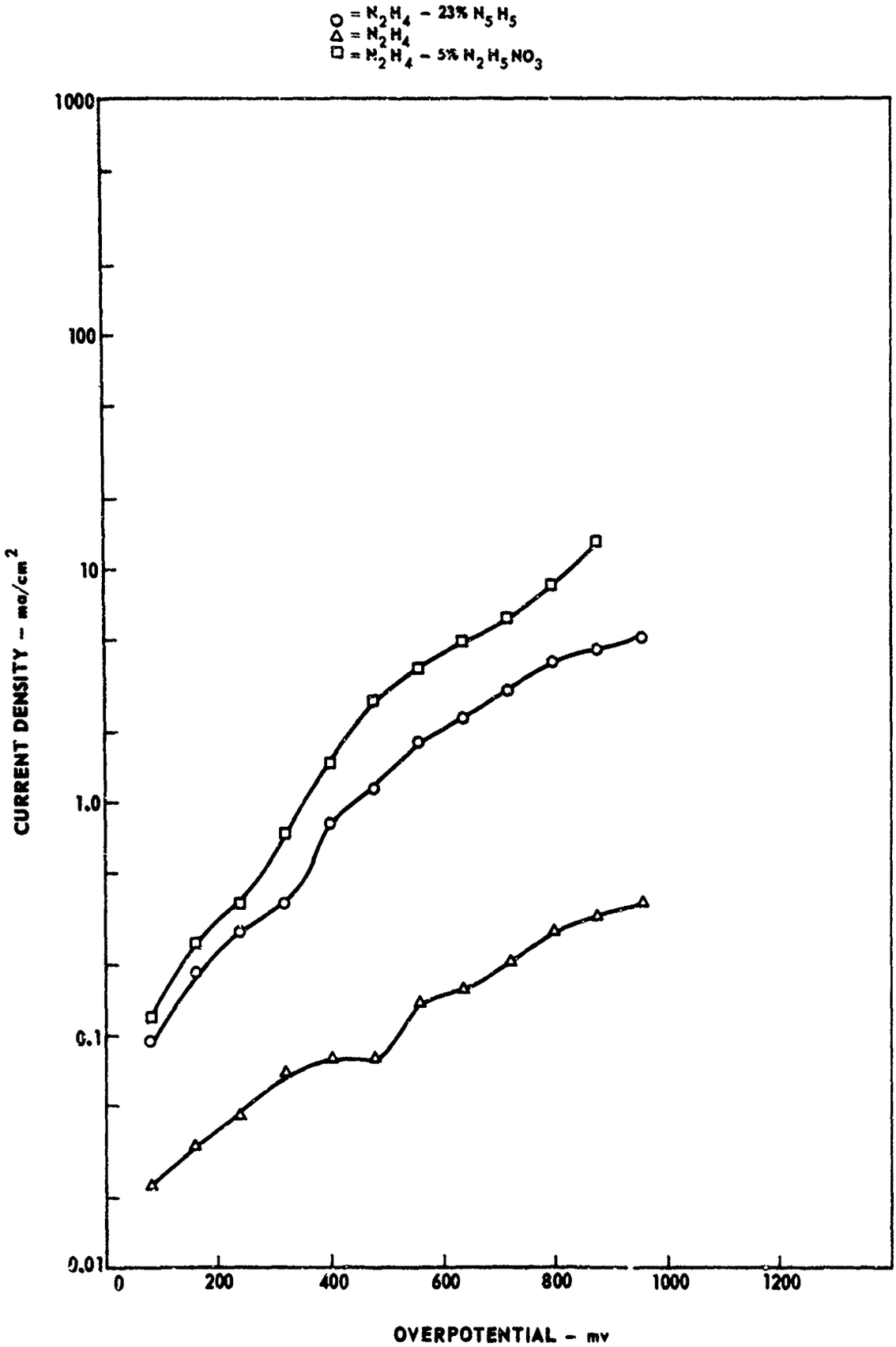

ANODIC POLARIZATION OF 304SS IN HYDRAZINE-BASE PROPELLANTS

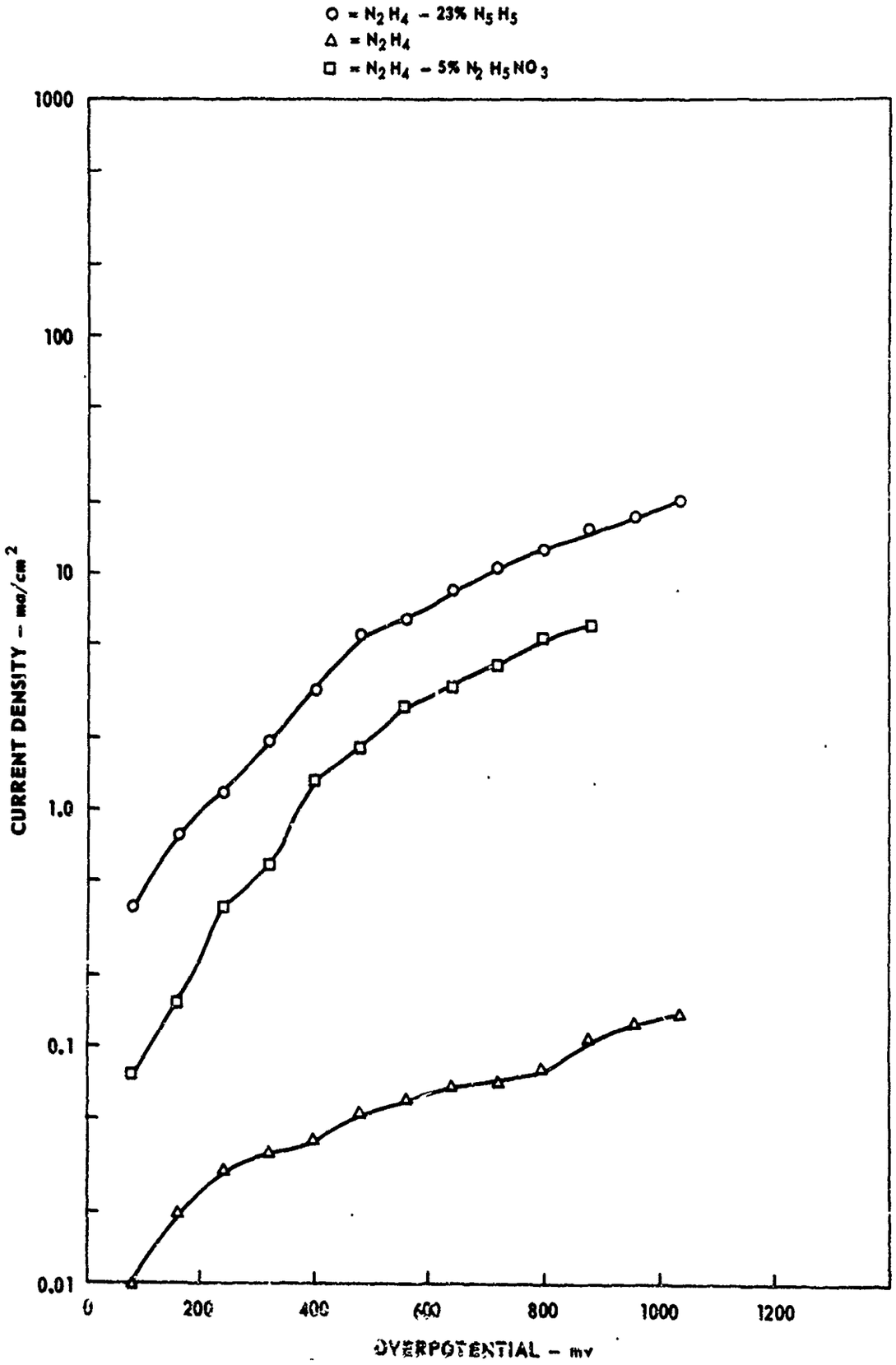

FIG. 4

ANODIC POLARIZATION OF AM 350 IN HYDRAZINE-BASE PROPELLANTS

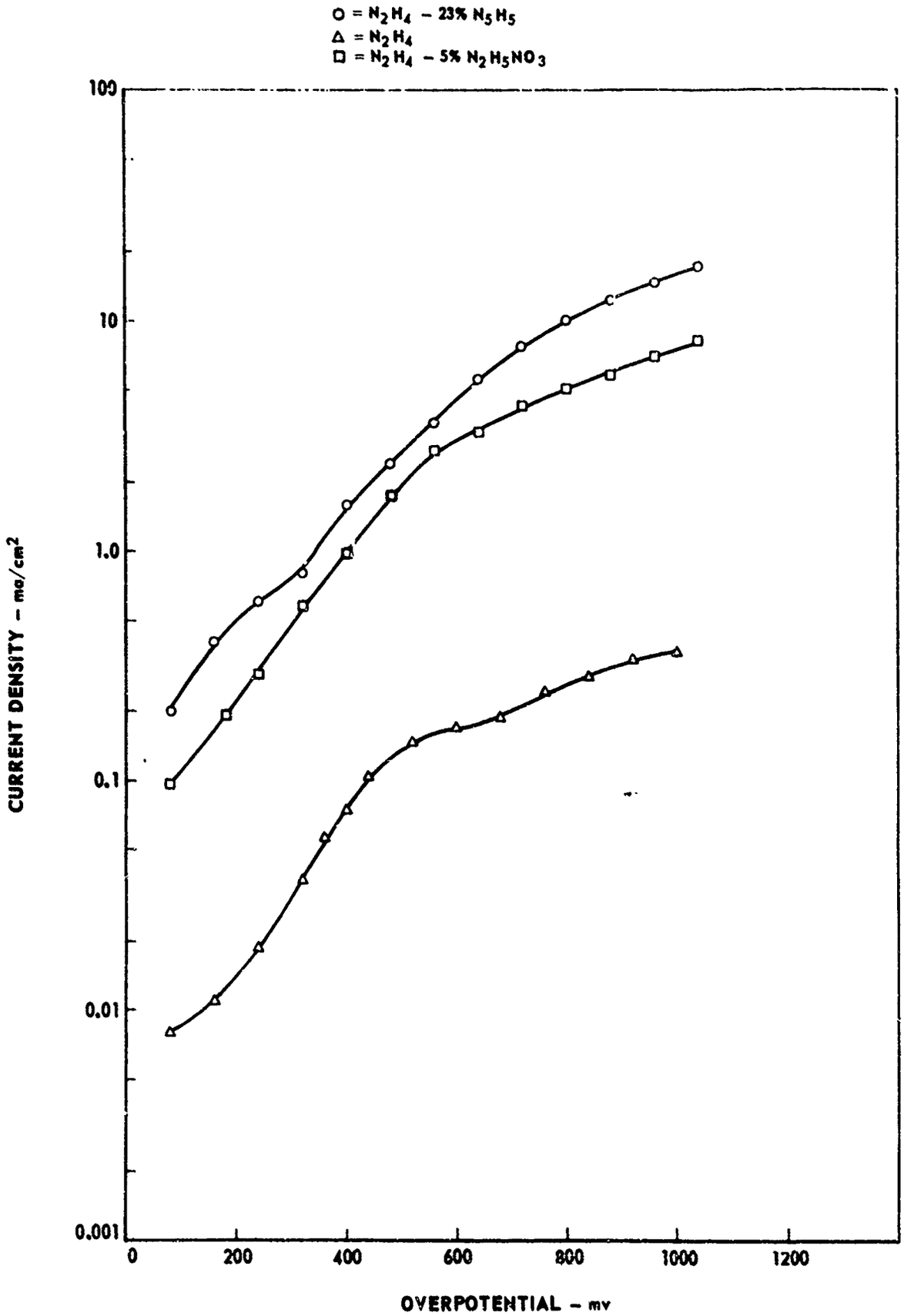

ANODIC POLARIZATION OF HS 1414 IN HYDRAZINE-BASE PROPELLANTS

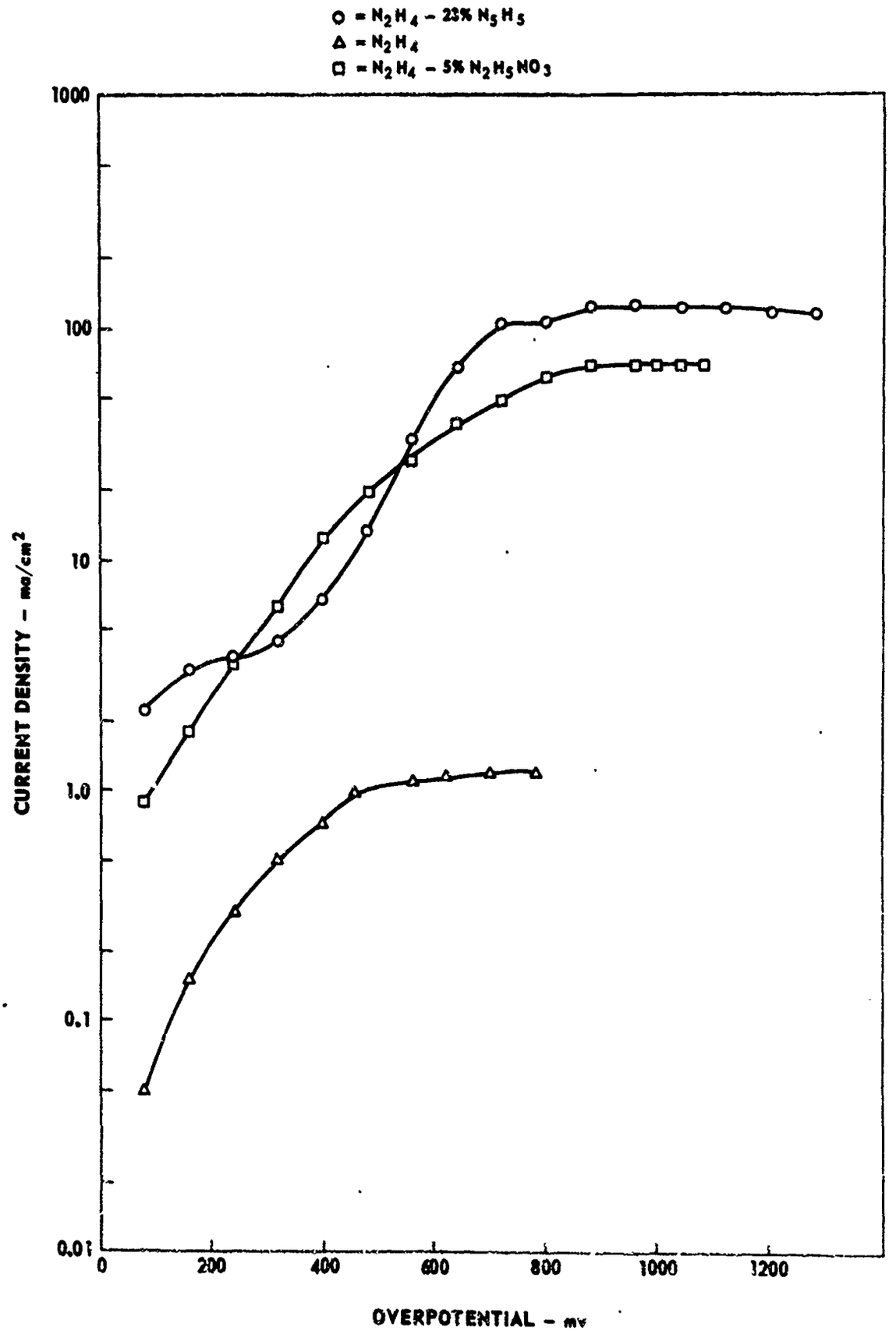

FIG. 6

ANODIC POLARIZATION OF PLATINUM IN HYDRAZINE-BASE PROPELLANTS

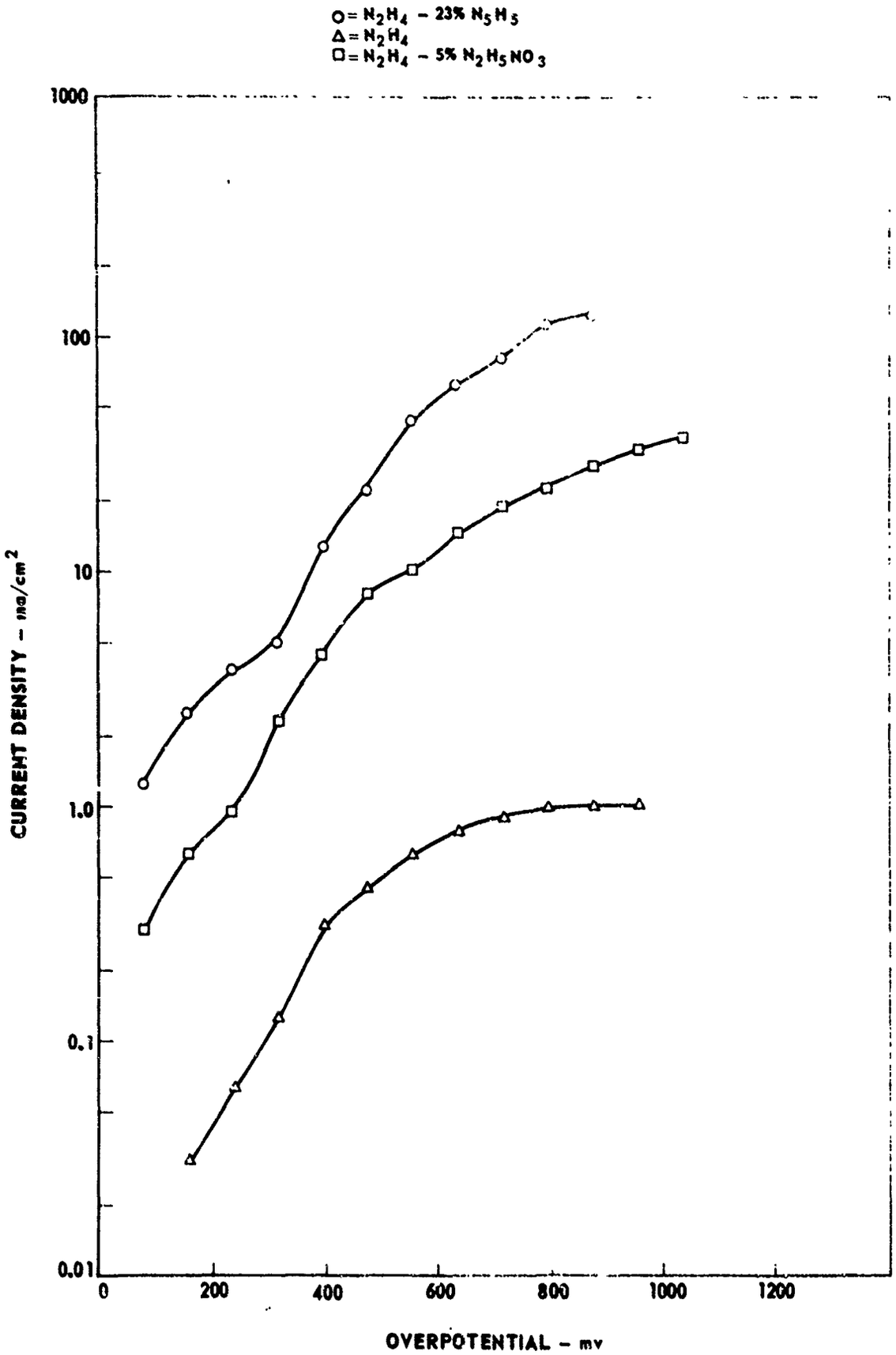

FIG. 7

ANODIC POLARIZATION OF GRAPHITE IN HYDRAZINE-BASE PROPELLANTS

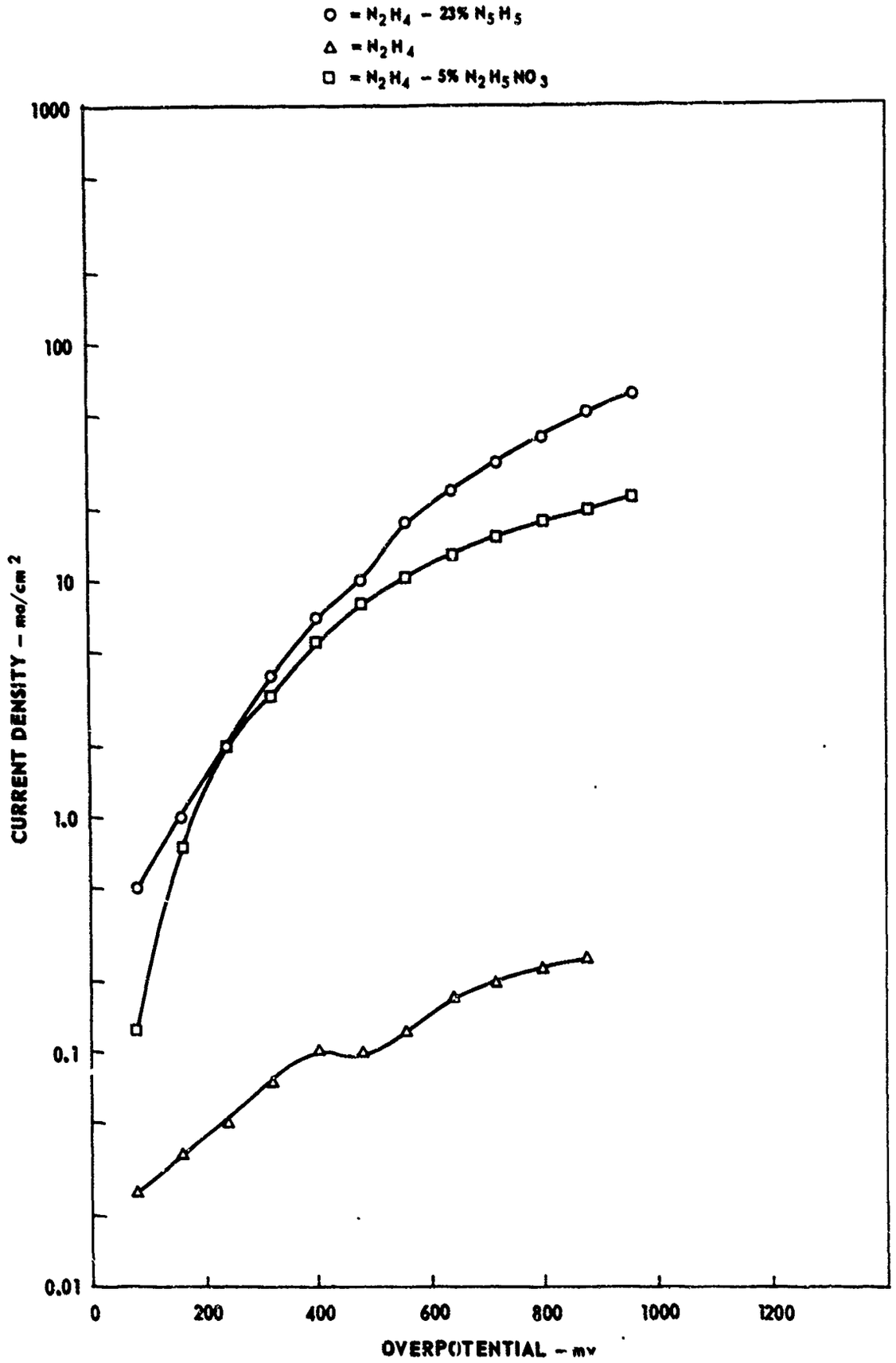

FIG. 8

ANODIC POLARIZATION OF AA 1100 IN HYDRAZINE-BASE PROPELLANTS

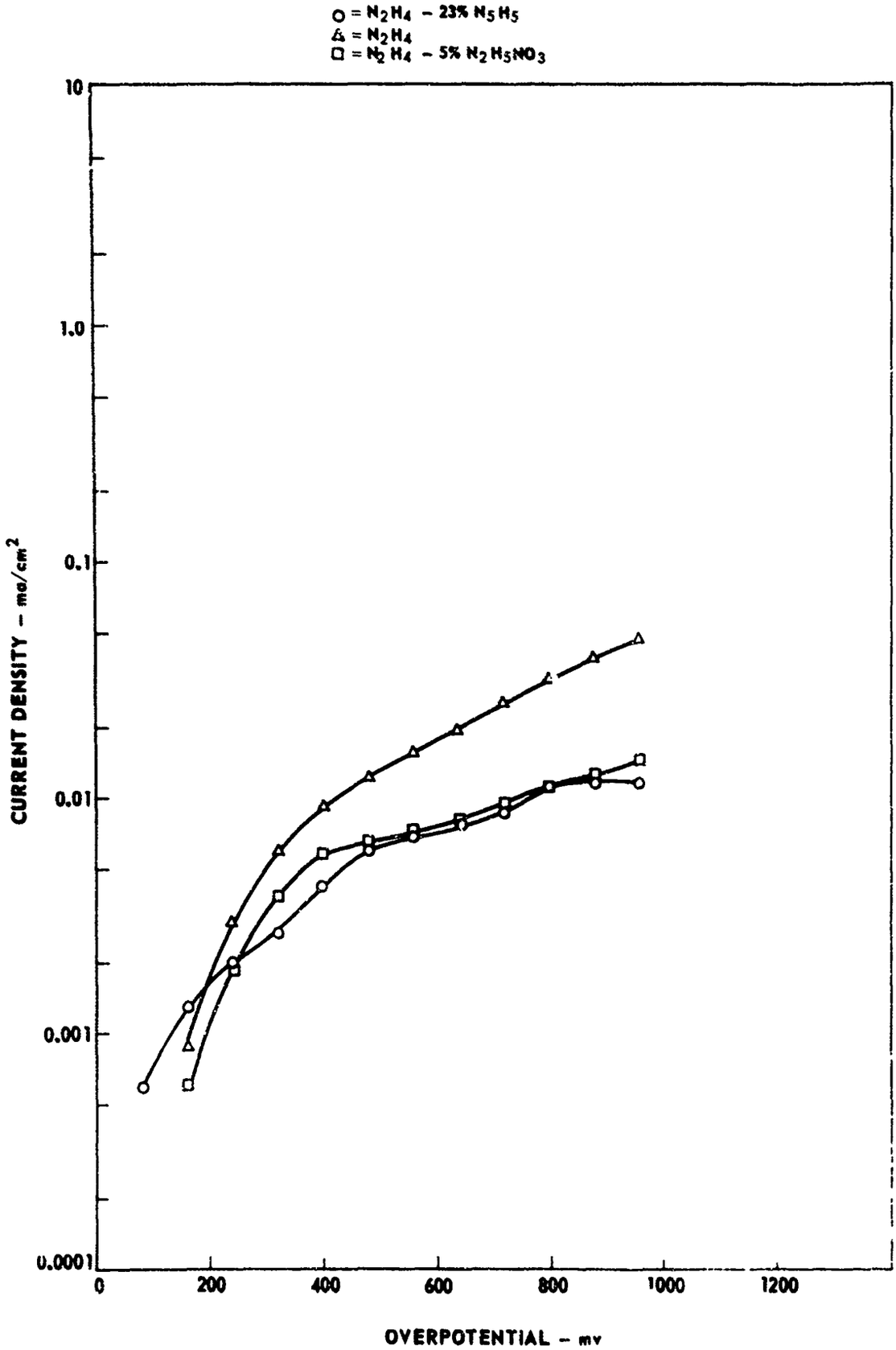

FIG. 9

ANODIC POLARIZATION OF AA 6061-T6 IN HYDRAZINE-BASE PROPELLANTS

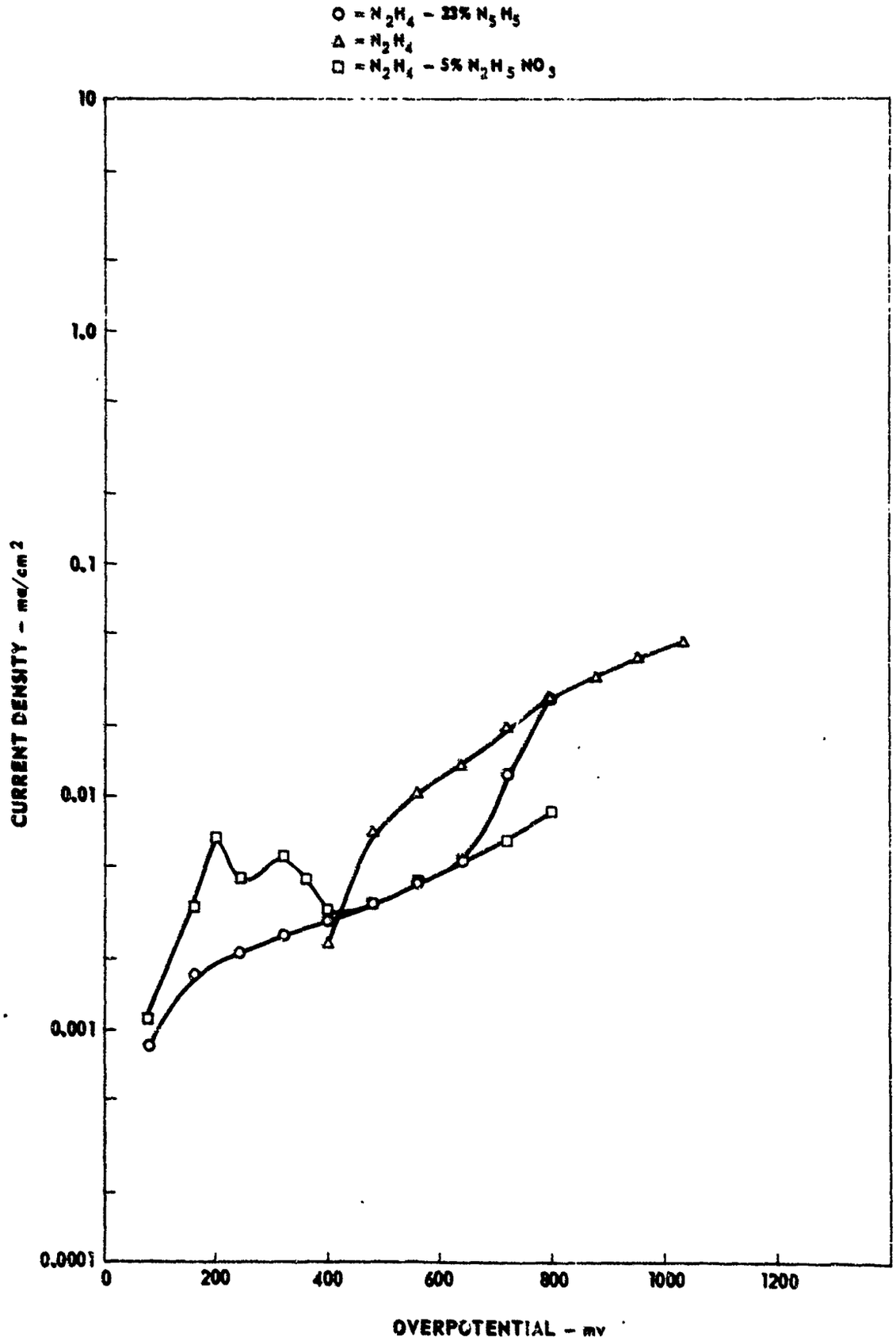

FIG. 10

CATHODIC POLARIZATION OF 17-7 PH IN HYDRAZINE-BASE PROPELLANTS

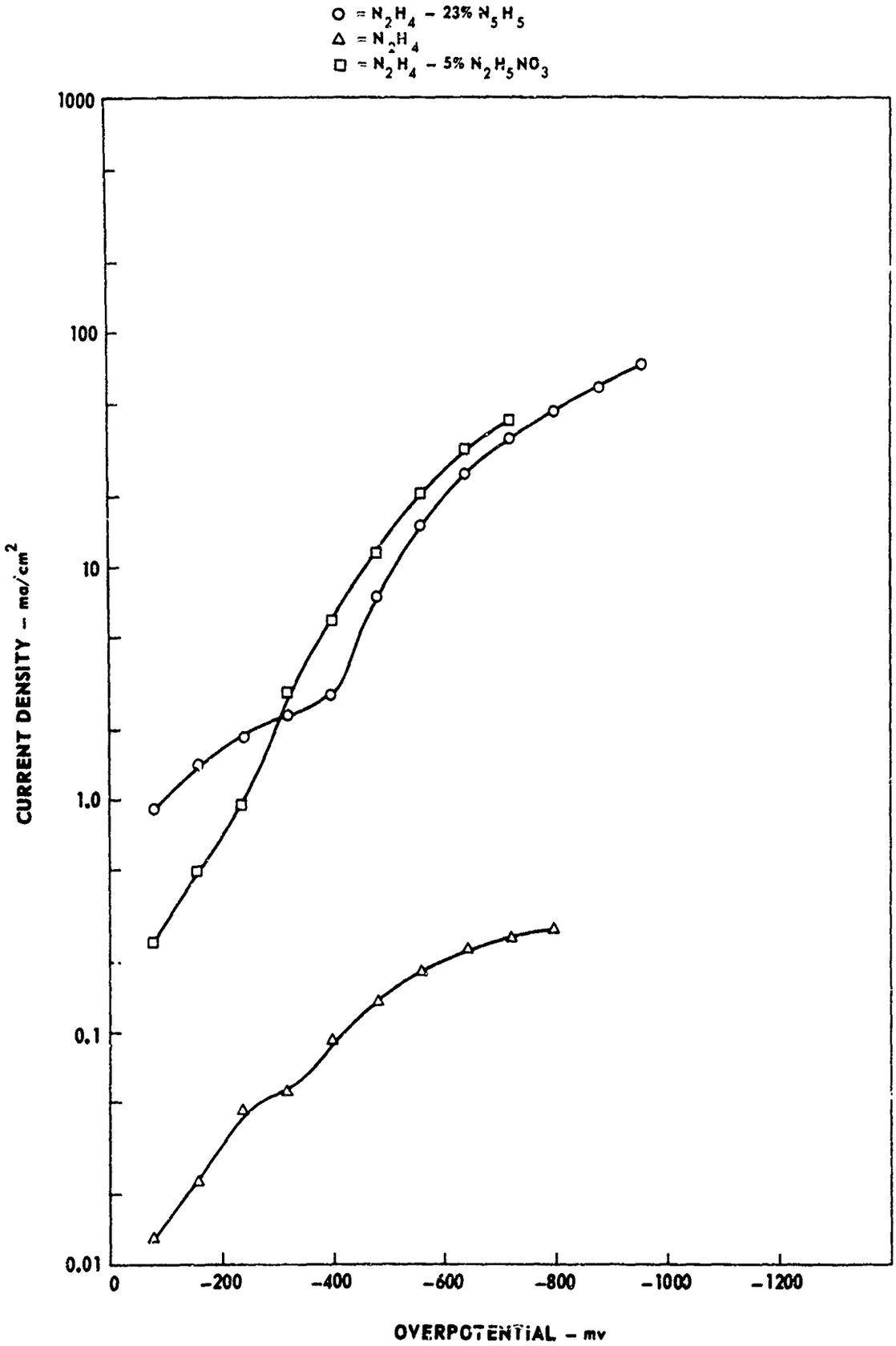

FIG. 11

CATHODIC POLARIZATION OF 304 SS IN HYDRAZINE-BASE PROPELLANTS

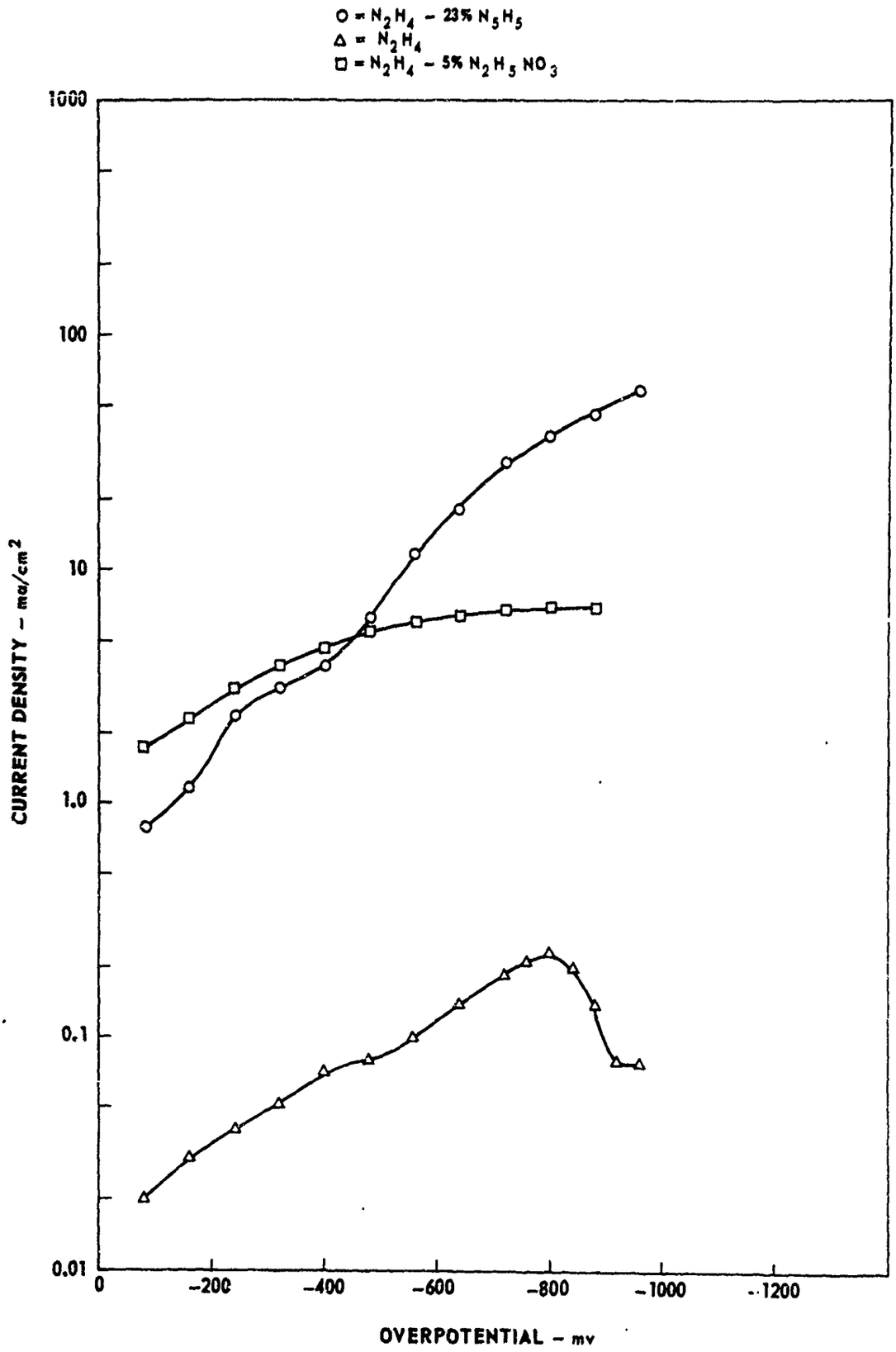

CATHODIC POLARIZATION OF AM 350 IN HYDRAZINE-BASE PROPELLANTS

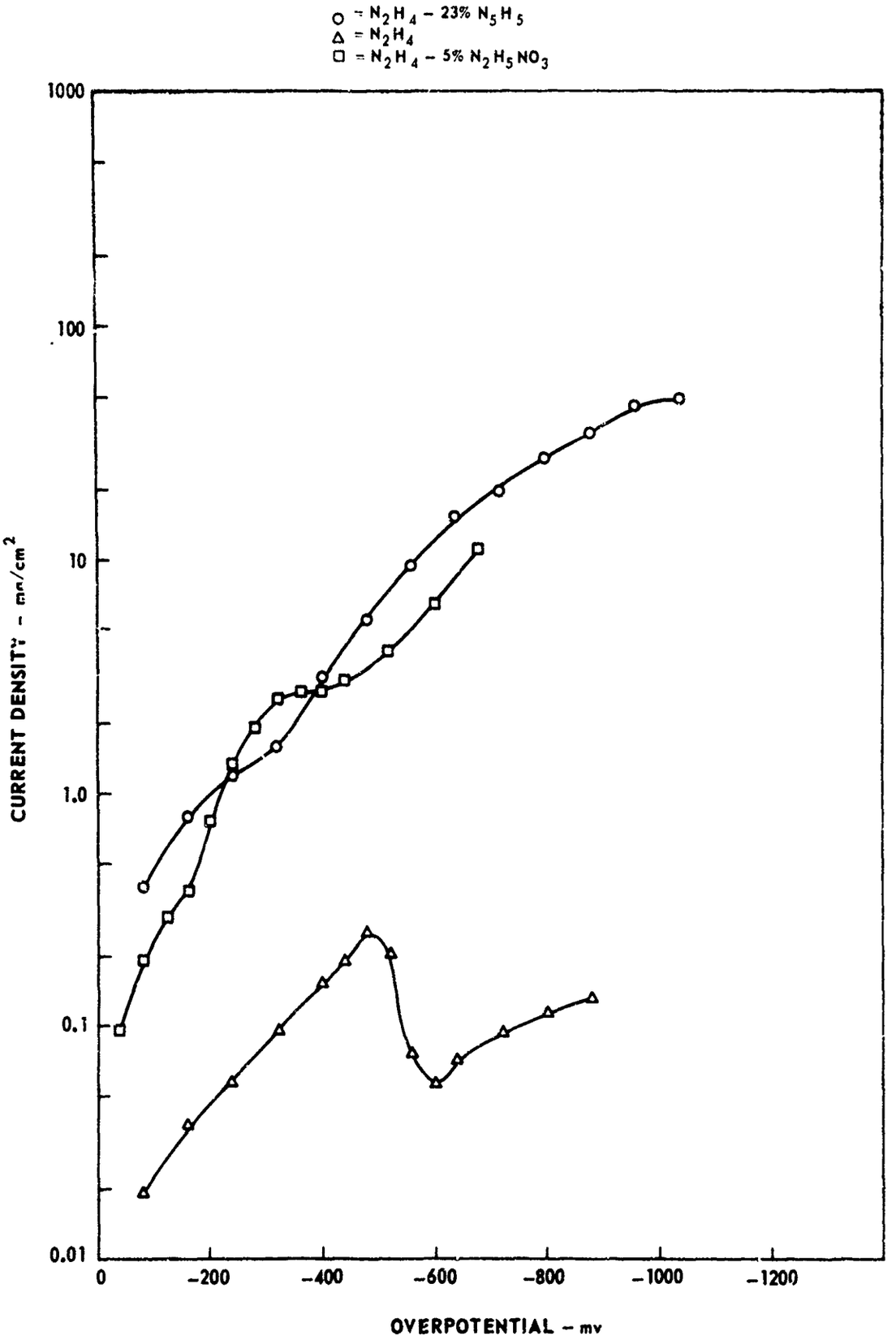

CATHODIC POLARIZATION OF HS 1414 IN HYDRAZINE-BASE PROPELLANTS

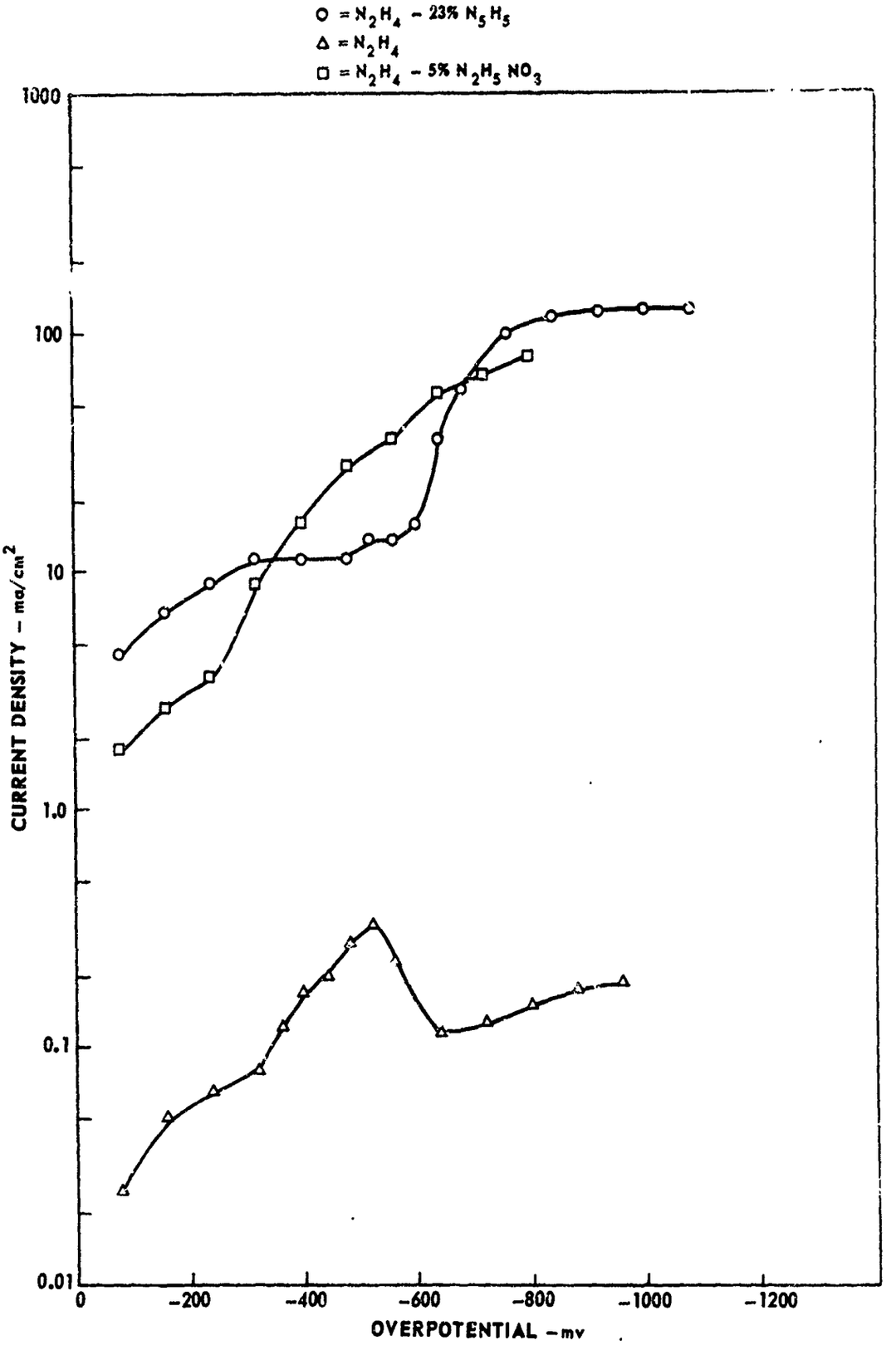

FIG. 14

CATHODIC POLARIZATION OF PLATINUM IN HYDRAZINE-BASE PROPELLANTS

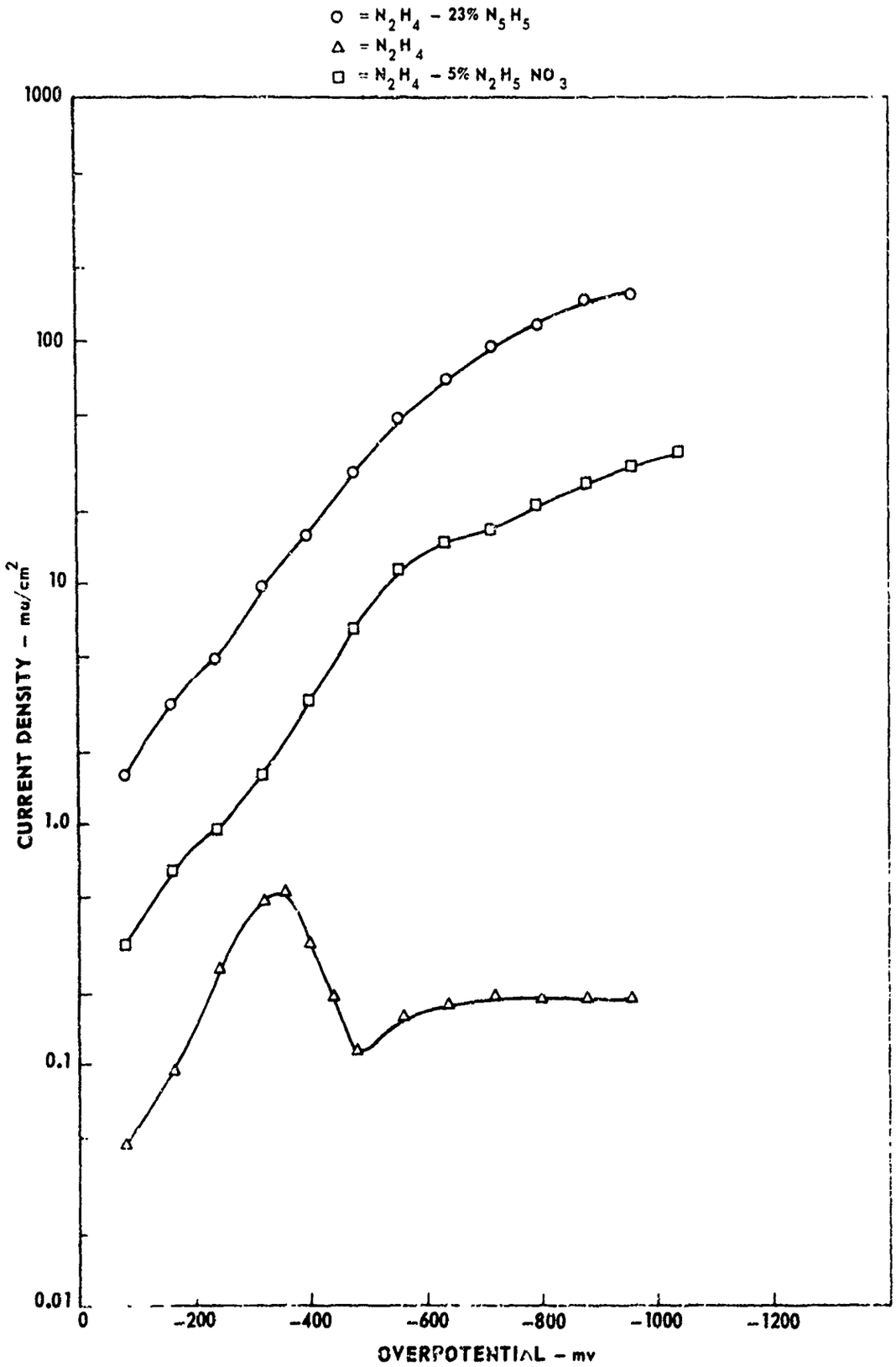

FIG. 15

CATHODIC POLARIZATION OF GRAPHITE IN HYDRAZINE-BASE PROPELLANTS

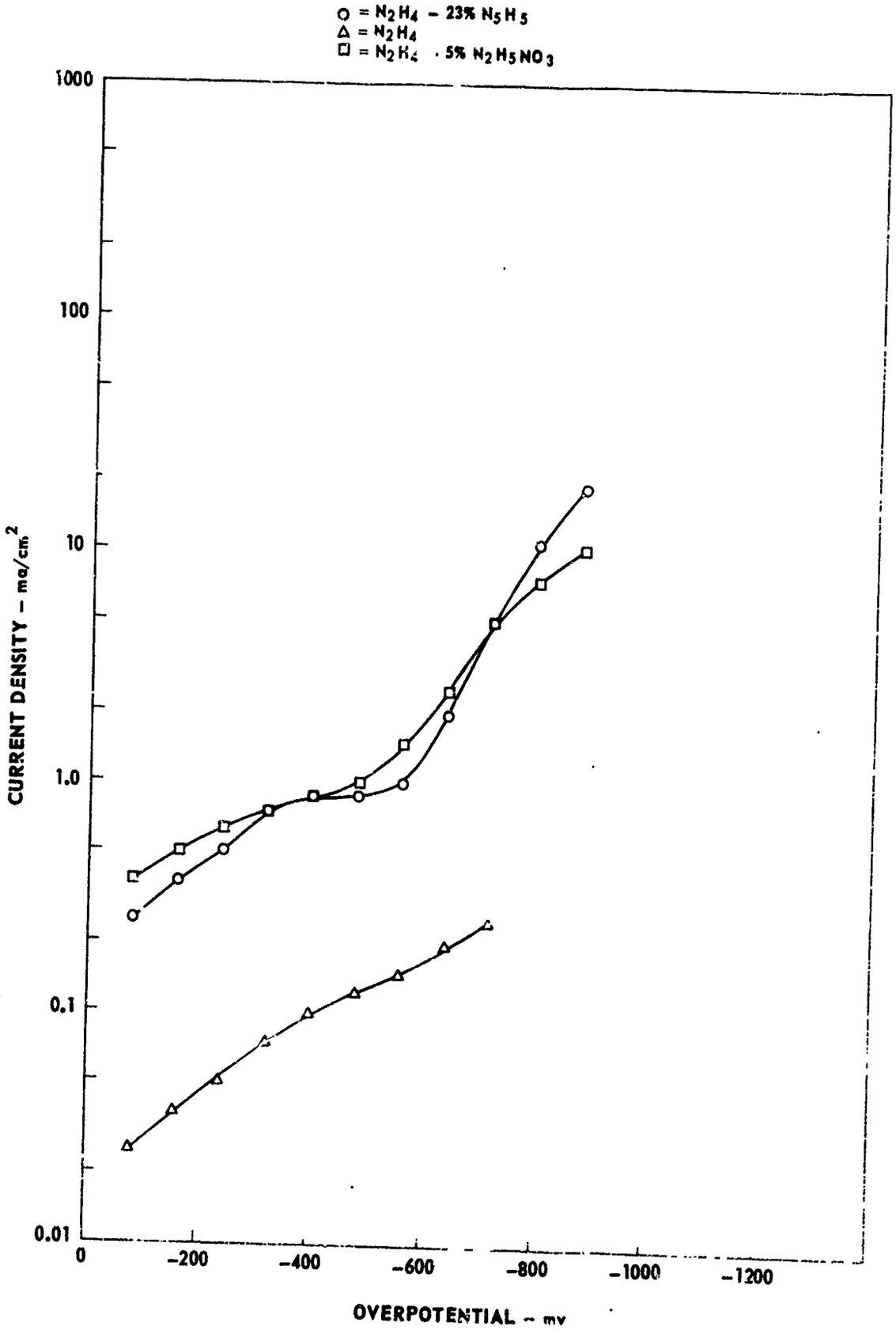

FIG. 16

CATHODIC POLARIZATION OF AA 1100 IN HYDRAZINE-BASE PROPELLANTS

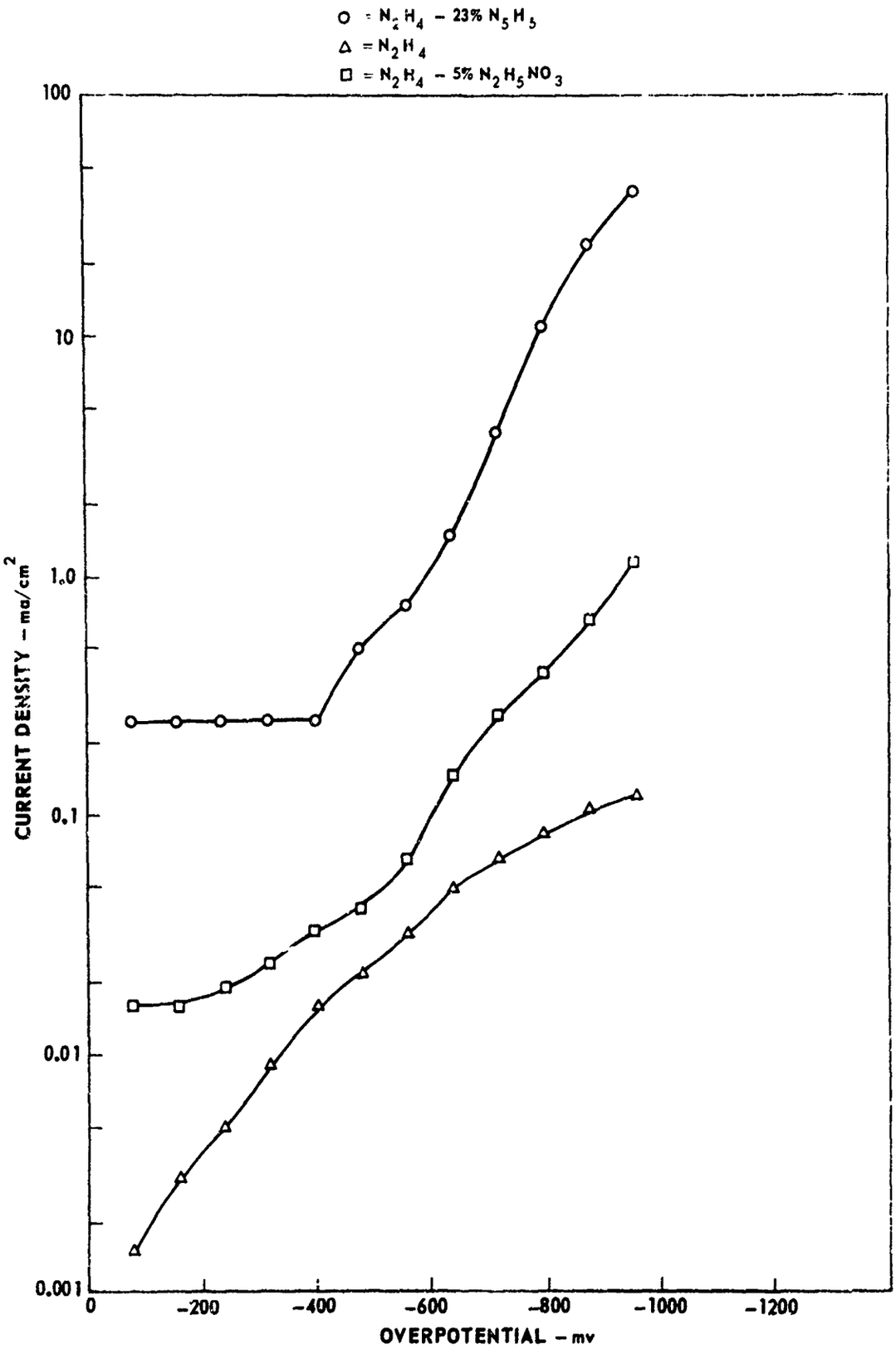

CATHODIC POLARIZATION OF AA6061-T6 IN HYDRAZINE-BASE PROPELLANTS

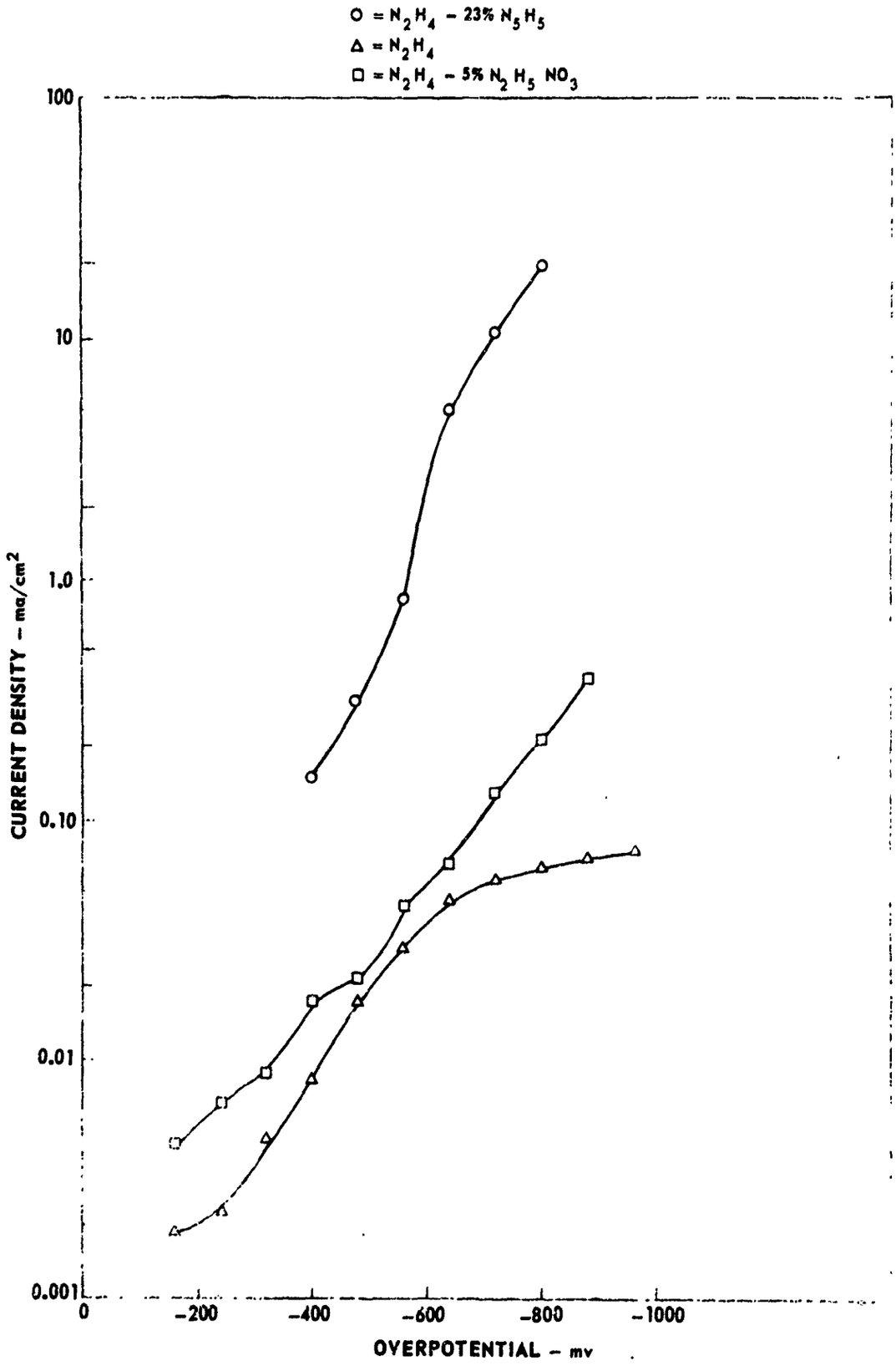

FIG. 18

ANODIC POLARIZATION OF 17 - 7 PH
IN 77% HYDRAZINE-23% HYDRAZINE AZIDE

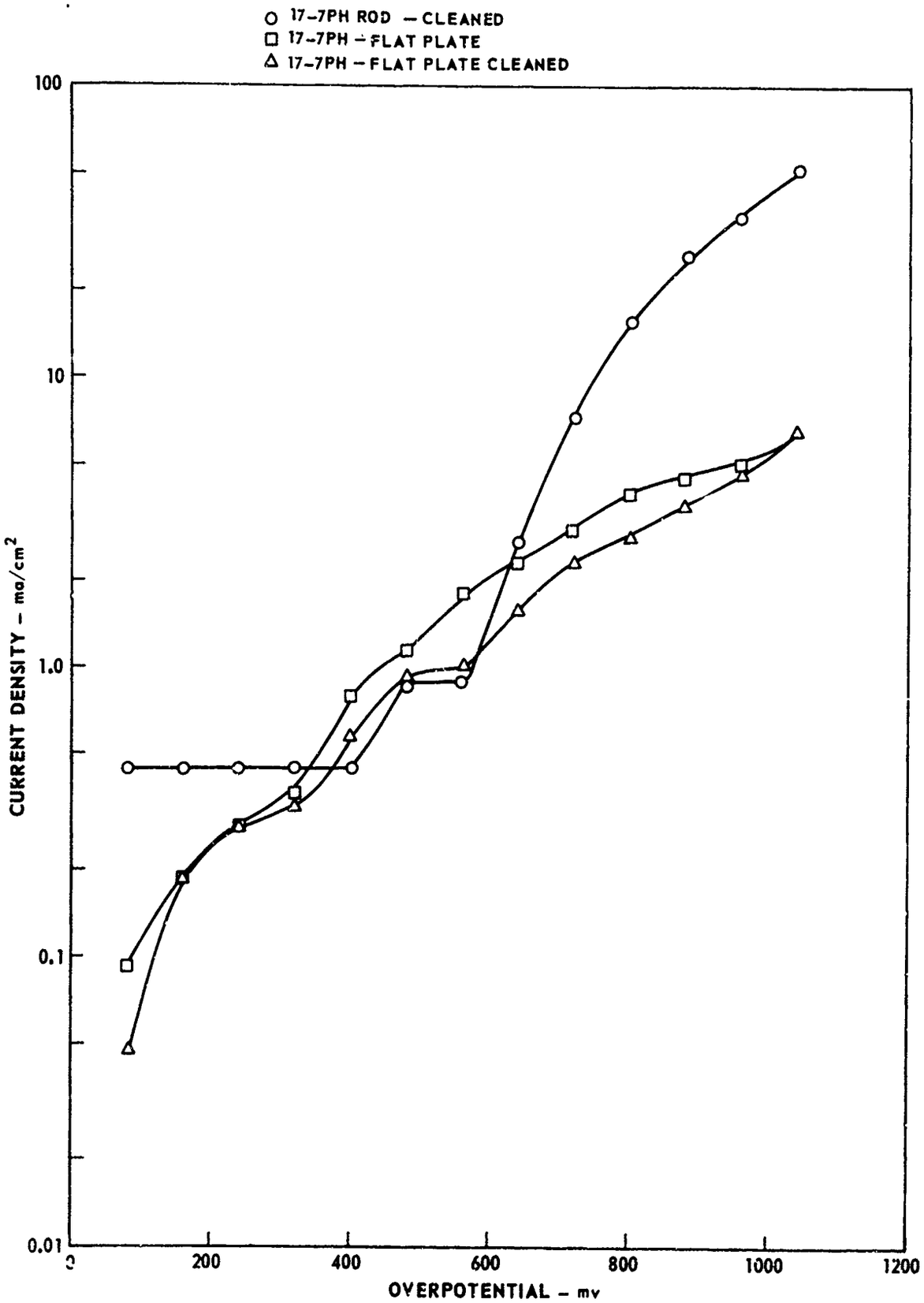

CATHODIC POLARIZATION OF AM 350
IN 77% HYDRAZINE-23% HYDRAZINE AZIDE

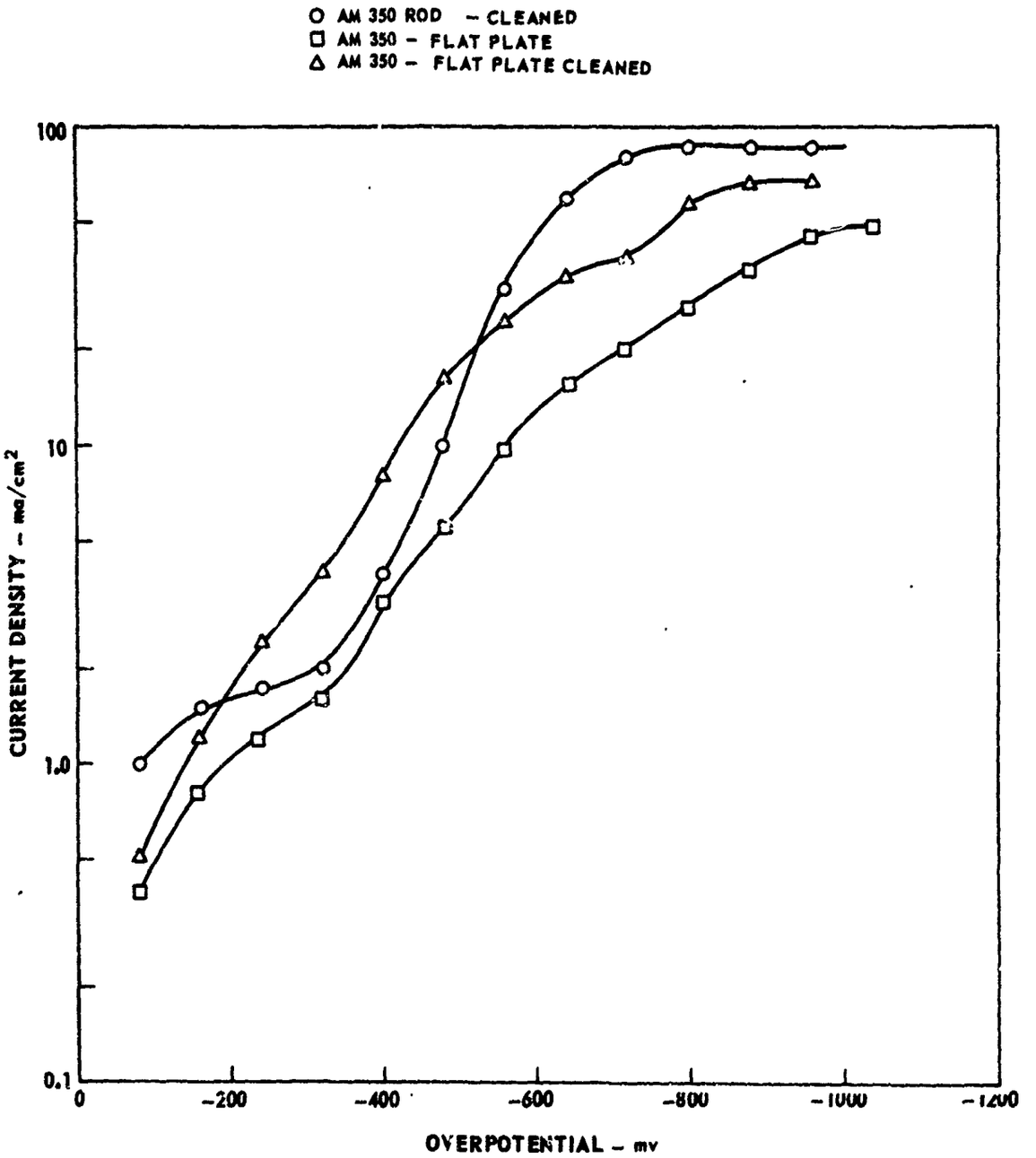

ANODIC POLARIZATION OF AM350 IN 77% HYDRAZINE – 23% HYDRAZINE AZIDE AND 88% HYDRAZINE – 12% HYDRAZINE AZIDE

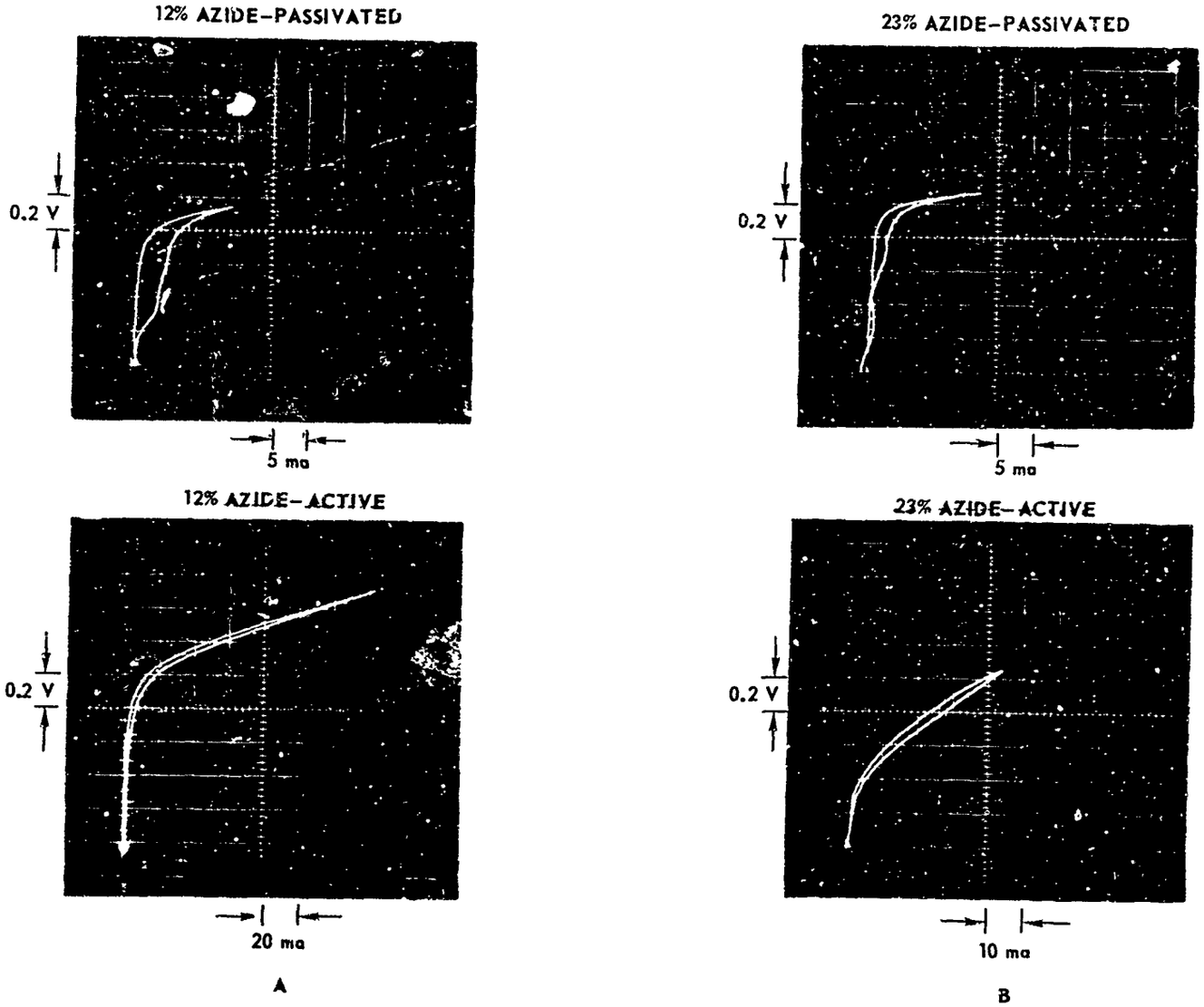

A B

FIG. 20

ANODIC POLARIZATION OF GRAPHITE IN 77% HYDRAZINE-23% HYDRAZINE AZIDE

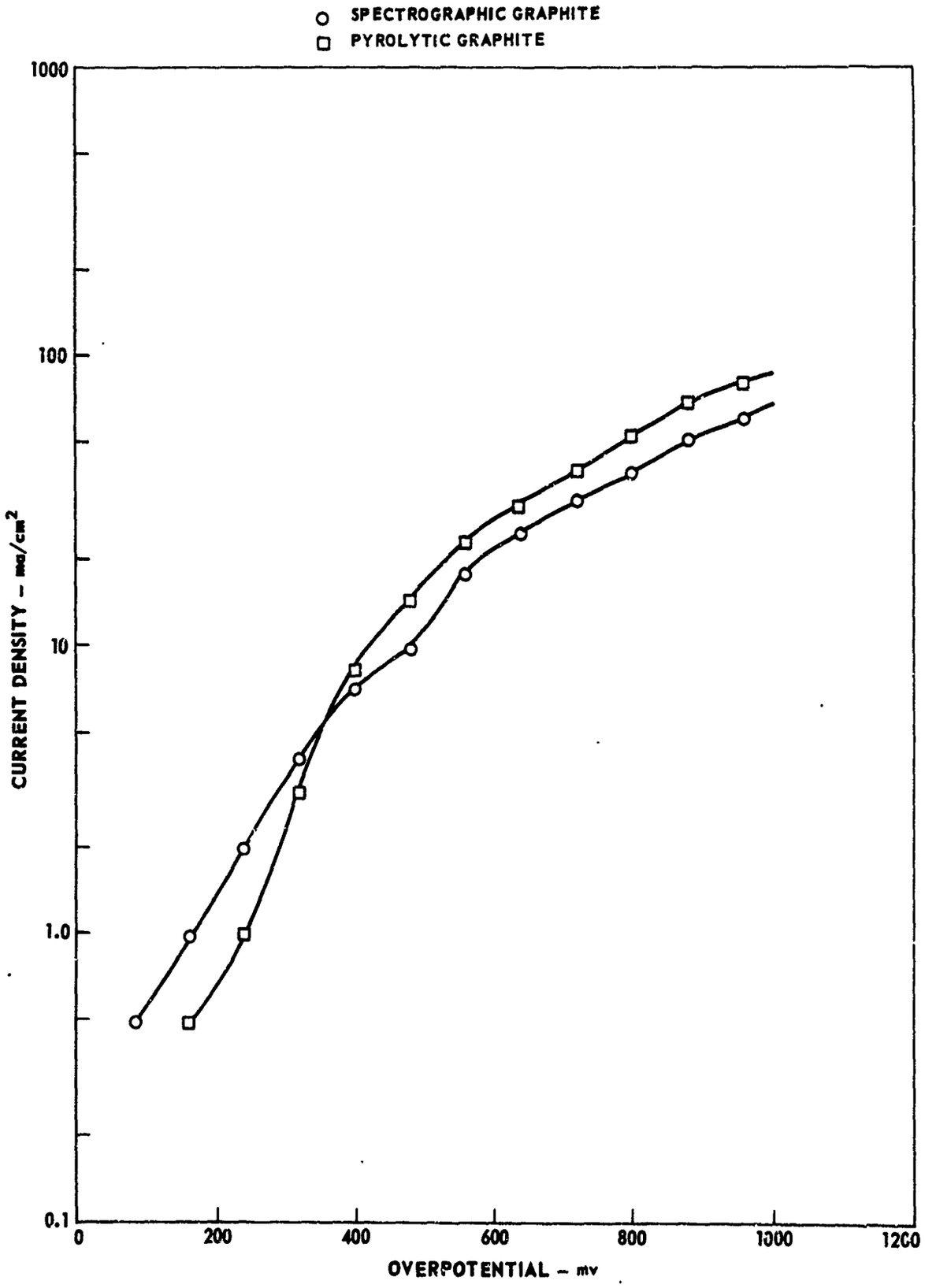

CATHODIC POLARIZATION OF GRAPHITE IN 77% HYDRAZINE-23% HYDRAZINE AZIDE

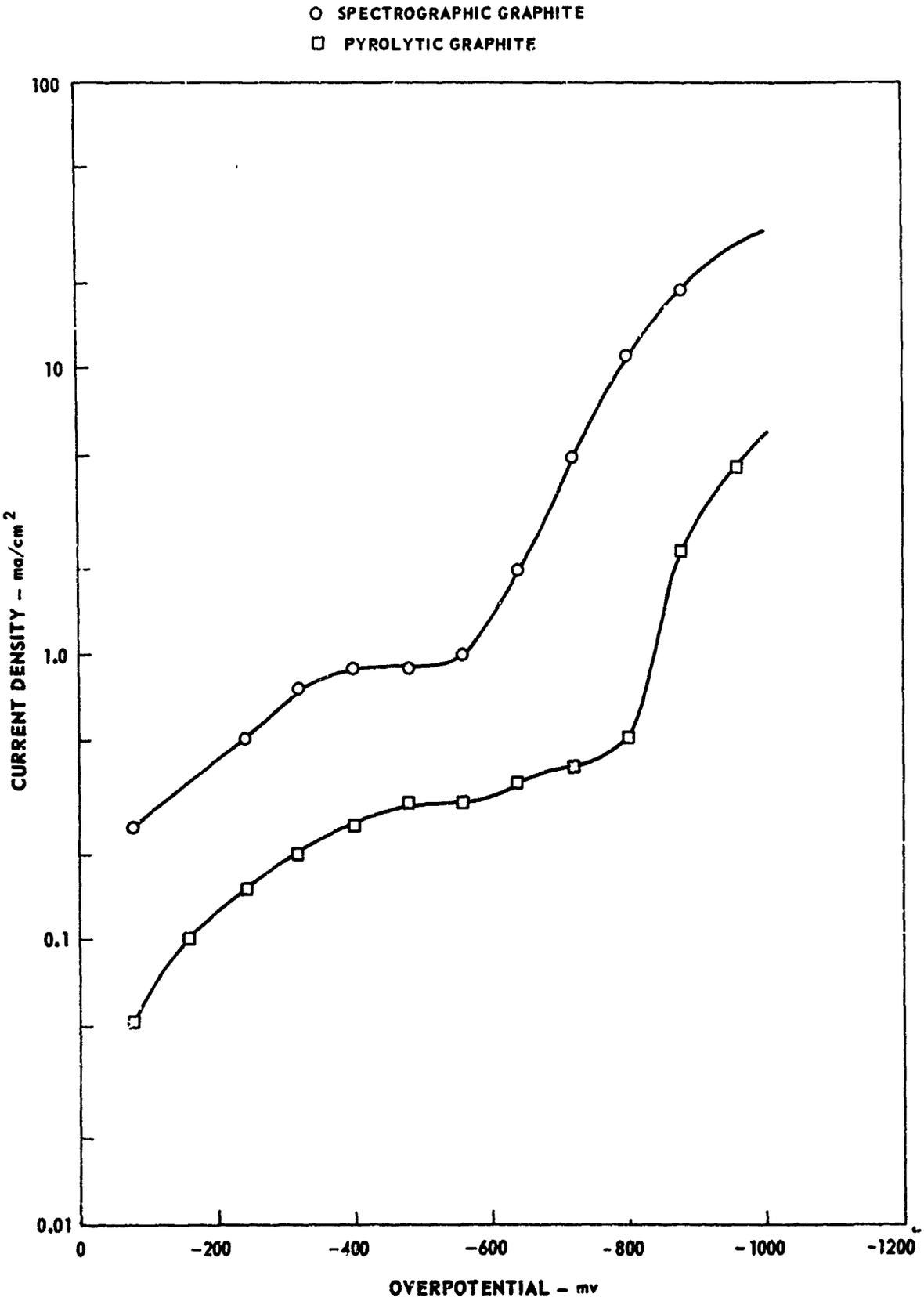

ANODIC POLARIZATION OF 304 SS AS A FUNCTION OF AZIDE CONCENTRATION

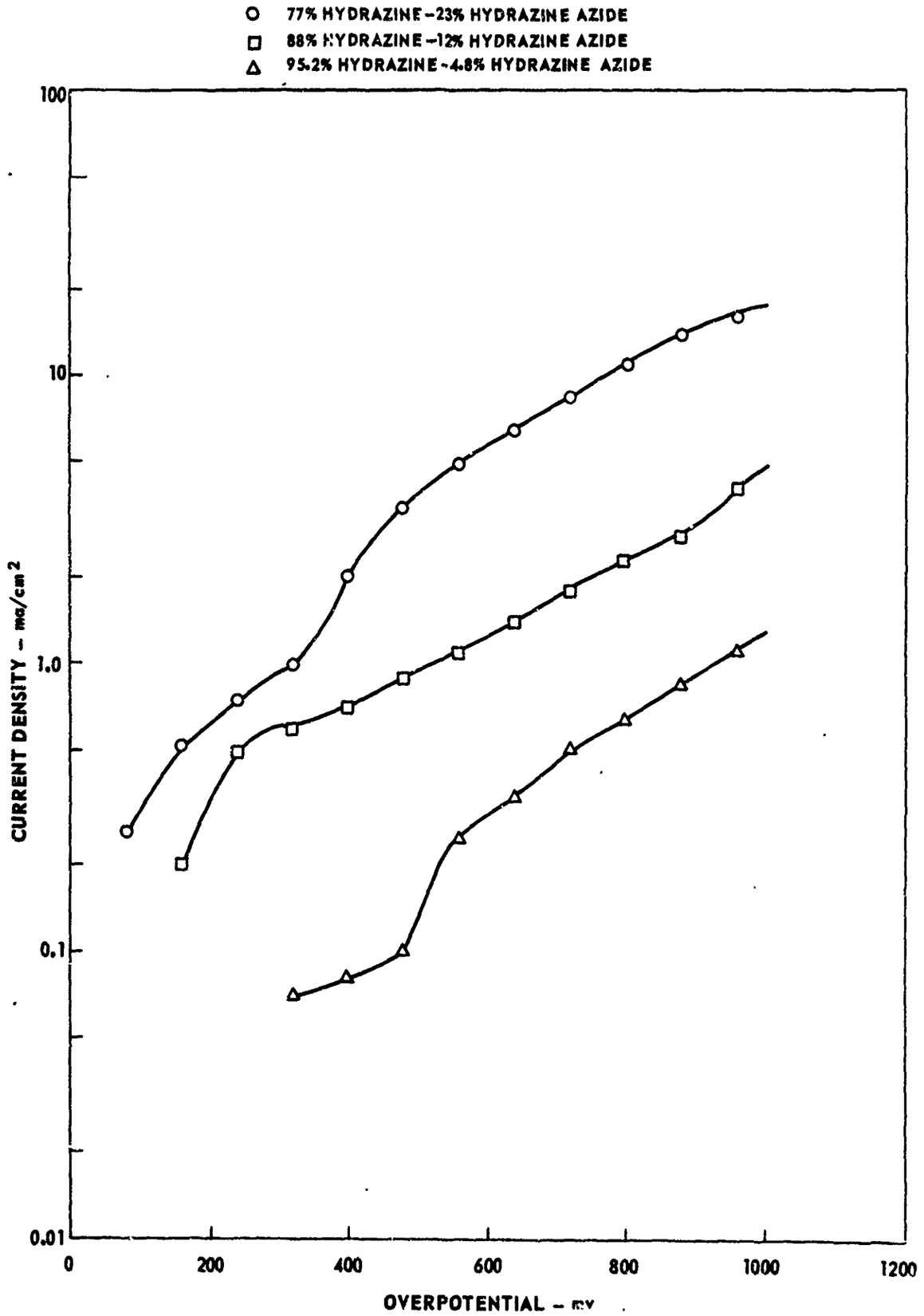

ANODIC POLARIZATION OF AM 350 AS A FUNCTION OF AZIDE CONCENTRATION

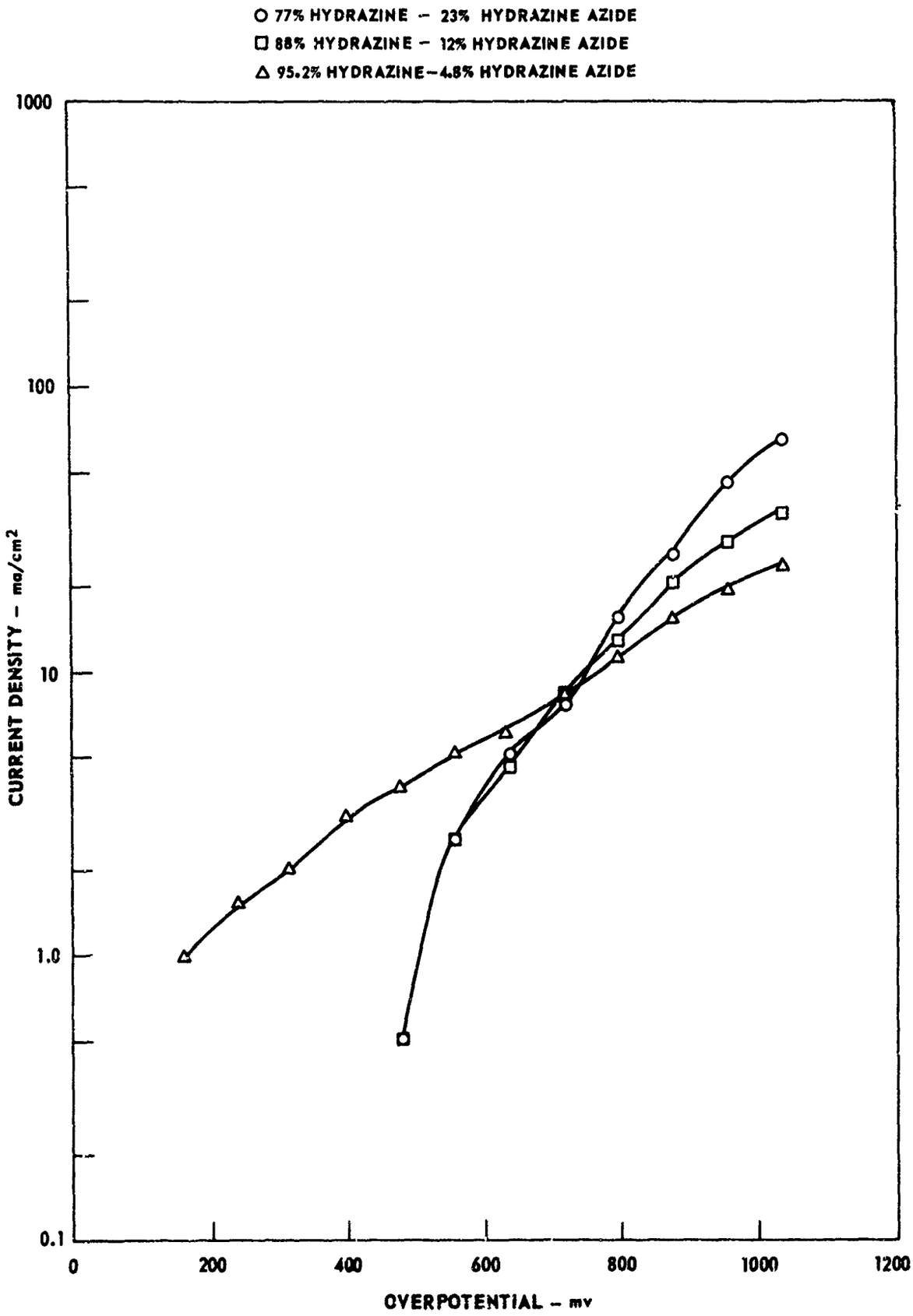

FIG. 25

ANODIC POLARIZATION OF PLATINUM AS A FUNCTION OF AZIDE CONCENTRATION

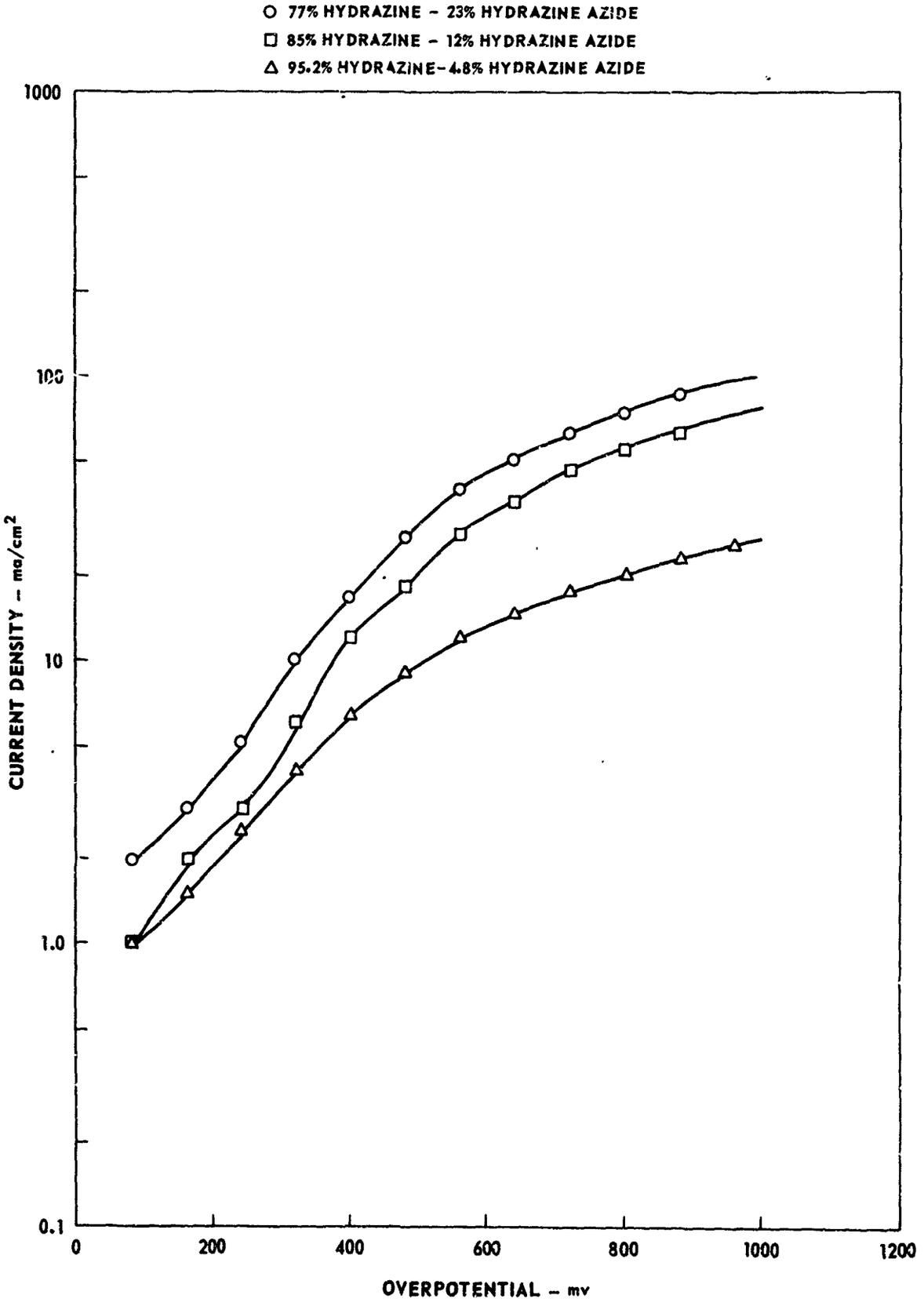

FIG. 26

ANODIC POLARIZATION OF PYROLYTIC GRAPHITE AS A FUNCTION OF AZIDE CONCENTRATION

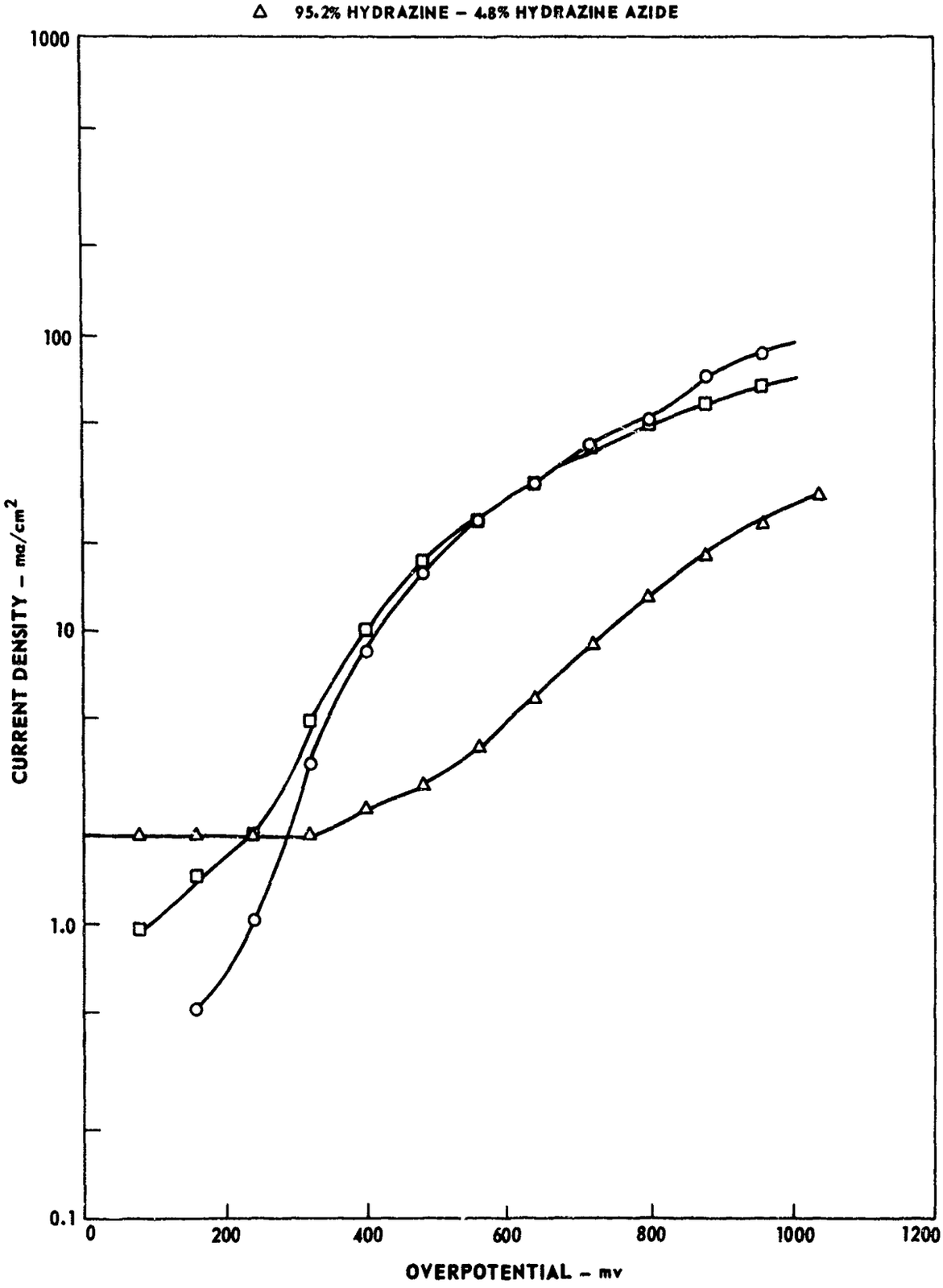

CATHODIC POLARIZATION OF 304 SS AS A FUNCTION OF AZIDE CONCENTRATION

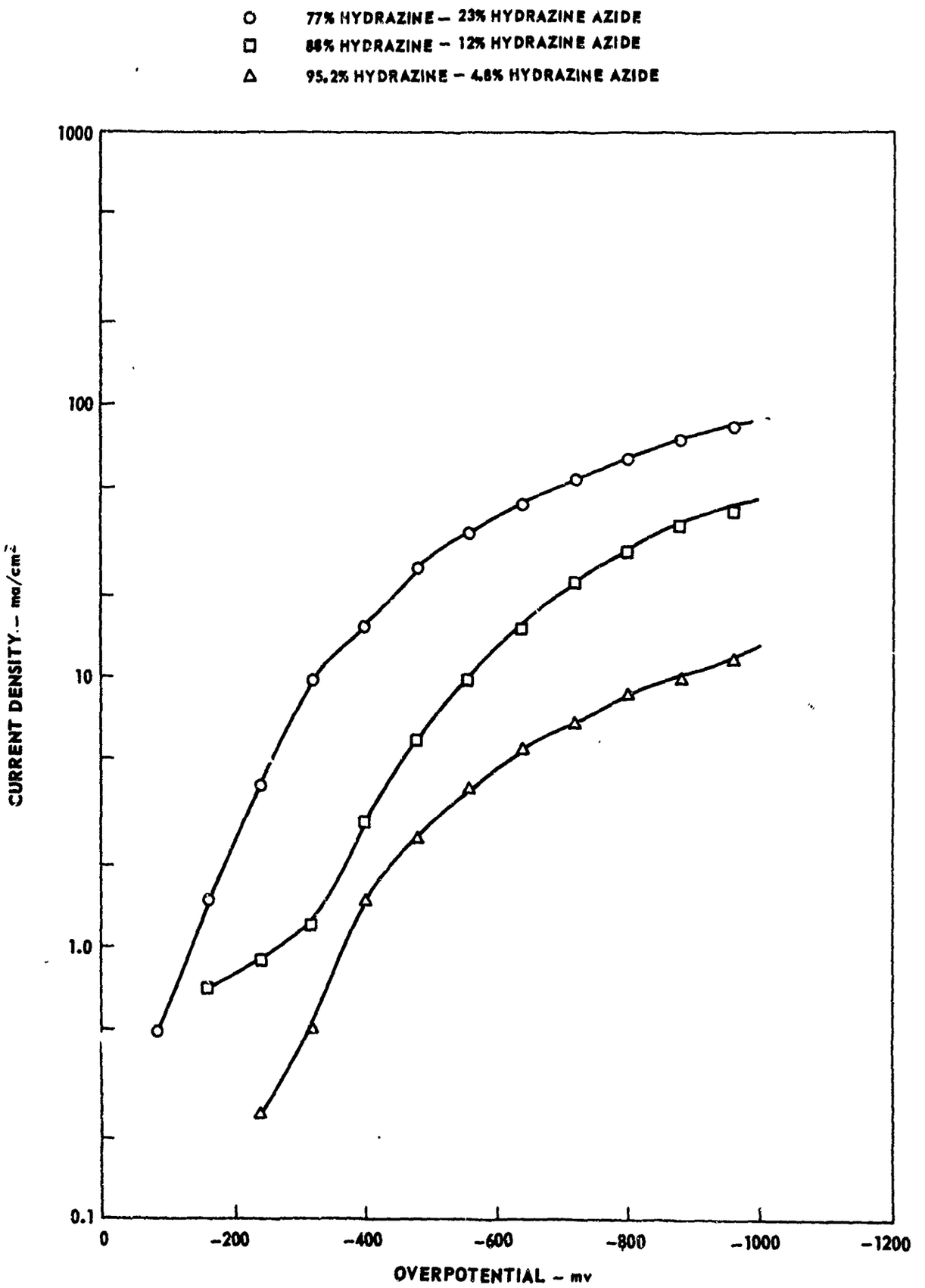

CATHODIC POLARIZATION OF AM 350 AS A FUNCTION OF AZIDE CONCENTRATION

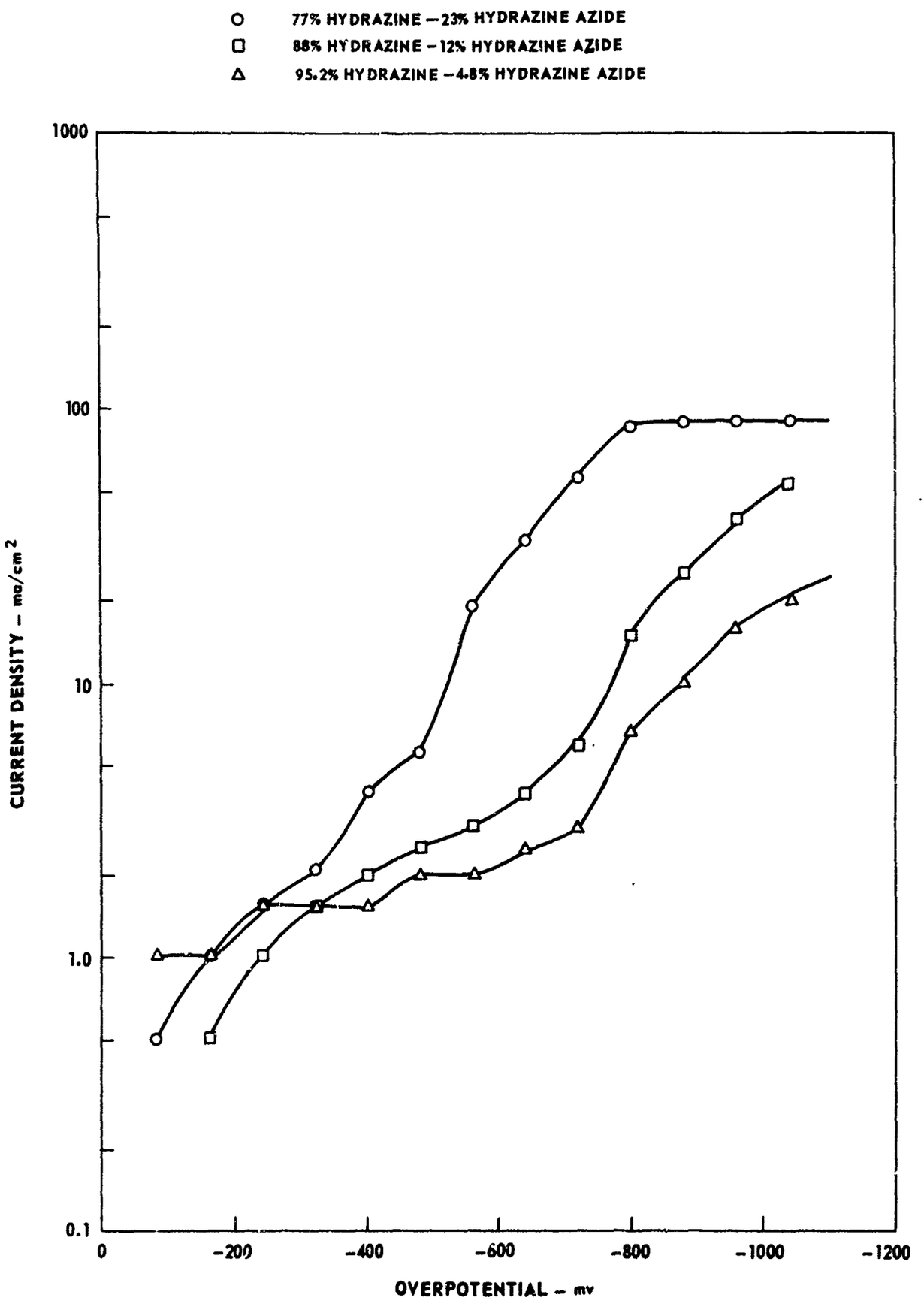

CATHODIC POLARIZATION OF PLATINUM AS A FUNCTION OF AZIDE CONCENTRATION

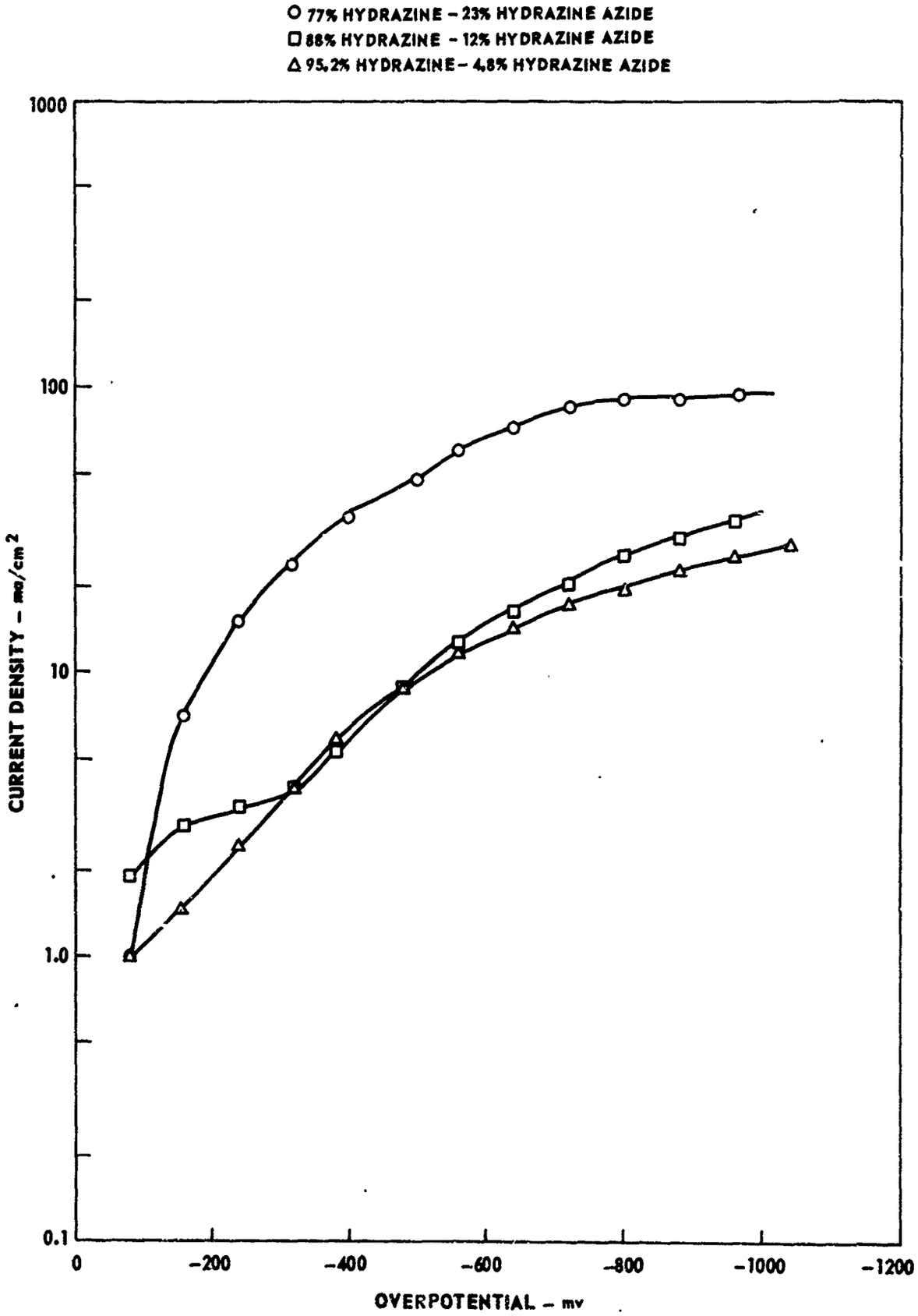

FIG. 30

CATHODIC CURRENT DENSITY VS AZIDE CONCENTRATION
AT η = 1000 mv

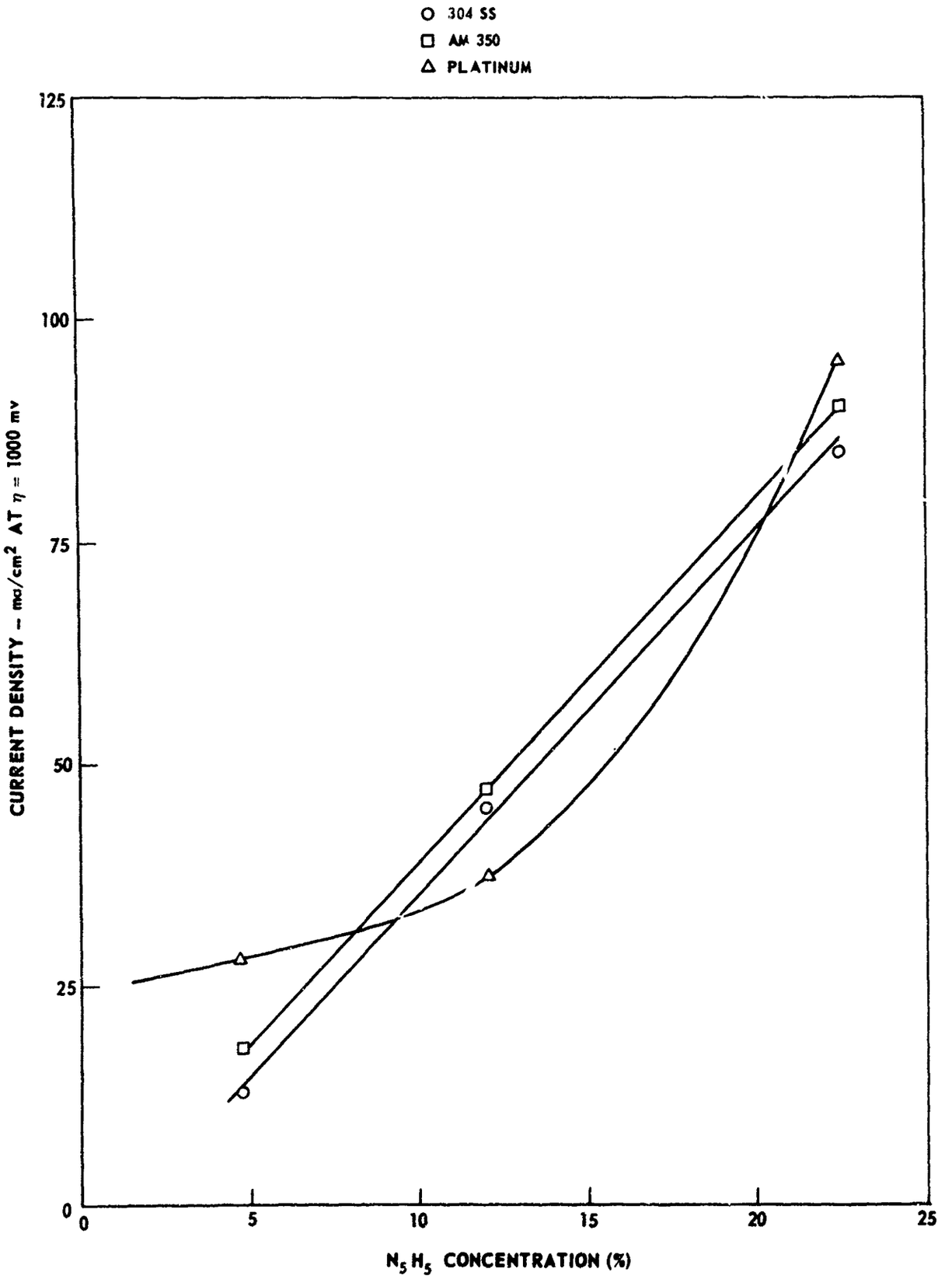

FIG. 31

ANODIC CURRENT DENSITY VS AZIDE CONCENTRATION AT η = 1000 mv

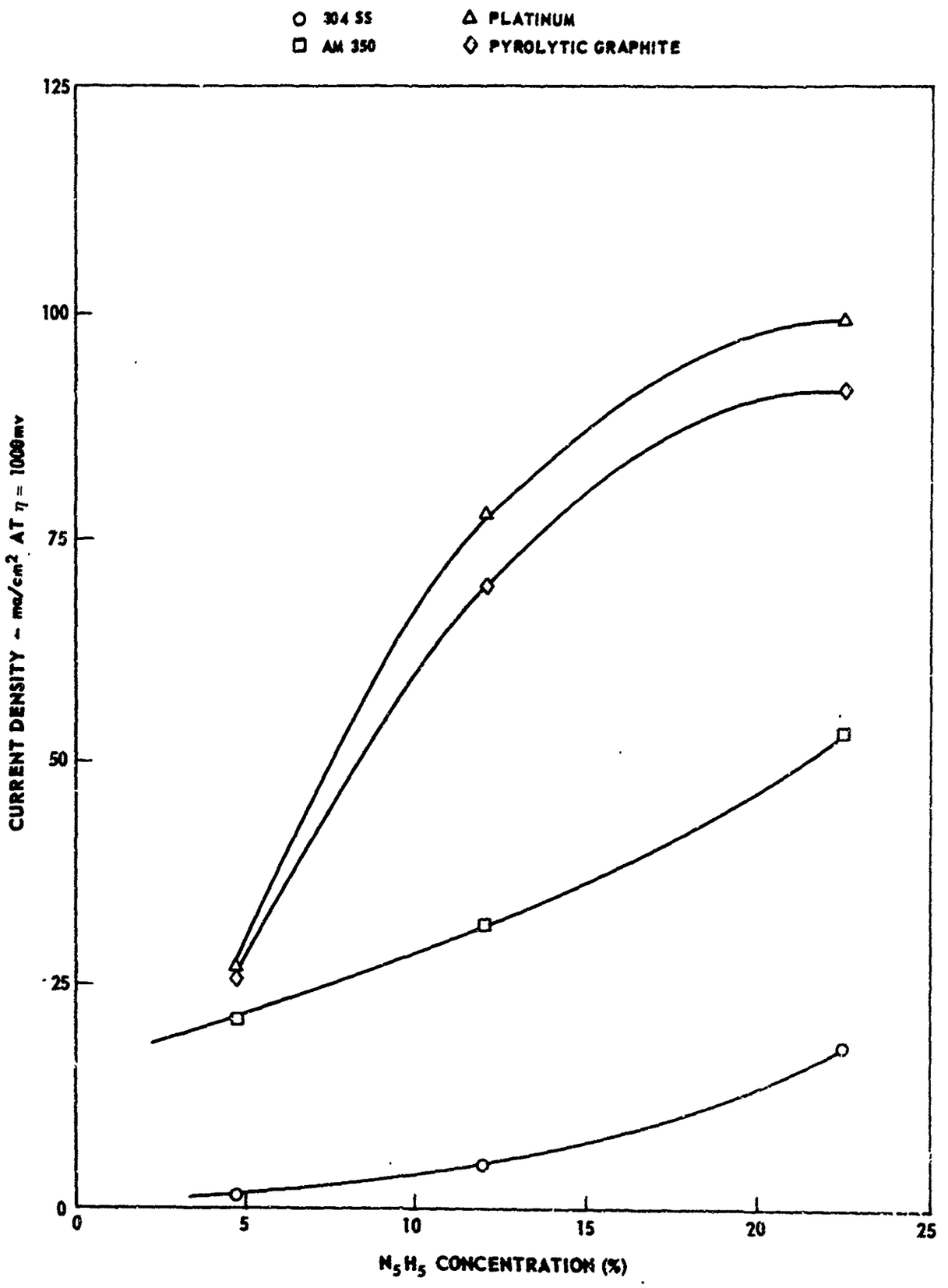

FIG. 32

ANODIC POLARIZATION OF 304 SS IN 6% HYDRAZINE NITRATE AND IN 4.8% HYDRAZINE AZIDE

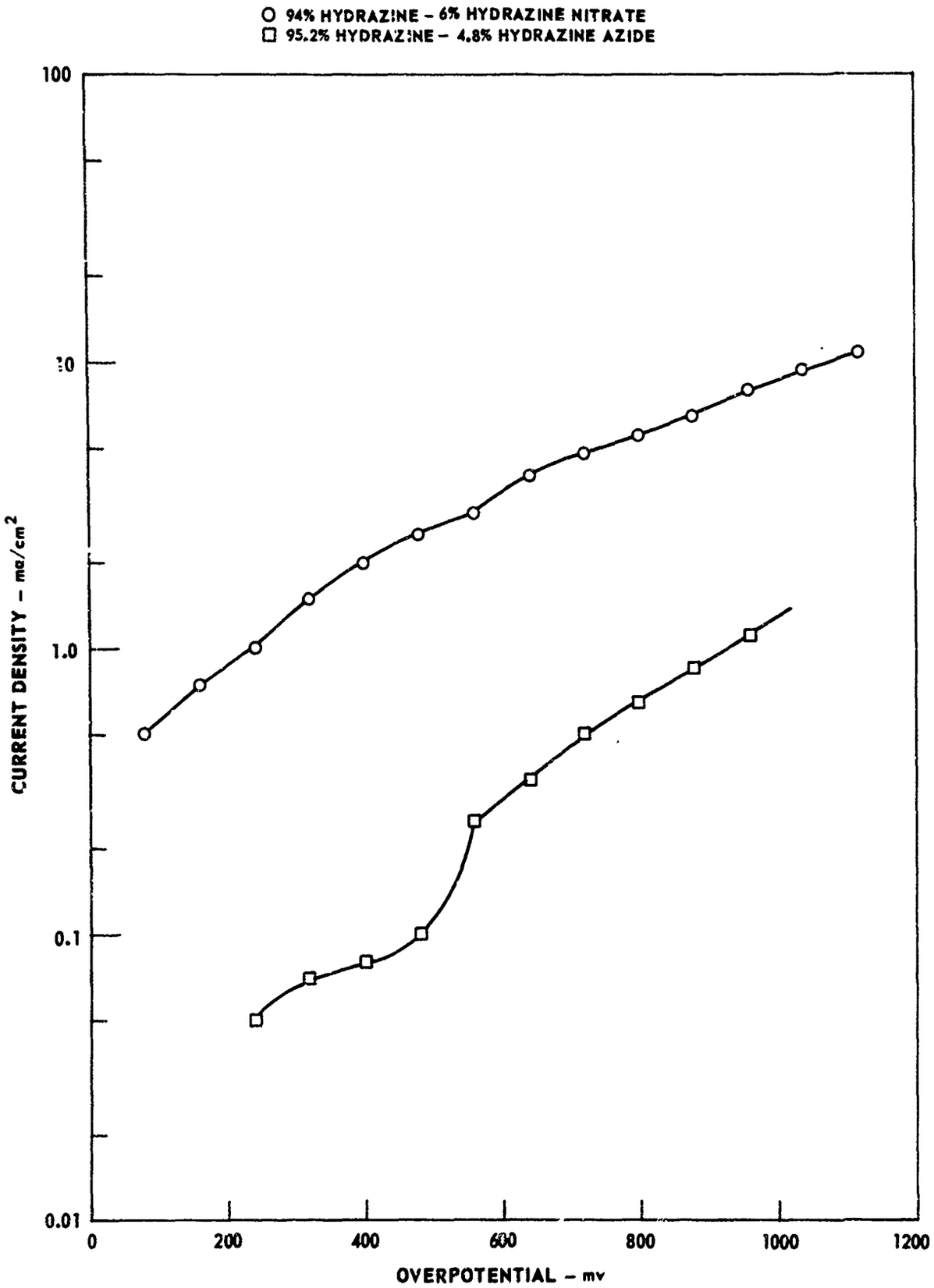

FIG. 33

ANODIC POLARIZATION OF AM 350 IN 6% HYDRAZINE NITRATE AND IN 4.8% HYDRAZINE AZIDE

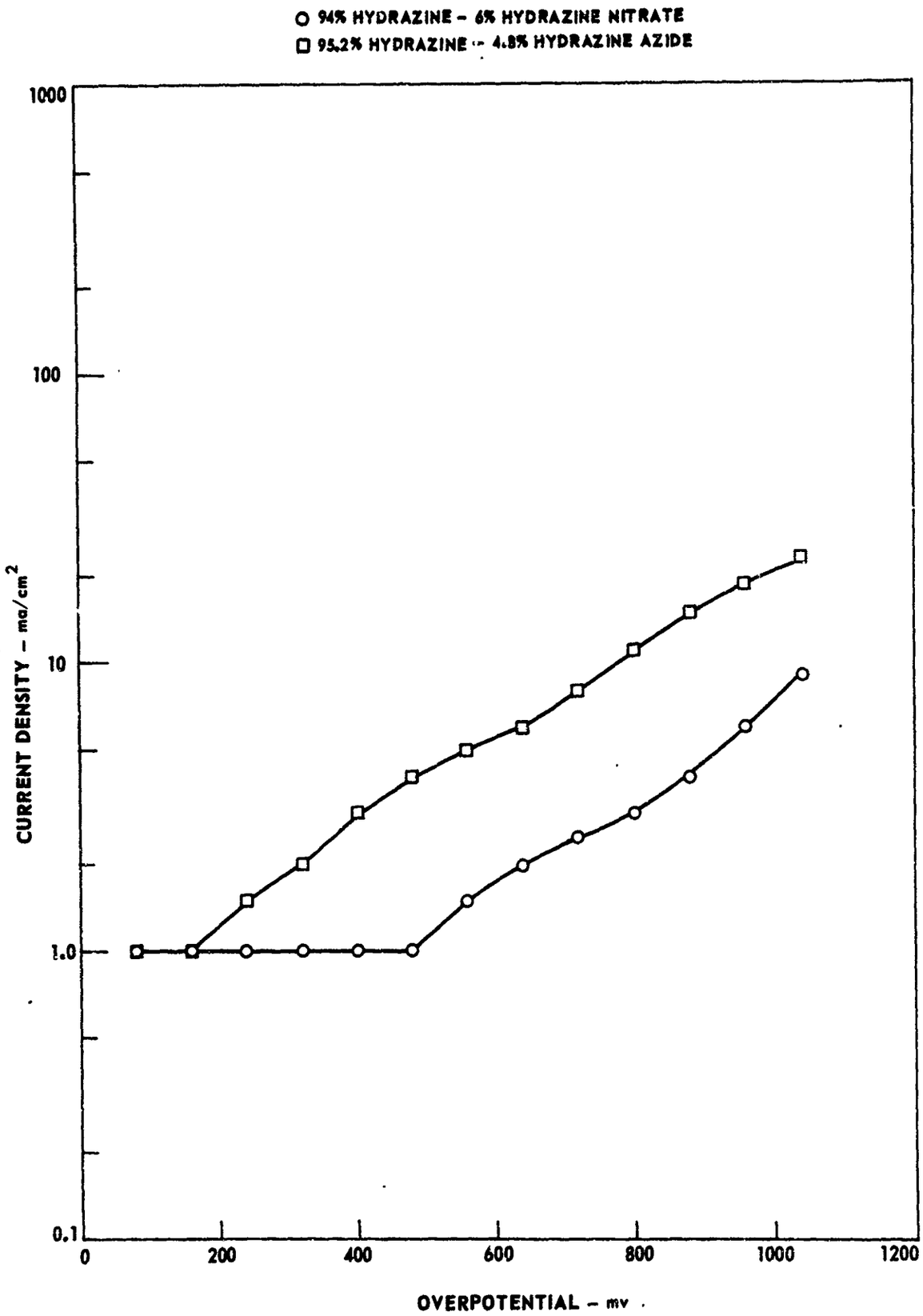

ANODIC POLARIZATION OF PLATINUM IN 6% HYDRAZINE NITRATE AND IN 4.8% HYDRAZINE AZIDE

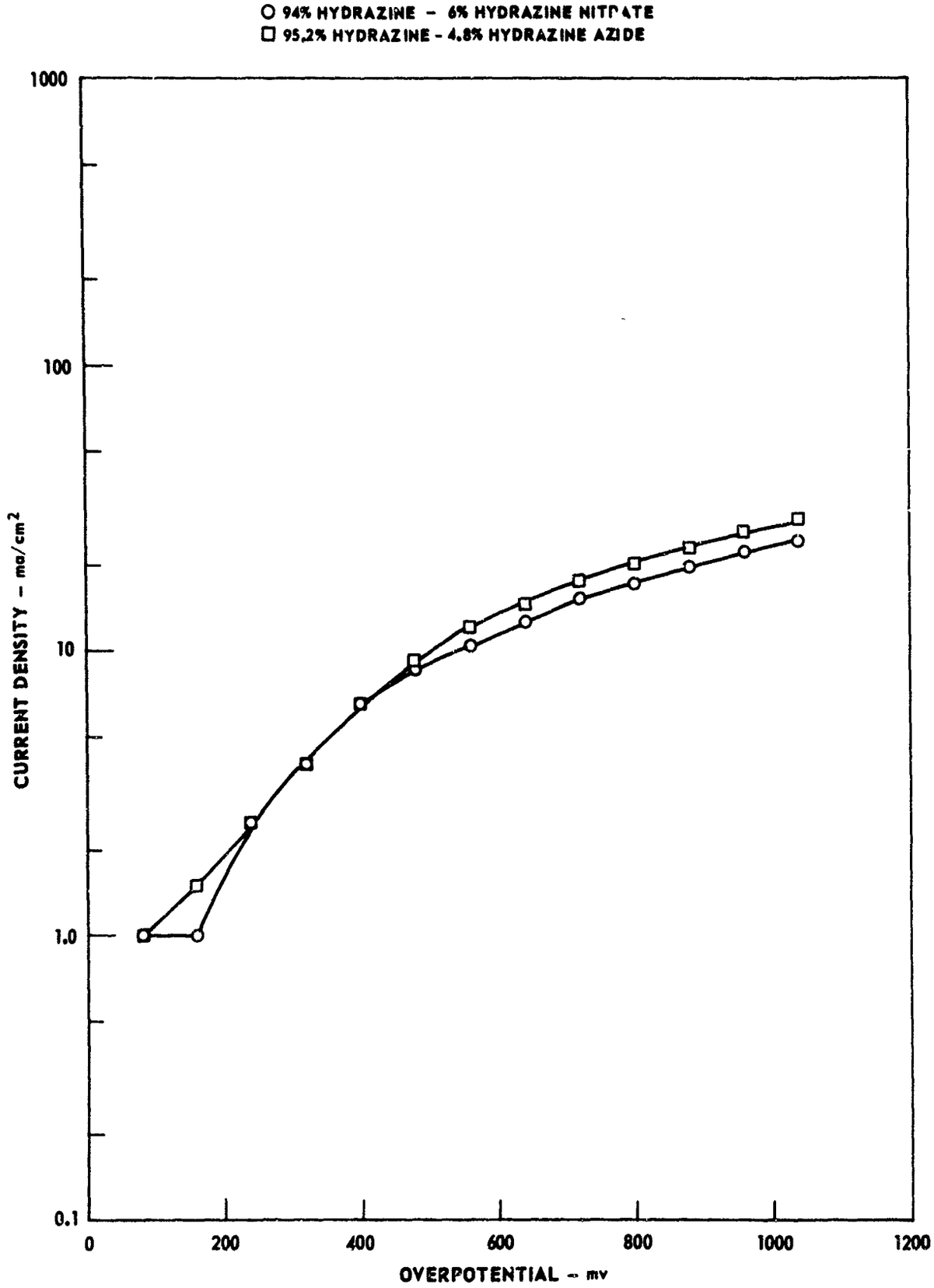

ANODIC POLARIZATION OF PYROLYTIC GRAPHITE IN 6% HYDRAZINE NITRATE AND IN 4.8% HYDRAZINE AZIDE

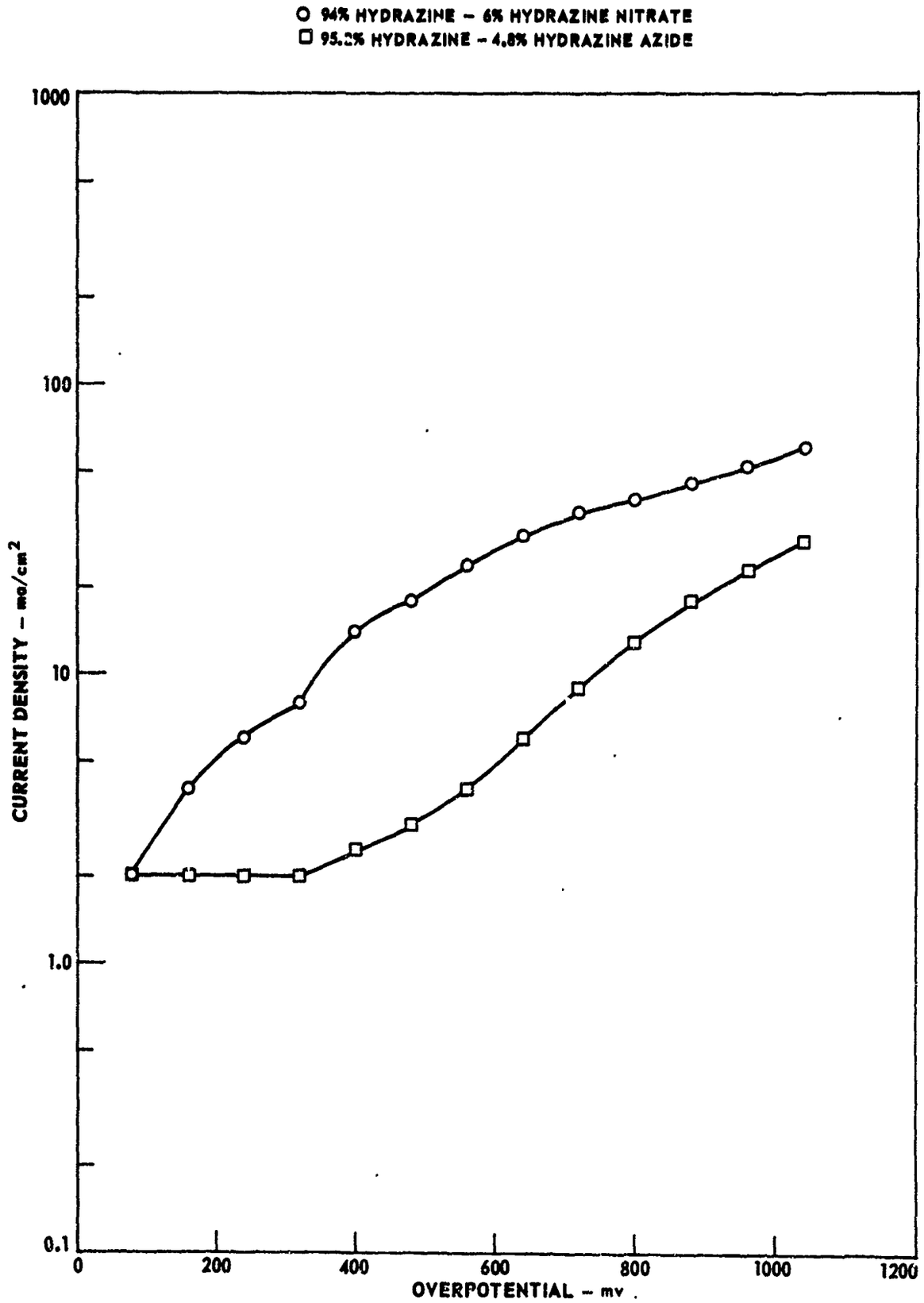

CATHODIC POLARIZATION OF 304SS IN 6% HYDRAZINE NITRATE AND IN 4.8% HYDRAZINE AZIDE

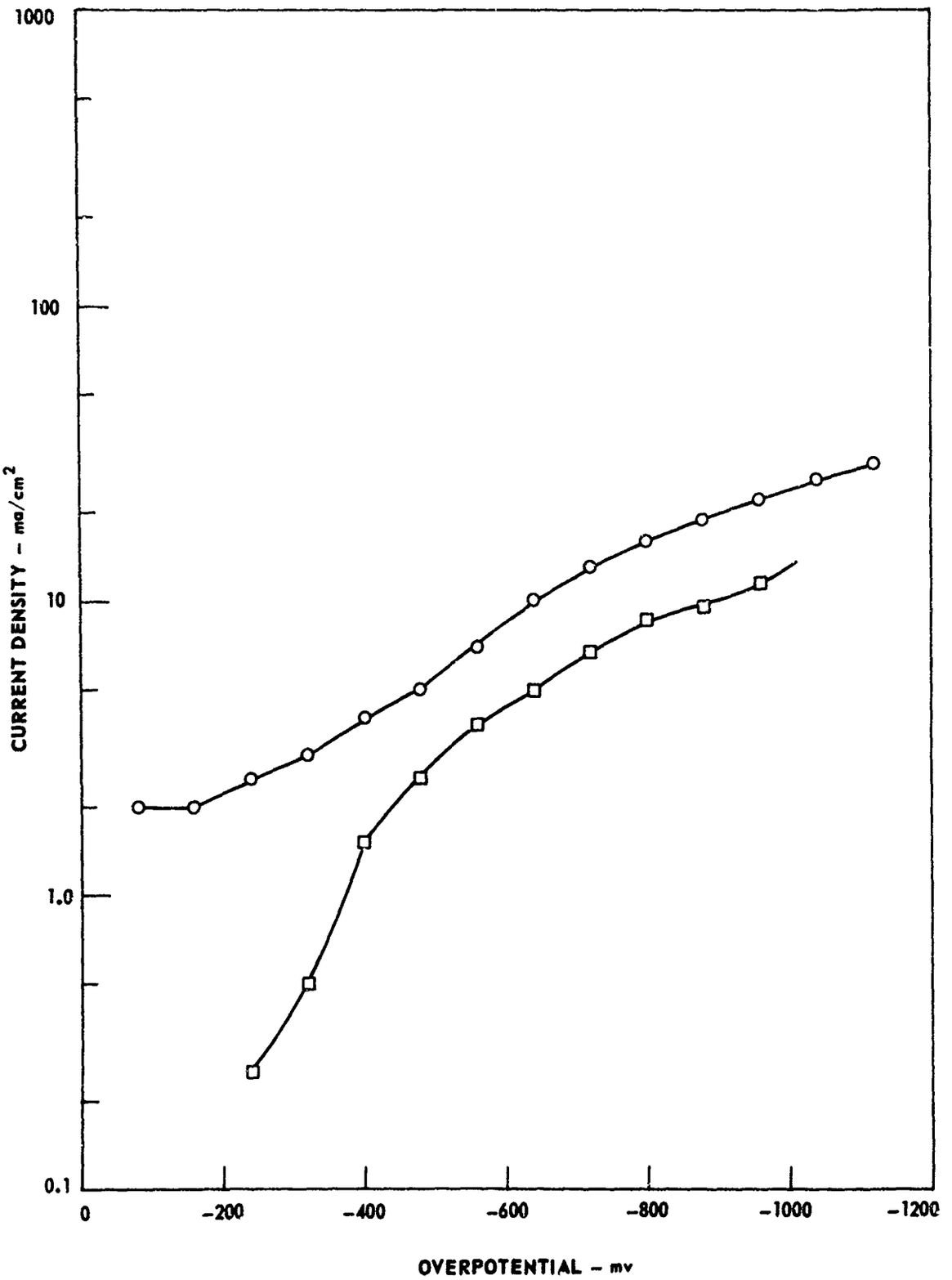

FIG. 37

CATHODIC POLARIZATION OF AM350 IN 6% HYDRAZINE AND IN 4.8% HYDRAZINE AZIDE

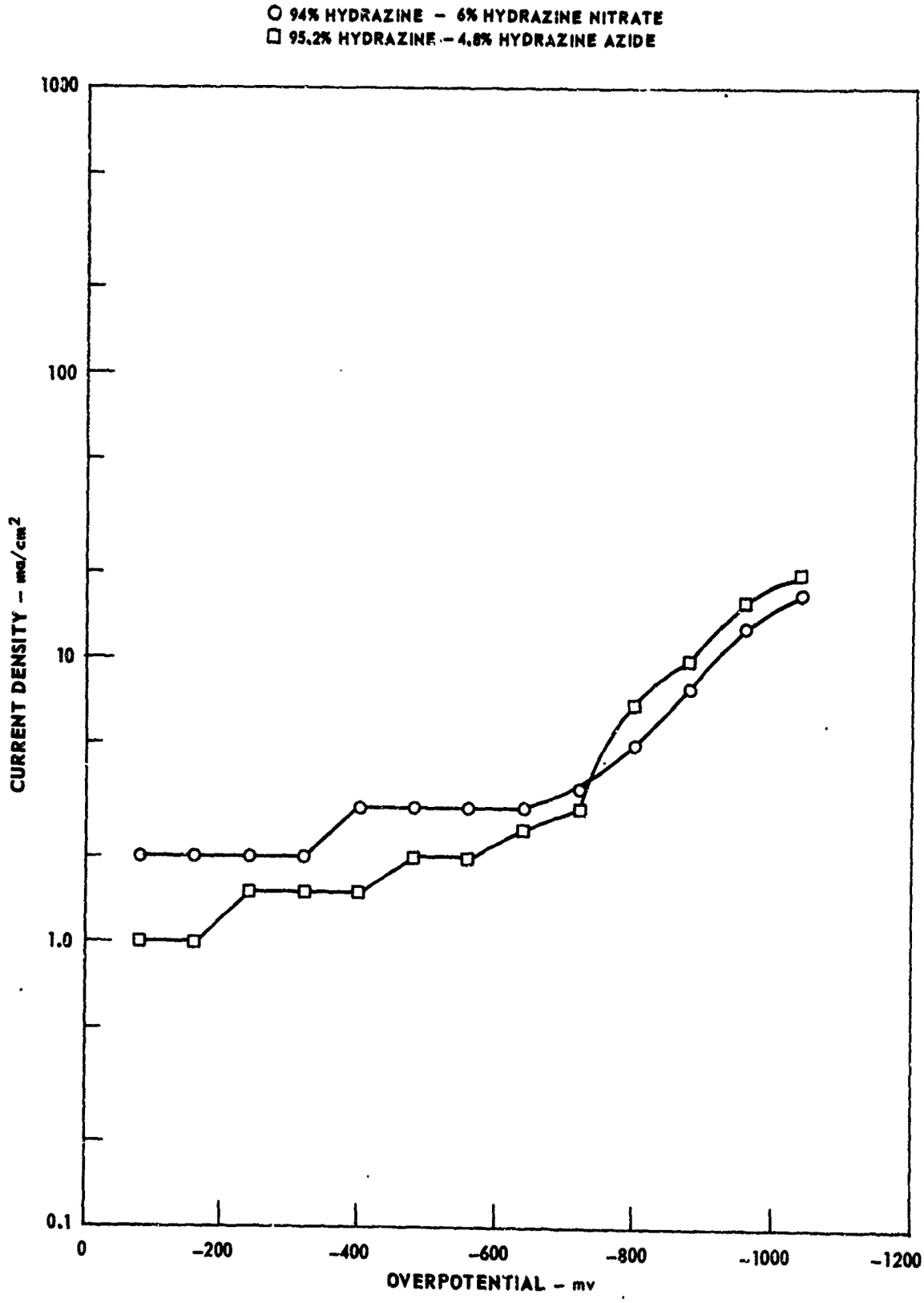

FIG. 38

CATHODIC POLARIZATION OF PLATINUM IN 6% HYDRAZINE NITRATE AND IN 4.8% HYDRAZINE AZIDE

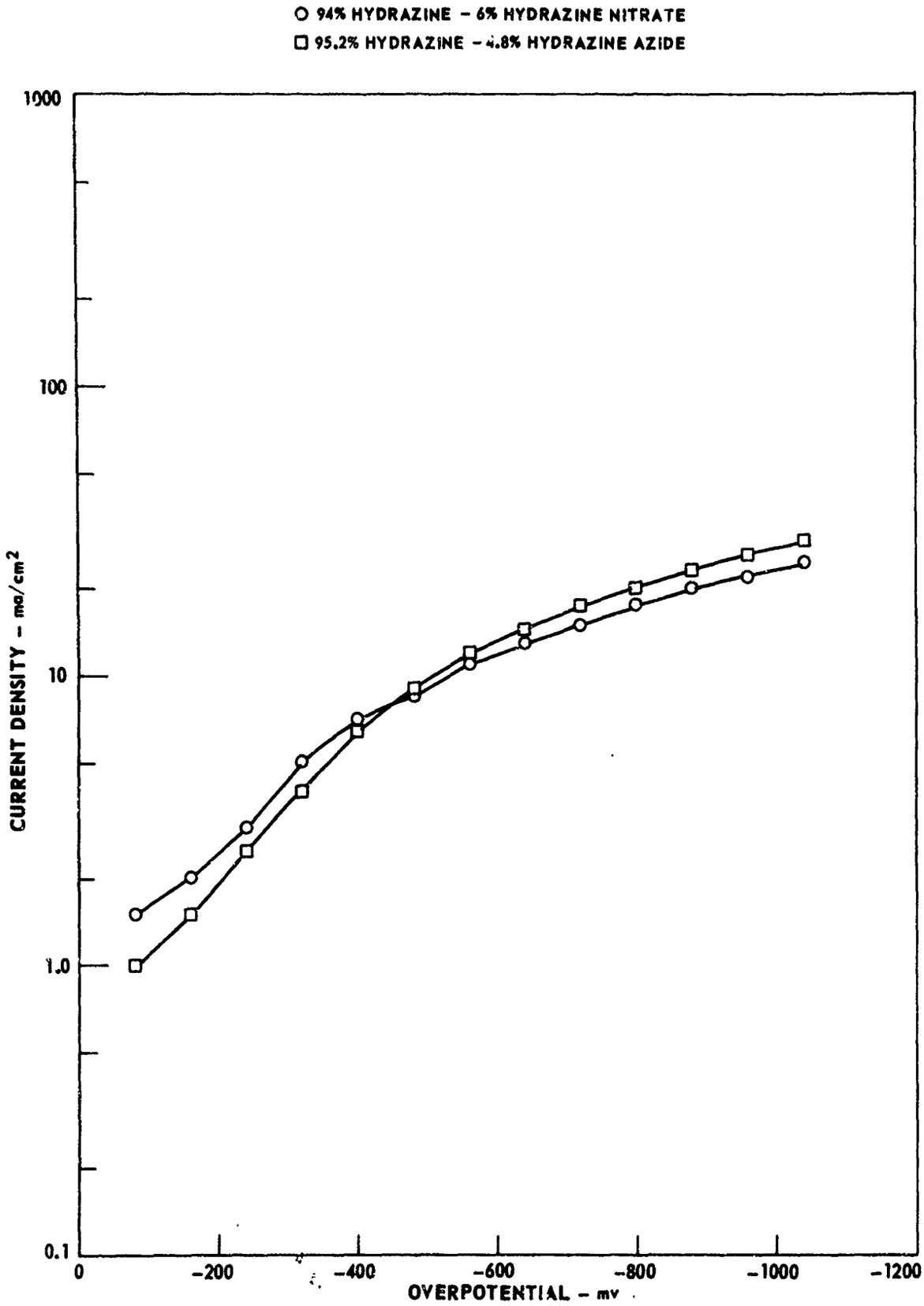

POTENTIAL-TIME RELATIONSHIPS AT 100 ma IN 77% HYDRAZINE - 23% HYDRAZINE AZIDE

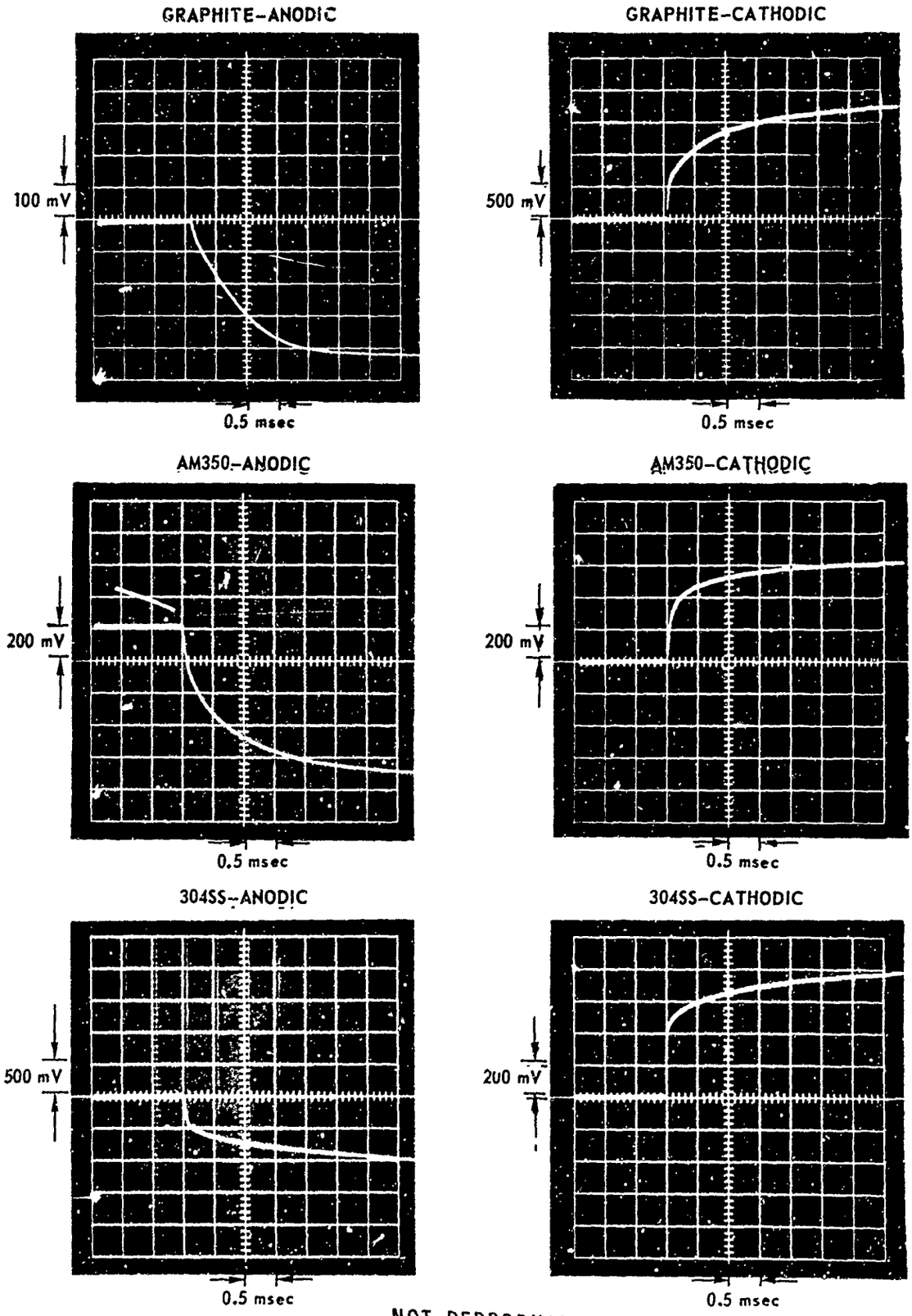

NOT REPRODUCIBLE

FIG. 40

ELECTROLYSIS CELL

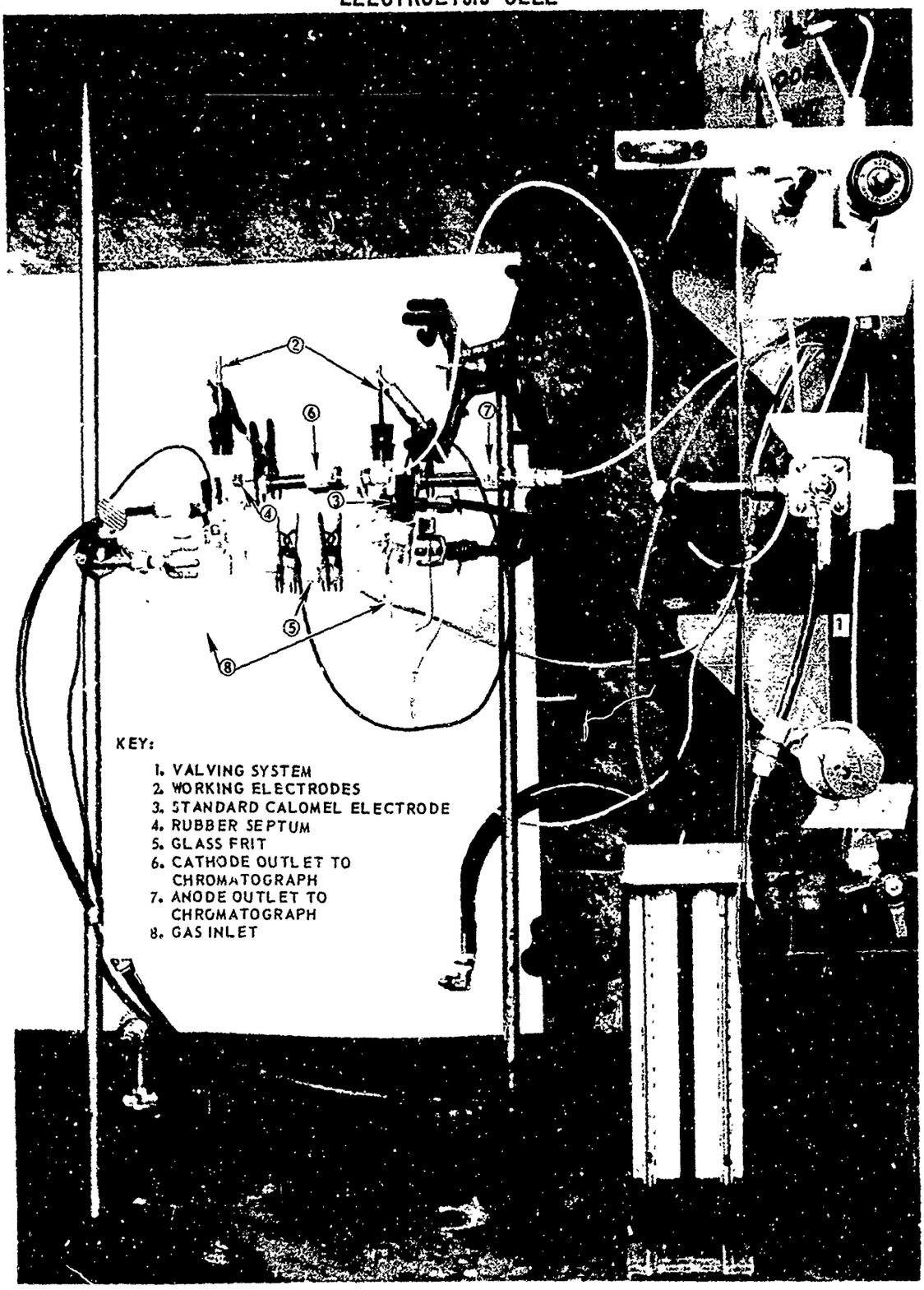

NOT REPRODUCIBLE

RL-70-294-B

NOT REPRODUCIBLE

FIG. 41

CHROMATOGRAPHY APPARATUS

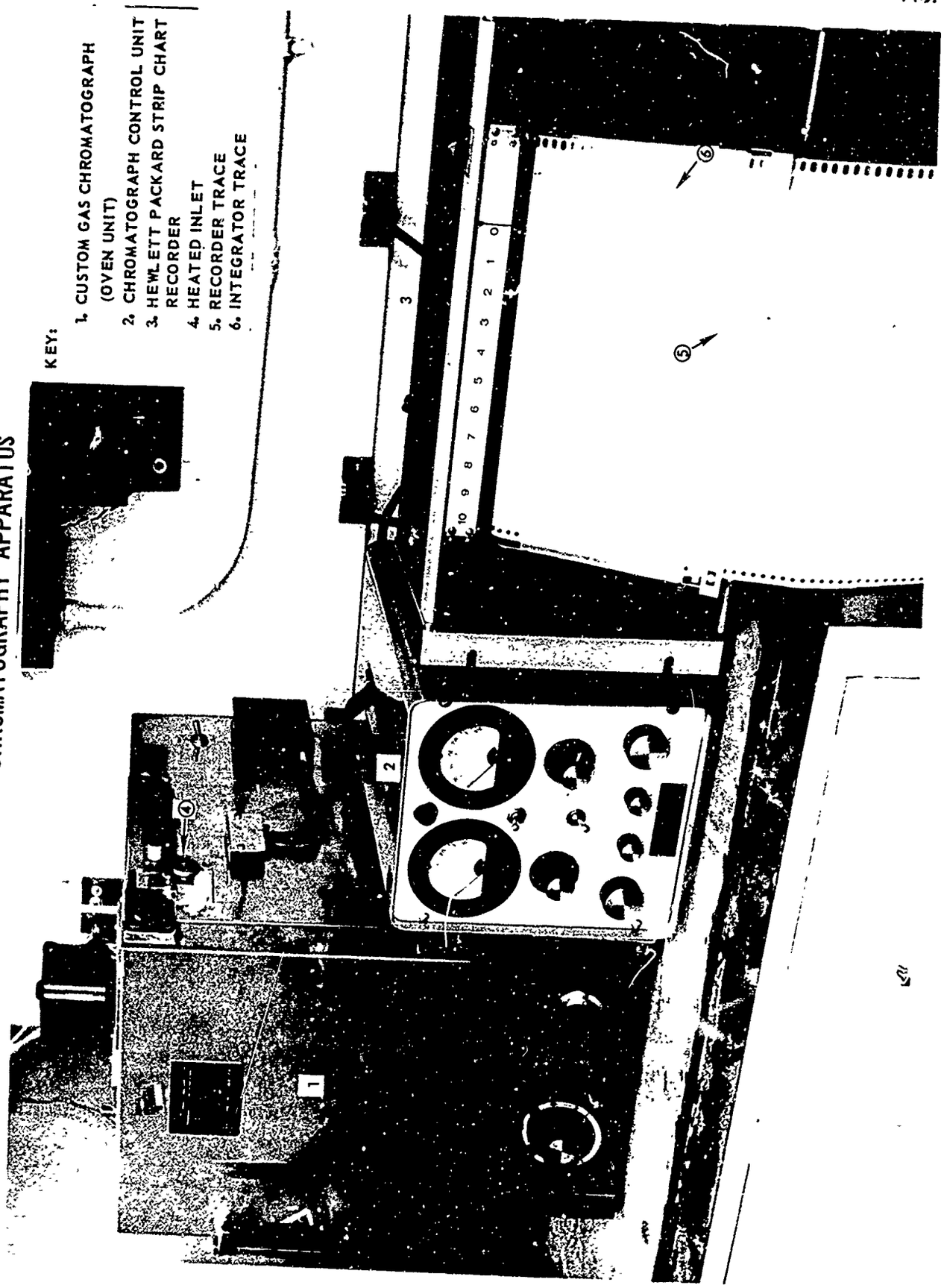

RL-70-294-C

Unclassified
Security Classification

DOCUMENT CONTROL DATA - R&D

(Security classification of title, body of abstract and indexing annotation must be entered when the overall report is classified)

1. ORIGINATING ACTIVITY *(Corporate author)* United Aircraft Research Laboratories	2a. REPORT SECURITY CLASSIFICATION Unclassified 2b. GROUP ---

3. REPORT TITLE

Electrolytic Ignition System for a Millipound Thruster

4. DESCRIPTIVE NOTES *(Type of report and inclusive dates)*

Phase I Special Report

5. AUTHOR(S) *(Last name, first name, initial)*

Brown, Charles T.

6. REPORT DATE January, 1971	7a. TOTAL NO. OF PAGES 89	7b. NO. OF REFS 2
8a. CONTRACT OR GRANT NO. F04611-70-C-0070 NEW b. PROJECT NO. c. d.	9a. ORIGINATOR'S REPORT NUMBER(S) 9b. OTHER REPORT NO(S) *(Any other numbers that may be assigned this report)*	

10. AVAILABILITY/LIMITATION NOTICES

This document is subject to special export controls and each transmittal to foreign governments or foreign nationals may be made only with prior approval of AFRPL (MOZT/STINFO) Edwards, California 93523

11. SUPPLEMENTARY NOTES	12. SPONSORING MILITARY ACTIVITY Air Force Rocket Propulsion Laboratory Edwards Air Force Base Edwards, California 93523

13. ABSTRACT The United Aircraft Research Laboratories have conducted a research program under Phase I of Contract F04611-70-C-0070, which had as its objective ~~the~~ selection of an electrolyte and electrode materials for an electrolytic ignition system for millipound thrusters. This report describes the evaluation of electrode polarization effects, ohmic effects due to both electrolytes and electrodes, and possible catalytic effects on electrode surfaces. Electrical conductivity measurements indicate that hydrazine-based salts must be added to hydrazine in order to minimize ohmic effects and that the mixture of 77% hydrazine-23% hydrazine azide is the most promising electrolyte candidate. Polarization studies have shown that platinum or pyrolytic graphite should be the best anode material for the electrolytic cell and that AM350 or 304SS should be the best cathode material in terms of minimizing the power needs for the cell. These electrodes were also found to catalyze the propellant decomposition reaction in addition to providing simple electrolytic decomposition. This result indicates that the reaction will be self-propagating at power inputs considerably below theoretical.

DD FORM 1 JAN 64 1473

Unclassified
Security Classification

Unclassified
Security Classification

14. KEY WORDS	LINK A ROLE	LINK A WT	LINK B ROLE	LINK B WT	LINK C ROLE	LINK C WT
Electrolytic ignition						
Monopropellants						
Hydrazine						
Hydrazine azide						
Millipound thrusters						

INSTRUCTIONS

1. ORIGINATING ACTIVITY: Enter the name and address of the contractor, subcontractor, grantee, Department of Defense activity or other organization *(corporate author)* issuing the report.

2a. REPORT SECURITY CLASSIFICATION: Enter the overall security classification of the report. Indicate whether "Restricted Data" is included. Marking is to be in accordance with appropriate security regulations.

2b. GROUP: Automatic downgrading is specified in DoD Directive 5200.10 and Armed Forces Industrial Manual. Enter the group number. Also, when applicable, show that optional markings have been used for Group 3 and Group 4 as authorized.

3. REPORT TITLE: Enter the complete report title in all capital letters. Titles in all cases should be unclassified. If a meaningful title cannot be selected without classification, show title classification in all capitals in parenthesis immediately following the title.

4. DESCRIPTIVE NOTES: If appropriate, enter the type of report, e.g., interim, progress, summary, annual, or final. Give the inclusive dates when a specific reporting period is covered.

5. AUTHOR(S): Enter the name(s) of author(s) as shown on or in the report. Enter last name, first name, middle initial. If military, show rank and branch of service. The name of the principal author is an absolute minimum requirement.

6. REPORT DATE: Enter the date of the report as day, month, year; or month, year. If more than one date appears on the report, use date of publication.

7a. TOTAL NUMBER OF PAGES: The total page count should follow normal pagination procedures, i.e., enter the number of pages containing information.

7b. NUMBER OF REFERENCES: Enter the total number of references cited in the report.

8a. CONTRACT OR GRANT NUMBER: If appropriate, enter the applicable number of the contract or grant under which the report was written.

8b, 8c, & 8d. PROJECT NUMBER: Enter the appropriate military department identification, such as project number, subproject number, system numbers, task number, etc.

9a. ORIGINATOR'S REPORT NUMBER(S): Enter the official report number by which the document will be identified and controlled by the originating activity. This number must be unique to this report.

9b. OTHER REPORT NUMBER(S): If the report has been assigned any other report numbers *(either by the originator or by the sponsor)*, also enter this number(s).

10. AVAILABILITY/LIMITATION NOTICES: Enter any limitations on further dissemination of the report, other than those imposed by security classification, using standard statements such as:

(1) "Qualified requesters may obtain copies of this report from DDC."

(2) "Foreign announcement and dissemination of this report by DDC is not authorized."

(3) "U. S. Government agencies may obtain copies of this report directly from DDC. Other qualified DDC users shall request through _____."

(4) "U. S. military agencies may obtain copies of this report directly from DDC Other qualified users shall request through _____."

(5) "All distribution of this report is controlled. Qualified DDC users shall request through _____."

If the report has been furnished to the Office of Technical Services, Department of Commerce, for sale to the public, indicate this fact and enter the price, if known.

11. SUPPLEMENTARY NOTES: Use for additional explanatory notes.

12. SPONSORING MILITARY ACTIVITY: Enter the name of the departmental project office or laboratory sponsoring *(paying for)* the research and development. Include address.

13. ABSTRACT: Enter an abstract giving a brief and factual summary of the document indicative of the report, even though it may also appear elsewhere in the body of the technical report. If additional space is required, a continuation sheet shall be attached.

It is highly desirable that the abstract of classified reports be unclassified. Each paragraph of the abstract shall end with an indication of the military security classification of the information in the paragraph, represented as *(TS), (S), (C), or (U)*.

There is no limitation on the length of the abstract. However, the suggested length is from 150 to 225 words.

14. KEY WORDS: Key words are technically meaningful terms or short phrases that characterize a report and may be used as index entries for cataloging the report. Key words must be selected so that no security classification is required. Identifiers, such as equipment model designation, trade name, military project code name, geographic location, may be used as key words but will be followed by an indication of technical context. The assignment of links, rules, and weights is optional